

Development of Effective Removal Methods of PFCs (Perfluorinated Compounds) in Water by Adsorption and Coagulation

By

Senevirathna Thennakoon Mudiyansele

Lalantha Dharshana Senevirathna

A thesis submitted in partial fulfillment of the requirements for
the degree of Doctor of Engineering

Nationality: Sri Lankan

Previous Degree: Master of Engineering in Environment

Asian Institute of Technology, Bangkok, Thailand

Scholarship Donor: Monbukagakusho Scholarship

Department of Urban and Environmental Engineering,
Graduate School of Engineering, Kyoto University, Japan

August 2010

ACKNOWLEDGEMENT

It is rather difficult to express in just few lines, my gratitude to all the people who helped me, in one way or another, to accomplish this work. I hope that those that I have mentioned realize that my appreciation extends far beyond the ensuing paragraphs.

First and foremost, I would like to thank my supervisor Professor Shigeo Fujii for inviting me and providing all the facilities and enough freedom for my research work. His direct and indirect guiding and monitoring made an exponential progress in my academic discipline, even though I resumed studies after seven years of field experiences. His enthusiasm and integral view on research and his mission for providing 'only high-quality work and no less', has made a deep impression on me which I will always cherish for the rest of my life. I owe him lots of gratitude for having shown me this way of research. I am really glad and proud that I have had an opportunity to work with such a wonderful person.

I wish to thank Professor Hiroki Tanaka, Professor Shimizu for serving on my PhD committee. Special thanks goes to Professor Shuhei Tanaka for many interesting discussions which we had on Tuesdays on adsorption, coagulation and treatment of PFCs and providing me all the requirements for the experiments within a short request.

My gratitude also goes to my colleagues in the PFOS group, and other lab members, especially Dr Chinagan Kunacheva, you are much younger than me in age, yet have learnt a lot from you.

Also I would like to express my deepest gratitude for the continuous support, care, understanding and love that I received from my wife, Shanu. Similar appreciation is extended to my parents. Last but certainly not least, I cherish my little princess, Himaya, who recharged my batteries every evening when I go back home with her nice smile.

Thank you all

Abstract

Perfluorinated compounds (PFCs) have been used for decades to make products that resist heat, oil, stains, grease and water. In the past, PFCs were not regulated. Common uses include nonstick cookware, stain-resistant carpets and fabrics, components of fire-fighting foam, industrial applications, coatings for packaging, such as milk cartons, cosmetic additives, and other personal products. Huge amount of PFCs have been already released in to the environment, which have been trickled down up to the glaziers in Antarctica. The chemical structure of PFCs makes them extremely resistant to breakdown in the environment.

Although PFCs have been used for decades, limited studies on human health effects have been carried out. In animal studies, high concentrations PFCs have shown adverse affects on the liver and other organs.

It is a reported fact by researchers that the conventional water and wastewater treatment facilities can not eliminate PFCs. Many studies have showed a positive correlation between the PFOS concentration in raw water and tap water samples suggesting minimum removal efficiency of conventional water purification systems. The main reason for the persistancy of PFCs is C-F bonds. The C-F bond length is shorter than any other carbon–halogen bonds, and shorter than the C-N and the C-O bonds. The high electro-negativity of fluorine gives the carbon–fluorine bond a significant polarity/dipole moment.

The overall objective of this research was to investigate on possible techniques to eliminate PFCs in water. Since PFCs are negatively charged by its atomic structure, the stagergy was to eliminate them by adsorption process. In this experiment, seven granular materials and nine coagulants were studied in detail for PFCs eliminations.

Six kind of synthetic resins and GAC were tested with a series of batch experiments for PFCs adsorption (Chapter 4). The batch experiment for kinetic and isotherm characteristics of each maretial was carried out in a shaker with 100 hrs shaking duration. Out of seven materials five were first time tested for PFCs. Faster kinetic characteristics were observed for GAC and ion exchange resins than non ion exchange resins. Considering the adsorption isotherms, synthetic resins were identified as better filter materials (in terms of adsorption capacity) to eliminate PFCs in water at a low concentration (1 µg/L).

The magnitude of Freundlich isotherm constants (K_f) decreases in the following order for most of the long chain and the medium chain PFCs tested: Ion-exchange polymers > Non ion-exchange polymers > GAC, sometimes at a further low equilibrium concentration (100 ng/L) non ion-exchange polymers showed higher adsorption capacity than other adsorbents. Amb IRA- 400 was identified as the best filter material to eliminate PFOS at equilibrium concentrations of >1 $\mu\text{g/L}$. Considering both adsorption isotherms and adsorption kinetics, Amb XAD 4 and Dow MarathonA were best candidate materials for eliminating PFOS at ng/L equilibrium concentrations. From the results for kinetic experiments, chemisorption was identified as the main attaching process in PFCs adsorption.

The process of coagulation was studied by a series of jar tests for PFCs elimination in this research (Chapter 5). There is limited published data on PFCs coagulation, especially by organic coagulants. Six long chain cationic coagulants were tested for anionic PFCs coagulation and the results were compared with three conventional inorganic coagulants. The results of the experiments with deionized water and wastewater spiked with PFCs showed that the PFCs coagulation by organic coagulants is double than that of inorganic coagulants. Among organic coagulants FL 2749 was identified as the best candidate material to eliminate PFCs. Jar test results with actual PFCs related industrial wastewater indicated that organic coagulants are not effective (as it showed in wastewater spiked with PFCs) to coagulate PFCs. The PFCs that appear in real wastewater seems to be incorporated with other polar molecules in wastewater. Organic coagulation followed by microfiltration was identified as an effective combination to eliminate PFCs for some wastewaters, but further studies have to be done on this topic.

The results of batch experiments (chapter 4 and 5) were further consolidated by the long run continuous experiments (60 days and 130 days). Non ion exchange polymers were further studied with a column experiment (Chapter 6) (60 days continuous run) and Amb XAD 4 was recognized as the best candidate among the tested four filter materials to eliminate PFOS. Amb XAD 4 removed 99.99% PFOS up to 23,000 bed volumes pass through with the condition of 10 $\mu\text{g/L}$ inflow concentration and flow rate of 15 ml/min (0.75 bed volumes/min). At the end of the column test, PFOS adsorbed granular materials were used to examine the material regeneratability with an organic solvent. Within 80 min, all most 100% PFOS was recovered from synthetic resins suggesting that

synthetic polymers can be effectively regenerated by an organic solvent.

A long run continuous experiment (130 days) showed the combined treatment process of coagulation (by organic coagulants) followed by adsorption and filtration is an excellent method to treat PFCs in water. The combination with some adsorbents, more than 99% removal was obtained even after 100 days of continuous run. Economical analysis with different scenarios for the level of treatment and regenerations indicated that AmbXAD 4 was the cheapest option for PFOS adsorption.

This experiment was limited for six synthetic resins and six long chain cationic organic coagulants. The results highly recommend to repeat the same experiments with more adsorbents and coagulants for material optimization. The materials tested in this experiment were limited for lab scale models and the same materials to be tested in the field. As the first step a filter column with Amb XAD4 can be installed at the discharge point of a wastewater treatment plant in a PFCs related industry.

Keyword

Perfluorinated compounds (PFCs), industrial wastewater, adsorption, coagulation, synthetic resins, organic coagulants

Table of Content

1. Introduction	1
1.1 Introduction	1
1.2 Research objectives	2
1.3 Dissertation framework	2
2. Literature survey	6
2.1 Introduction	6
2.2 Manmade fluorinated compounds	6
2.3 Applications of PFCs	7
2.4 Occurrence of PFCs	7
2.5 Properties of PFCs	8
2.5.1 Persistence	8
2.5.2 Bioaccumulation	8
2.5.3 Toxicity	9
2.5.4 Physiochemical properties of PFCs	10
2.5.5 Molecular structure of PFCs	12
2.6 PFCs and Stockholm Convention	12
2.6.1 Acceptable purposes	13
2.6.2 Specific exemptions	13
2.7 Treatment of PFCs	13
2.7.1 PFCs removal at conventional water treatment process	13
2.7.2 Membrane filtration	14
2.7.3 PFCs adsorption	15
2.7.4 PFCs oxidation	17
2.7.4 .1 Advanced oxidation processes (AOPs) - Oxygen-containing radicals	17
2.7.4 .2 Persulfate photolysis— Sulfate radical oxidation	19
2.7.4 .3 Direct UV photolysis	21
2.7.4 .4 Phosphotungstic acid photocatalysis	24

3. Ferrate oxidation of PFCs	29
3.1 Introduction	29
3.1.1 Ferrate Oxidation	30
3.1.2 Ferrate production	31
3.1.3 Application of ferrate oxidation in water and wastewater treatment	31
3.1.4 Ferrate oxidation of PFCs	33
3.2 Aims	33
3.3 Experimental method	34
3.3.1.1 Chemicals	34
3.3.1.2 Analytical equipments and methods	34
3.3.1.3 Oxidation tests of PFC	34
3.3.2 Determination of optimum Molar ratio	35
3.3.3 Mixture of PFCs oxidation by ferrate	36
3.4 Results and discussion	37
3.4.1 Oxidation test of PFOA in a ferrate solution	37
3.4.1.1 Stability of PFOA chain	37
3.4.1.2 Oxidation of PFOA by Ferrate	38
3.4.2 CPC oxidation by ferrate - reference study	39
3.4.2.1 Kinetic of TOC reduction by ferrate oxidation	40
3.4.2.2 TOC reduction at the ferrate oxidation of PFOA and CPC	41
3.4.3 Ferrate oxidation of a mixture of PFCs	41
3.5 Summery	44
4. PFCs adsorption (batch experiment)	45
4.1 Introduction	45
4.1.1.Process principle	45
4.1.2 Synthetic Polymer Production	46
4.1.3 Non ion-exchange Resins	47

4.1.4 Ion exchange resins	47
4.1.4.1 Fundamentals of Ion Exchange	47
4.1.4.2 Cation Exchange Resins.	48
4.1.4.2 Anion Exchange Resins.	48
4.1.4.3 Resins Capacity.	48
4.2 Aims and objectives	48
4.3 Experimental Description	49
4.3.1 Materials	49
4.3.2 Material cleaning - Synthetic polymer materials.	50
4.3.3 Material cleaning - Cleaning of GAC.	50
4.3.4 Preparation of PFCs solutions	51
4.4 Experimental methods	51
4.4.1 Experimental apparatus	51
4.4.2 Experimental conditions	52
4.4.2.1 Isotherm experiments with different changing parameters	52
4.4.2.2 Batch test to determine isotherm characteristics of Individual PFCs	52
4.4.2.3 Batch test to examine the applicability of new materials to real wastewater	53
4.4.2.4 Batch test to determine kinetic characteristics.	55
4.5 Modeling and simulation	55
4.5.1 Adsorption isotherms models	55
4.5.2 Kinetics models	57
4.6 Results and Discussion	58
4.6.1 Time required to reach equilibrium concentration	58
4.6.2 Determination of isotherm characteristics with different methodologies	58
4.6.3 Isotherm experiment for individual coagulants with individual PFCs	60
4.6.3.1 Non Ion-Exchange polymers	60

4.6.3.2 Adsorption by ion-exchange polymers	66
4.6.3.3 PFOS adsorption	68
4.6.3.3.1 Adsorption of PFOS onto Granular Activated Carbon	68
4.6.3.3.2 Adsorption of PFOS onto ion-exchange polymers	70
4.6.3.3.3 Adsorption of PFOS onto non ion-exchange polymers	71
4.6.3.3.4 Sorption kinetics of PFOS	72
4.6.4 Adsorption kinetics of non ion-exchange polymers	73
4.6.5 Adsorption kinetics of ion-exchange polymers	77
4.6.6 Batch test with industrial wastewater	77
4.7 Conclusion	81
5. PFCs coagulation	82
5.1 Introduction	82
5.1.1 Inorganic Coagulants	82
5.1.2 Organic Polymers	82
5.1.3 Use and Benefits of organic polymers in Water Treatment	83
5.1.4 Coagulation of anionic particles by cationic polymer coagulants	83
5.2 Aims and Objectives	84
5.3 Materials and Method	85
5.3.1 Materials	85
5.3.2 Jar test	86
5.3.3 Methodology - Experiment 1 (Optimum dosage of organic coagulants)	86
5.3.4 Methodology Experiment 2 (Performance of organic and inorganic coagulants)	87
5.3.5 Methodology Experiment 3 (PFCs coagulation as a mixture)	87
5.3.6 Methodology Experiment 4 (Coagulation of wastewater spike with a mixture of PFCs)	88
5.3.7 Methodology Experiment 5 (Experiment with industrial waste water)	88

5.4 Results and discussion	89
5.4.1 Experiment 1 - Optimum dosage of organic coagulants	89
5.4.2 Experiment 2- Performance of organic and inorganic coagulants	90
5.4.3 Experiment 3 PFCs coagulation as a mixture	91
5.4.3.1 PFCs coagulation by organic coagulants	94
5.4.4 Experiment 4 – Coagulation of wastewater spike with a mixture of PFCs	95
5.4.5 Experiment 5 – Experiment with real waste water	96
5.4.6 The role of filtration in the treatment process.	99
5.4.7 Possible removal mechanism of organic coagulants for PFCs spiked wastewater	99
5.5 Conclusion	101
6. PFOS adsorption (column experiment)	102
6.1 Introduction	102
6.1.1 Key variables for the design of synthetic resin sorbent systems	102
6.1.1.1 Type of synthetic resin	103
6.1.1.2 Background water quality	103
6.1.1.3 Process flow configuration	103
6.1.2 Regeneration of granular materials	104
6.1.2 .1 Steam Regeneration	105
6.1.2 .2 Solvent Regeneration	105
6.1.2 .3 Microwave Regeneration	105
6.2 Aims and objectives	106
6.2.1 Objectives	106
6.3 Methodology	106
6.3.1 Adsorbent Pretreatment	106
6.3.2 Analytical Equipments and Methods for PFOS Determination	107
6.3.3 Column Experiment	107
6.3.4 PFOS regeneration	107

6. 4 Results and discussion	108
6.4.1 Forces effect on adsorption	108
6.4.1.1 PFOS-surface electrostatic interaction	109
6.4.1.2 PFOS-PFOS electrostatic interaction	109
6.4.1.3 Other non-electrostatic interactions.	109
6.4.1. 4 Effect of pH.	109
6.4.1.5 Effect of ionic strength.	110
6.4.2 Overall Performance of the columns with time	110
6.4.2 .1 Dowex L493	111
6.4.2 .2 Amberlite XAD 4	112
6.4.2 .3 Granular Activated carbon	112
6.4.2 .4 Dowex V493	113
6.4.3 Column rest results and Batch test results	113
6.4.4 Mathematical modeling	114
6.4.5 Material regeneration by organic solvents	116
6.5 Summery	119
7. Combined treatment of PFOS	120
7.1 Introduction	120
7.2 Aims and objectives	120
7.3 Methodology	121
7.3.1 Adsorbent Pretreatment	121
7.3.2 Analytical Equipments and Methods for PFOS Determination	121
7.3.3 Column Experiment	121
7.4 Results and discussion	123
7.4.1 Reduction of PFOS by coagulation and filtration process in the combine treatment process	125
7.4.2 Reduction of PFOS by adsorption process in the combine treatment process	126

7.4.3 TOC and PFOS removal	126
7.5 Economic Analysis	128
7.5.1 Objective and Background	128
7.5.2 Assumptions	128
7.5.3 Cost Scenarios	129
7.5.4 Methodology	129
7.5.4.1 Material installation cost	129
7.5.4.2 Material regeneration interval	130
7.5.4.3 Material regeneration cost	130
7.5.5 Results	134
7.5.5.1 Factors affect on cost effectiveness	134
7.6 Summery	135
8. Conclusions and Recommendations	136
8.1 Conclusions	136
8.2 Recommendations	139

List of Figures

Figure 1.1	Scope of the study	4
Figure 1.2	Structure of the thesis	5
Figure 2.1a	Molecular structure PFOS	12
Figure 2.1b	Molecular structure PFOA	12
Figure 3.1	Flow chart of the batch experiments	36
Figure 3.2	Schematic diagram for the batch experimental setup with magnetic stirrer	36
Figure 3.3	Ferrate(VI) degradation of PFOA with time	37
Figure 3.4	Oxidation numbers in PFOA chain	39
Figure 3.5a	The changing rate of TOC with remaining TOC level. (This study)	40
Figure 3.5b	The changing rate of TOC with remaining TOC level (Yong et al (2006))	40
Figure 3.6	Percentage TOC reduction with time for CPC and PFOA	41
Figure 3.7	Ferrate(VI) degradation of PFCs with different initial concentrations and molar ratios	42
Figure 4.1	Schematic diagram of batch test experiment to understand isotherm and kinetic characteristics of different granular materials	52
Figure 4.2	Time requirement for different granular materials to reach equilibrium concentration	59
Figure 4.3	Freundlich isotherm curve drawn with different experimental methods	60
Figure 4.4	Adsorption isotherm of PFDA onto GAC and non ion-exchange polymers	63
Figure 4.5	Adsorption isotherm of PFOA onto GAC and non ion-exchange polymers	64
Figure 4.6	Adsorption isotherm of PFHpA onto GAC and non ion-exchange polymers	64
Figure 4.7	Adsorption isotherm of PFHxA onto GAC and non ion-exchange polymers	65
Figure 4.8	Adsorption isotherm of PFBA onto GAC non ion-exchange polymers	66
Figure 4.9	Adsorption isotherm of PFOA onto ion-exchange polymers	67
Figure 4.10	Adsorption isotherm of PFHxA onto ion-exchange polymers	68
Figure 4.11	Adsorption isotherm of PFOS onto GAC	69
Figure 4.12	Adsorption isotherm of PFOS onto ion-exchange polymers	70
Figure 4.13	Adsorption isotherm of PFOS onto non ion-exchange polymers	71
Figure 4.14	Adsorption Kinetics of PFOS onto GAC, ion-exchange polymers and non ion-exchange polymers and pseudo second-order kinetic curve	73

Figure 4.15	Adsorption kinetics (for initial concentrations 500mg/L and 5000mg/L) for the PFCs of (a) PFBA 5000mg/L, (b) PFBA 500mg/L, (c) PFHpA 5000mg/L, (d) PFHpA 500mg/L, (e) PFDA 5000mg/L, (f) PFDA 500mg/L, and modeling using the pseudo second- order equation.	75
Figure 4.16	Adsorption Kinetics of PFHxA and PFOA onto GAC, ion-exchange polymers and non ion-exchange polymers and pseudo second-order kinetic curve	76
Figure 4.17	Adsorption isotherm of PFOA occurred in PFCs related industrial WW onto ion-exchange polymers, non ion-exchange polymers and GAC	79
Figure 5.1	A diagram to explain conceptual mechanism of PFCs elimination by organic coagulants	84
Figure 5.2	Basic steps involved with Jar test	87
Figure 5.3	percentage PFOA removal with different dose of coagulants	90
Figure 5.4	Percentage PFOA removal with different type of coagulants	91
Figure 5.5	Percentage reduction of each PFCs by various organic and inorganic coagulatnts for MilliQ water spike with a mixture of PFCs	93
Figure 5.6	PFCs with different chain lengths removal by coagulation	94
Figure 5.7	the effect of molecular Wt on PFCs coagulation for organic coagulants	95
Figure 5.8	Percentage reduction of each PFCs by various organic and inorganic coagulatnts for MilliQ water spike with a mixture of PFCs and industrial wastewater spike with a mixture of PFCs	97
Figure 5.9	Percentage reduction of each PFCs by various organic and inorganic coagulatnts for actual PFCs related industial wastewater	98
Figure 5.10	Schematic diagram to explain possible PFCs coagulation mechanism. (a) Mixing (b) attachment (c) rearrangement (d)flocculation	100
Figure 6.1	Column experiment setup for PFOS adsorption onto different filter materials	108
Figure 6.2a	Variation of percentage PFOS removal with time (60 days) for different filter materials in the column experiment	110
Figure 6.2b	Variation of effluent PFOS concentration with operation time and filtered bed volume	111
Figure 6.3	Fractional effluent PFOS concentration in the column with DOW L493	111
Figure 6.4	(a) Fractional effluent PFOS concentration in the column with Amb XAD 4; (b) Basic structure of Amb XAD 4;	112
Figure 6.5	Fractional effluent PFOS concentration in the column with F400	113

Figure 6.6	Fractional effluent PFOS concentration in the column with DOW V493	113
Figure 6.7	Schematic representative of a column for modeling	
Figure 6.8	Linear plot of t vs. $\ln[C/(C_0-C)]$ (a) and comparison of the observed and predicted breakthrough curves (b) of PFOS adsorption in columns with different filter materials.	119
Figure 6.9	Variation of cumulative PFOS accumulation on various filter materials with time	120
Figure 6.10	Variation of percentage PFOS recovery with time by organic solvent	119
Figure 7.1	Schematic diagram of the experimental setup for combined treatment processes	122
Figure 7.2	Percentage PFOS removal with time by adsorption process and combined coagulation and adsorption process for non ion exchange filter materials.	123
Figure 7.3	schematic diagram to explain the combined treatment process	124
Figure 7.4	Percentage PFOS removal with time by coagulation and filtration process	125
Figure 7.5	Percentage PFOS removal by adsorption (with and without coagulation process)	126
Figure 7.6	Variation of TOC in the effluent of each column at the combine treatment process	127

List of Tables

Table 2.1	Basic information of PFCs considered in this study	11
Table 2.2	Basic physiochemical properties of PFCs	11
Table 2.3	Summary of previous studies on materials to adsorb PFOS	18
Table 2.4	Summary of previous studies on materials to adsorb PFOA	18
Table 2.5	Summary of previous studies on PFOA degradation	25
Table 2.6	Summary of previous studies on PFOS degradation	27
Table 3.1	Oxidation potential of common oxidants	31
Table 3.2	Ferrate oxidation of various organic compounds	33
Table 3.3	Summary of the conditions for experiments	35
Table 3.4	Bond energies in PFOA molecule	39
Table 3.5	Summarized results of ferrate oxidation of PFCs	43
Table 4.1	Physical properties of non ion-exchange polymers	49
Table 4.2	Physical properties of ion-exchange polymers	49
Table 4.3	Physical properties of GAC (Filtersorb 400, coal based)	50
Table 4.4	Experiment condition for sorption isotherm experiment	53
Table 4.5	Different sorbent-sorbate combinations considered for individual batch experiments to determine the characteristics of sorption isotherms kinetics	53
Table 4.6	Experiment condition for sorbent-sorbate combination (Table 4.4) for the sorption isotherm experiment-2	54
Table 4.7	Experiment condition for sorption isotherm for industrial wastewater	54
Table 4.8	Experiment condition for sorbent-sorbate combination (Table 4.5) for the sorption kinetic experiment	55
Table 4.9	summary of adsorption isotherm models developed with various assumptions	56
Table 4.10	Freundlich constants for different sorbent/ sorbate combinations and calculated q_c for different C_e (ng/L) based on K_f and n values	62
Table 4.11	Freundlich constants for different sorbent/ sorbate combinations and calculated q_c for different C_e (ng/L) based on K_f and n values	67
Table 4.12	Freundlich constants for PFOS with different adsorbents and calculated q_c for different C_e (ng/L) based on K_f and n values	72
Table 4.13	Pseudo-second-order kinetic parameters for different non ion-exchange sorbent/ sorbate combinations	76

Table 4.14	Pseudo-second-order kinetic parameters of PFHxA, PFOA and PFOS with different ion-exchange, non ion-exchange and GAC	77
Table 4.15	Initial PFCs concentration of the wastewater	78
Table 4.16	adsorption characteristics of different filter materials with PFCs related industrial Wastewater	80
Table 5.1	Commonly used inorganic coagulants	83
Table 5.2	Physico chemical properties of organic coagulants used in the experiment	85
Table 5.3	Physico chemical properties of inorganic coagulants used in the experiment	86
Table 5.4	Summary of the experimental conditions	89
Table 5.5	Levels of PFCs in the wastewater used in this study	96
Table 6.1	Design flow rats for some GAC filters available in the market	104
Table 6.2	The basic steps involve with GAC regeneration	104
Table 6.3	Parameters of the theoretical model proposed by Lin and Huang (Lin and Hung 1999) for a column experiment for PFOS adsorption onto different filter materials.	116
Table 7.1	Experimental conditions for combined treatment process	123
Table 7.2	Cost of Granular Materials	129
Table 7.3	Drop of PFOS removal efficiencies with time	130
Table 7.4	Results of economic analysis for three times material regenerations	133
Table 7.5	Results of economic analysis for five times material regenerations	131
Table 7.6	Results of economic analysis for eight times material regenerations	133

Abbreviation

AC	activated carbon	PFBuS	perfluorobutane sulfonate
AFFF	aquous fire fighting foam	PFCA	perfluorocarboxylates
Amb XAD 4	Amberlite XAD 4	PFCs	perfluorochemicals
AOPs	advanced oxidation processes	PFDA	perfluorodecanoic acid
BP	bottle-Point experiment	PFHpA	perfluoroheptanoic acid
C-F	carbon-fluorine bond	PFHxA	perfluorohexanoic acid
Dow L493	Dowex Optipore L493	PFHxS	perfluorohexane sulfonate
Dow V493	Dowex Optipore V493	PFNA	perfluorononanoic acid
Dow V503	Dowex Optipore V503	PFOA	perfluorooctane acid
ESI	electrospray ionization	PFOS	perfluorooctane sulfonate
F400	Calgon filtratorb 400	PFPeA	perfluoropentanoic acid
GAC	granular activated carbon	PFTeDA	perfluorotetradecanoic acid
LC	liquid chromatograph	PFUnA	perfluoroundecanoic acid
MS/MS	tandem mass spectrometer	POPs	persisted organic pollutants
MTBE	methyl t-butyl ester	RE	removal efficiency
PBT	Persistence, bioaccumulation and toxicity	RO	reverse osmosis
PD	pore diffusion	SF	sand filtration
PFAS	perfluoroalkyl sulfonates	UV	ultra violet
PFBA	perfluorobutyric acid	WWTP	wastewater treatment plant

Chapter 1 Introduction

1.1 Introduction

Industrialization and technological development processes have led to the introduction of new hazardous chemicals into the water environment. Most of these chemicals are synthesized with unique characteristics for a specific application, but ultimately those contribute to pollute water environment. Perfluorinated compounds (PFCs) are such tracer level emerging water pollutants, which are synthesized by replacing all C-H bonds of a hydrocarbon by C-F bond. The C-F bond is the strongest bond in organic chemistry and fluorine always prefers to have -1 oxidation state. The ultimate result of replacing all C-H bonds by C-F bond in the synthesis process is a PFCs molecule with polarity, (negatively charged) which is strong, difficult to oxidize and sustainable in the environment (O'Hagan., 2008).

The exact toxicity of each PFCs for human being is still unclear. Some researchers have reported adverse health effects of some PFCs. Perfluorooctane Sulfonate (PFOS) were recently categorized as a POP by the Stockholm convention (Earth 2009).

On the other hand, development in instrumental chemistry has facilitated the measurement of new pollutants more accurately at low concentrations. Both tap water and discharge industrial wastewater quality standards are expanding into wider spectrum of parameters. As emerging persistent toxic pollutants, PFCs are now discussed to include drinking water quality parameters and researchers are working on how to treat them at water and wastewater purification plants.

Researchers have already identified that conventional tap water and wastewater purification plants could not remove PFCs (Fujii *et al*, 2007 and Takagi *et al*, 2008). Previous studies have identified adsorption as an effective process to eliminate PFCs from water. Different kind of granular activated carbon (GAC), some ion-exchange resins, high silica zeolite, and anaerobic sludge have been tested to evaluate the PFCs adsorption capacity (Qiang *et al*. 2009; Ochoa-Herrera *et al*. 2008). In general, PFCs treatment research has been limited for unrealistic PFCs concentrations at mg/L levels.

The overall objective of this research was to investigate on possible PFCs treatment techniques. The research was limited for wastewater as it was identified as the main PFCs polluter. **Figure 1.1** shows the flow of PFCs through different treatment processes and this research studied some physico-chemical treatment processes for PFCs elimination. The main

objectives of this study can be summarized as;

1.2 Research objectives

1. To study the oxidation characteristics of PFCs by ferrate techniques.
2. To determine the PFCs adsorption characteristics of ion-exchange polymers, non ion-exchange polymers and activated carbon while establishing a methodology for the batch experiment.
3. To simulate the real application of selected polymers by a long run column experiment to adsorb PFCs.
4. To identify possible candidate coagulants to eliminate PFCs for wastewater treatment process.
5. To examine the improvement of adsorption process by prior coagulation with organic coagulants.

A main part of this study was dedicated to investigate the PFCs adsorption characteristics of non ion-exchange polymers, ion-exchange polymers and granular activated carbon at low concentrations. Seven synthetic polymer materials and one GAC material were investigated in this study. Both batch experiments (with shaking time of 100 hrs) and column experiments (operation time of 100 days) were conducted to determine sorption isotherms, sorption kinetics and the applicability in the field. Out of the eight materials investigated in this study, six materials were tested for the first time for PFCs and the experiment conditions were set such that it simulates real ground situation with low PFCs concentrations.

Since the PFCs are negatively charged, long chain polymeric cationic coagulants were tested and results were compared with the conventional inorganic coagulants for PFCs elimination.

The individual positive results obtained for adsorption and coagulation were combined at the latter part of the study and the effect on adsorption by coagulation was observed.

1.3 Dissertation framework

This dissertation consists of eight chapters. Overall content of the thesis is schematically shown in **Figure 1.2**.

Chapter 1 gives a brief introduction of this research, including research background, objectives and dissertation structures.

Chapter 2 reviews current available literature on PFCs, mainly recent developments on treatment of PFCs and management strategies to control PFCs.

Chapter 3 describes ferrate oxidation of PFCs. PFCs oxidation by conventional oxidants in water and wastewater treatment is already known. Ferrate has been identified as an emerging oxidative agent to apply in water and wastewater purification industry with highest redox potential among all conventional oxidants. This study was conducted as there is no prior data available for PFCs oxidation by ferrate.

Chapter 4 shows the characteristics of PFCs adsorption onto polymers. Batch experiments were conducted to obtain adsorption isotherms and kinetics for eight granular materials including ion-exchange polymers, non ion-exchange polymers and GAC. Published data on the six polymers tested is very limited. Freundlich equation and pseudo second-order model were successfully applied to explain isotherm and kinetic data.

Chapter 5 shows coagulation of PFCs. A comparative study of polymer type organic coagulant and conventional inorganic coagulants was carried out in a series of Jar tests. Six organic coagulants and three conventional inorganic coagulants were used in the study. Published data on PFCs coagulation by organic coagulants is rarely available.

Chapter six is dedicated for the column experiment with non ion-exchange polymers. The polymers used in this experiment were selected by the results of Chapter 5. A set of columns with four non ion-exchange granular materials were continuously run for sixty days. After the experiment, the same materials in the columns were used to determine the PFOS regeneratability by organic solvents.

Chapter 7 explains combine treatment of PFCs (Adsorption + Coagulation). A treatment process of coagulation followed by adsorption was simulated by a lab scale model and it was continuously run for 130 days. The combined performance was compared with the individual performances as obtained in Chapter 5 and Chapter 6. Later part of the chapter is reserved for economical analysis for synthetic polymers and GAC.

Chapter 8 gives conclusions of this study and recommendations for further research.

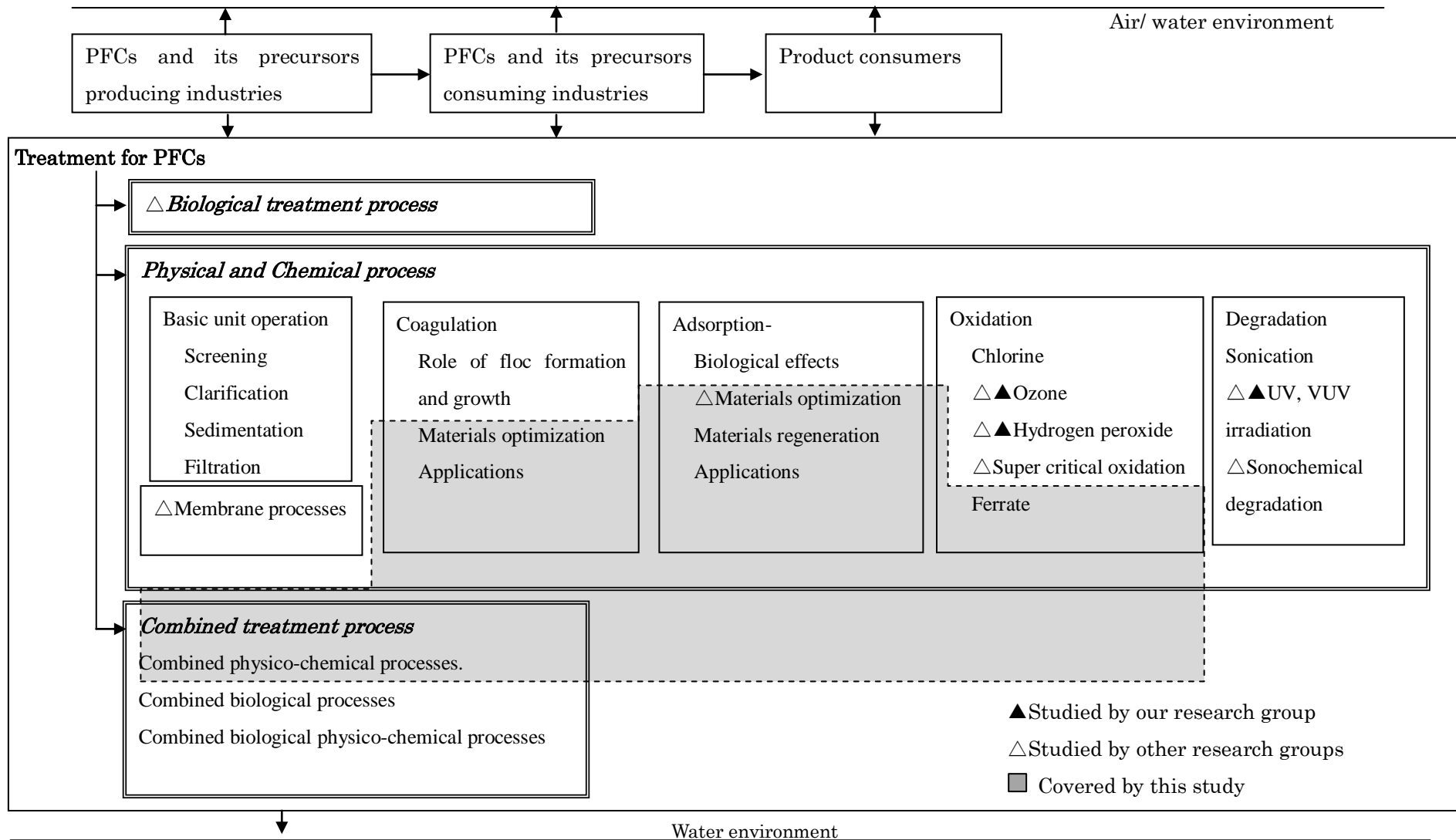


Fig. 1.1 Scope of the study

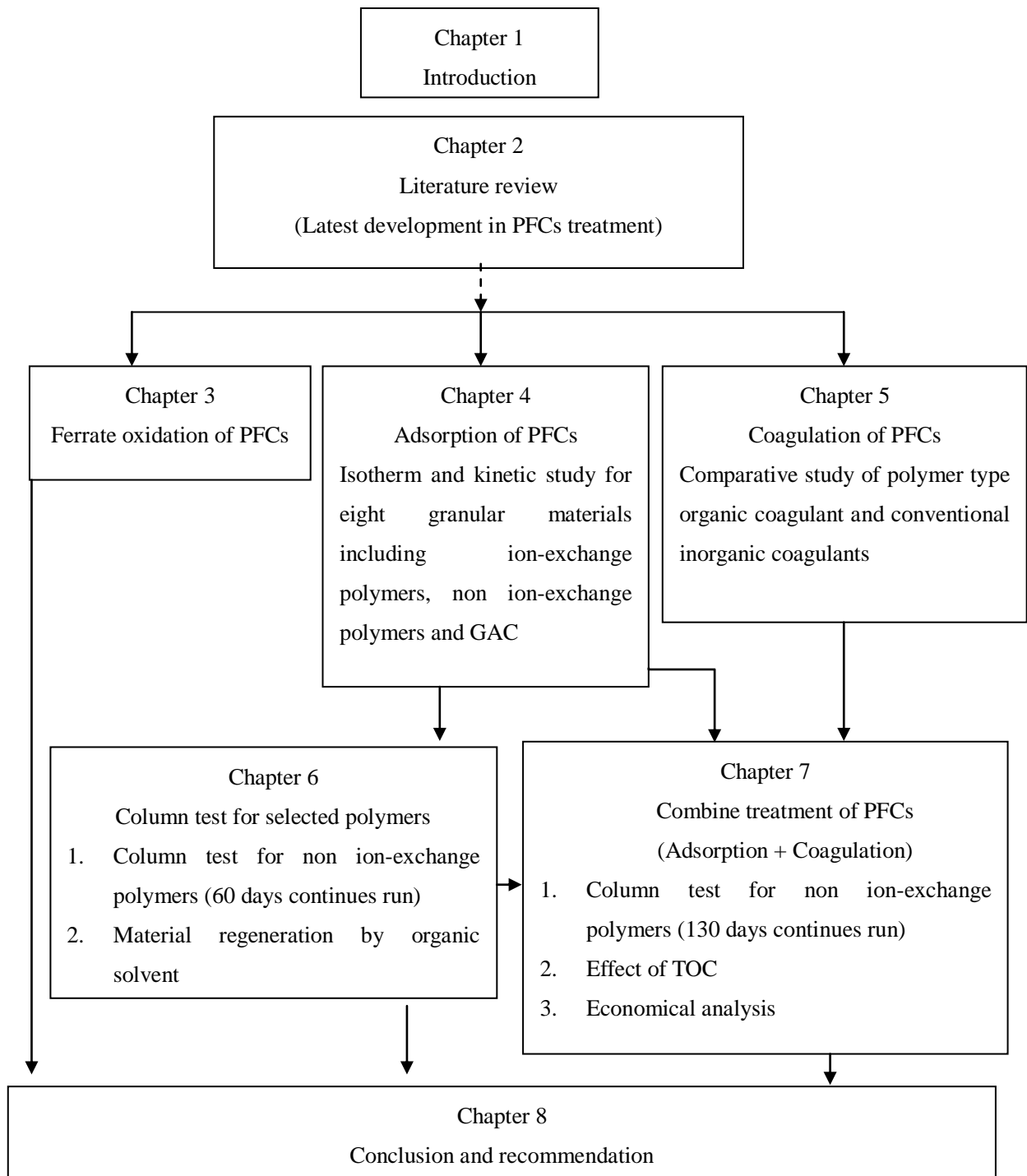


Fig. 1.2 Structure of the thesis

Chapter 2 Literature survey

2.1 Introduction

The entire story in this study begins with the carbon–fluorine bond which is a common component of all PFCs. This bond is the strongest bond in organic chemistry. The length of the carbon–fluorine bond is typically about 1.35 angstrom (1.39 Å in fluoromethane), which is shorter than any other carbon–halogen bonds, and shorter than carbon–nitrogen and carbon–oxygen bonds. The short length of the bond can also be attributed to the ionic or electrostatic attractions between the partial charges on carbon and fluorine. The bond also strengthens and shortens as more fluorines are added to the identical carbon on a chemical compound. The high electronegativity of fluorine (4.0 for F vs. 2.5 for C) gives the carbon–fluorine bond a significant polarity/dipole moment. The electron density is concentrated around the fluorine, leaving the carbon relatively electron poor. This introduces ionic character to the bond through partial charges ($C\delta^+—F\delta^-$). The partial charges on the fluorine and carbon are attractive, contributing to the unusual bond strength of the carbon–fluorine bond (O'Hagan, 2008). Carbon–fluorine bonds can have a bond dissociation energy (BDE) of up to 130 kcal/mol (Lemal, 2004). The BDE is higher than other carbon–halogen and carbon–hydrogen bonds. For example, the molecule represented by CH_3X has a BDE of 115 kcal/mol for carbon–fluorine while values of 104.9, 83.7, 72.1, and 57.6 kcal/mol represent carbon–X bonds to hydrogen, chlorine, bromine, and iodine, respectively (Blanksby and Ellison, 2003). The ultimate result of all the characteristics is a strong polar organic compound of PFCs, which is persistent in environment and toxic to the living beings.

2.2 Manmade fluorinated compounds

There are about 30 natural organofluorine molecules in the environment (Hekster et al., 2003). These molecules contain only one fluorine atom per molecule. In contrast, man-made fluorinated organic compounds often contain many fluorine atoms, thus they are called polyfluorinated (Key et al. 1997). In perfluorinated compounds (PFCs), all the carbon–hydrogen bonds are replaced with carbon–fluorine bonds (Renner, 2001) except one bonding site at the end of chain. PFCs are composed of a carbon–fluorine chain and generally have side moieties attached such as carboxylic acids or sulfonic acids (Giesy and Kannan 2002). The strong carbon–fluorine bond in PFCs gives thermal and chemical stability to many PFCs (So et al., 2004). The stability that makes fluorinated

compounds desirable for commercial use also makes them potentially significant environmental contaminants due to their resistance to natural breakdown processes, that is, their persistence (Key et al., 1997). Research over the past few years has shown that the PFCs are now widespread environmental contaminants and found in living organisms globally.

2.3 Applications of PFCs

PFCs are manufactured because of their specific physical and chemical properties such as chemical and thermal inertness and special surface-active properties (Hekster et al., 2003). They repel both water and oil and act as surfactants, that is, they reduce surface tension and do so better than other surfactants. These properties have led to the use of perfluorinated compounds in a wide variety of applications. For instance, their unique properties of repelling both water and oil has led to their use as coatings for carpet protection, textile protection, leather protection, and paper and board protection. They are also used in firefighting foams and as polymerisation aids. In addition they are used as speciality surfactants, for example, in cosmetics, electronics, etching, medical use and plastics (Hekster et al., 2003, So et al., 2004). They are also widely employed in different industrial processes such as wiring insulation for telecommunications, aerospace, electronics (semiconductors), and medical use (Martin et al., 2004b; Prevedouros et al., 2006). In particular, PFOA is used as adjuvant in the production of fluoropolymers such as PTFE, Teflon or similar products, and occurs in these applications as aqueous and gaseous process emission (Fricke and Lahl, 2005; Davis et al., 2007). Point source manufacturing facilities of fluorochemicals are one of the largest sources of emissions for PFCs (Prevedouros et al., 2006; Davis et al., 2007).

2.4 Occurrence of PFCs

PFCs, especially PFOS and PFOA, have been found in surface waters in Japan (Saito et al., 2004), USA (Hansen et al., 2002; Boulanger et al., 2004, 2005), and Europe (Skutlarek et al., 2006; Loos et al., 2007; McLachlan et al., 2007). PFOA has been found in relatively high concentration levels near fluorochemical manufacturing facilities in USA, (500 ng/L) in the Tennessee River (Hansen et al., 2002), in the Ohio River (Davis et al., 2007), and in Germany up to 56ng /L in the River Alz (near a fluorochemical factory). In addition, it has been found in drinking waters, up to 519 ng/L in Germany (Schaefer, 2006; Skutlarek et al.,

2006) and in ground water near the Ohio River, USA (Davis et al., 2007). Moreover, PFOS and PFOA have also been analyzed in ocean waters with detected concentrations up to 100 pg /L and marine mammals (Kannan et al., 2002; Yamashita et al., 2004, Haukas et al., 2007). An OECD hazard assessment from the year 2002 (OECD, 2002) identified PFOS as a PBT-chemical (persistent, bioaccumulative, toxic). In December 2006, the European Parliament and the Council decided to restrict marketing and use of PFOS with a few exceptions by amending Council Directive 76/769/EC on dangerous substances for PFOS (European Commission, 2006). It is currently being discussed if PFOA should be included in this Directive. In addition, it is investigated to introduce PFOS and PFOA as so-called priority substances regulated by the Water Framework Directive (WFD).

2.5 Properties of PFCs

2.5.1 Persistence

3M Company published its reports on hydrolysis and aqueous photolytic degradation (Hatfield, 2001) of PFOA, which showed rather long half-life times in natural environment. PFOS also showed its resistance to advanced oxidation processes including ozone, ozone/UV, ozone/H₂O₂ and Fenton reagent (Schröder and Meesters, 2005). Also it has been reported that almost all PFCs had no response to oxidation by chromium potassium oxide (Cr₂O₇²⁻) or potassium permanganate acid (MnO₄⁻), which confirmed their stabilities in critic environment.

2.5.2 Bioaccumulation

K_{ow}, known as partition coefficient between octane and water phases, is useful to estimate bioaccumulation potentials. However, it is not available for most of PFCs because PFCs are surfactants and third layer is formed during measurement (OECD, 2002; US EPA, 2002). Bioaccumulation factors (BAFs) or bioconcentration factors (BCFs) are calculated by dividing the average concentrations in organism by the concentrations in water environment. BAFs represent accumulation potentials of organics from environment to organisms.

Previous researchers have reported that their preliminary study showed dietary BAFs of PFOS were 2,796 in bluegill sunfish and 720 in carp (OECD,

2002) respectively. BAFs of PFOA were about 2 in fathead minnow and 3~8 in carp, which are quite lower than PFOS. First survey of PFOS in Japan showed quite high BAFs of PFOS to fishes in Tokyo Bay, which were as high as 1,260~19,950 (Taniyasu, et al., 2002). Survey in Great Lakes has also shown that BAFs of PFOS is about 1,000 for benthic invertebrates (Kannan, et al., 2005). Another research in Ai river of Japan showed rather high BAF of PFOS in wild turtles as 10,964 and very low BAF of PFOA equal to 3.2. Similar situation occurred for rainbow trout under synthetic PFCs spiking waters. Dietary BAFs of PFCAs have ranged from 0.038 to 1.0, while BAFs of PFASs have ranged from 4 to 23,000, both increased with length of carbon chain (Martin, et al., 2003). The research on lake trout in Great Lakes in North America also showed similar trend of increasing BAFs by carbon chain length. BAFs of PFCA showed linear increase from 3.2 to 3.9, while BAFs of PFAS changed from 500 to 12,600 (Furdui, et al., 2007). Increase of BAFs by ascendant PFCs carbon chain length indicated that long-chained PFCs or more hydrophobic PFCs had stronger bioaccumulative potentials and bioconcentration levels. Furthermore, BAFs of PFASs were greater than PFCAs in equivalent carbon chain length, which indicated that acid function groups also played important role to determine accumulation potentials.

Biomagnification factors (BMFs) are calculated by dividing the average concentrations in predators to those in preys. BMFs can be applied to estimate accumulation potentials of organics in food chains. One study in Great Lakes reported BMF of PFOS to be 10~20 for mink or bald eagles to their prey items (Kannan, et al., 2005). Another survey of US coastal marine food chain showed that BMFs of bottlenose dolphin are 0.1-13.0 for PFCA and 0.8~14 for PFAS, which were also increased by ascendant carbon chain length (Houde, et al., 2006). It can be concluded that BMFs of PFCs were around 10 in aquatic ecosystems.

2.5.3 Toxicity

Since PFCs differ from normal lipophilic toxic substances, their toxicokinetics is still unknown in mechanism and need more studies to elucidate the profile. Although a lot of researches have been conducted on the toxicity of PFCs, the results were in diverse qualities. Generally, medium and long-chained PFCs may be more toxic than short-chained ones by their longer

half life in rodents. Review on PFOS toxicity showed that subchronic exposure led to significant weight loss accompanied by hepatotoxicity, and reductions of serum cholesterol and thyroid hormones (OECD, 2002). Reviews also revealed the influence of PFOS on generations of laboratory rodents (Lau, et al., 2003; Thibodeaux, et al., 2003) and on human birth in Japan (Inoue, et al., 2004a).

US EPA reviewed studies on toxicity of PFOA, which showed diverse behavior between gender and generations of laboratory animals. Average half life of PFOA in human body was estimated to be 4.37 years (US EPA, 2003). PFOA behaved in different ways between species and sexes due to renal clearance, and undergoes enterohepatic circulation. However, it was also reported that PFOA can be eliminated and detoxified in the human body (Kudo and Kawashima, 2003). Pharmacokinetic profiles of PFOA in the adults may be different from those in sexually immature rats (Lau, *et al.*, 2004).

Studies on toxicity of PFCs other than C8 were still very few. PFBuS has much shorter half-life time than PFOS, therefore seems less toxic. PFHxS was detected in human serum in similar level of PFOA and 10 times less than PFOS (verbal communication with US-EPA). Both PFNA and PFDA were peroxisome proliferators, and PFDA has longer half-life time in rats and shows quite high toxic potency (Lange, *et al.*, 2006). Pharmacokinetic and structure-activity studies on the relationship between toxicity and carbon chain length would arouse interests of toxicologists in future.

2.5.4 Physiochemical properties of PFCs

PFCs are either in liquid form or in solid form depending on the chain length. They are heavier than water and miscible with most organic solvents (ethanol, acetonitrile, methanol). They have relatively low solubility in water, and water has a very low solubility in them. The number of carbon atoms in a PFCs molecule largely determines most physical properties. The greater the number of carbon atoms, the higher the boiling point, density, viscosity, surface tension, critical properties, vapor pressure and refractive index. Some physical properties of PFCs considered for this study is shown in **Table 2.1 and 2.2**.

Table 2.1 Basic information of PFCs considered in this study

Abbr. name	Full name	Molecular Structure	m.w	CAS No.
PFBA	Perfluorobutyric Acid	$\text{CF}_3(\text{CF}_2)_2\text{COOH}$	214	375-22-4
PFHxA	Perfluorohexanoic Acid	$\text{CF}_3(\text{CF}_2)_4\text{COOH}$	314	307-24-4
PFHpA	Perfluoroheptanoic Acid	$\text{CF}_3(\text{CF}_2)_5\text{COOH}$	364	375-85-9
PFOA	Perfluorooctane Acid	$\text{CF}_3(\text{CF}_2)_6\text{COOH}$	414	335-67-1
PFDA	Perfluorodecanoic Acid	$\text{CF}_3(\text{CF}_2)_8\text{COOH}$	514	335-76-2
PFOS	Perfluorooctane Sulfonate	$\text{CF}_3(\text{CF}_2)_7\text{SO}_3$	500	2795-39-3

Abbr.name – Name abbreviated m.w – molecular weight

Table 2.2 Basic physiochemical properties of PFCs

PFCs	pK_a^a	Melting point ^b C°	Boiling point ^c C°	Specific Gravity	Texture
PFBA			120.8-121.0	1.65	yellow liquid
PFHxA			159-160	1.76	clear liquid
PFHpA			175	1.79	crystalline
PFOA	2.50	55-56, 37-50	189	1.70	white powder
PFDA		83-85, 88	218		white powder
PFOS	3.27	>400, 277		2.05	white powder

Note: *a* = PFOA (OECD, 2002), PFOS (US EPA, 2002); *b* = melting point, data from material safety data sheet (MSDS) of Wako Company and ExFluor Company; *c* = boiling point, from ExFluor MSDS.

2.5.5 Molecular structure of PFCs

PFCs molecules consist of a perfluorinated carbon chain and one special functional group at a corner of the chain. This functional group is either carboxylic or sulfonic group (**Figure 2.1a,b**). Fully fluorinated carbon chain of



Fig 2.1.a molecular structure PFOS Fig 2.1.b molecular structure PFOA

the PFCs makes it hydrophobic and functional group at the end makes PFCs hydrophilic. Different hydrophilic functional groups show diverse behavior in aqueous environment. The perfluorinated tail is covered by strongest C-F bonds, and surrounded by fluorine atoms which have similar size with the carbon atom.

2.6 PFCs and Stockholm Convention

The Stockholm Convention on Persistent Organic Pollutants (POPs) is a global treaty to protect human health and the environment from chemicals that remain intact in the environment for long periods, become widely distributed geographically and accumulate in the fatty tissue of humans and wildlife. This convention was adopted in 2001 and entered into force in 2004. By signing this convention the parties agree to take measures to eliminate or reduce the release of POPs into the environment. The Convention is administered by the United Nations Environment Programme and is based in Geneva, Switzerland.

A separate committee has been established (POPRC) as a subsidiary body to the Stockholm Convention for reviewing new chemicals. One of the known PFCs of PFOS was reviewed by the 4th POPs review committee and recommended to categorized it as a POPs (<http://chm.pops.int/Convention/POPsReviewCommittee/hrPOPRCMeetings/POPRC4/POPRC4ReportandDecisions/tabid/450/language/en-US/Default.aspx>).

This recommendation was seriously considered at the fourth meeting of the Conference of the Parties (COP4) to the Stockholm Convention and decided to amend part I of Annex B of the Convention to list perfluorooctane sulfonic acid (PFOS), its salts and perfluorooctane sulfonyl fluoride with the acceptable purposes and specific exemptions (decision SC-4/17).

2.6.1 Acceptable purposes

Eventhough PFOS was categorized as a POPs by the Stockholm convention, provision was given to further use of PFOS for the following applications. Photo-imaging, photo-resist and anti-reflective coatings for semi-conductor, etching agent for compound semi-conductor and ceramic filter, aviation hydraulic fluids, metal plating (hard metal plating) only in closed-loop systems, certain medical devices (such as ethylene tetrafluoroethylene copolymer (ETFE) layers and radio-opaque ETFE production, in-vitro diagnostic medical devices, and CCD colour filters), fire-fighting foam, insect baits for control of leaf-cutting ants from *Atta* spp. and *Acromyrmex* spp.

2.6.2 Specific exemptions

A special exemption was given to use PFOS for the following application by Stockholm convention. Photo masks in the semiconductor and liquid crystal display (LCD) industries, metal plating (hard metal plating, decorative plating), electric and electronic parts for some color printers and color copy machines, insecticides for control of red imported fire ant, and termites, chemically driven oil production, carpets, leather and apparel, textiles and upholstery, paper and packaging, coatings and coating additives, rubber and plastics.

2.7 Treatment of PFCs

2.7.1 PFCs removal at conventional water treatment process

Few researchers have already reported a positive correlation between the PFOS concentration in raw water and tap water samples suggesting minimum removal efficiency at conventional water purification systems (Fujii et al, 2007; and Takagi et al, 2008).

Ground water and drinking water around a Teflon manufacturer in Virginia, USA was found to be contaminated with PFOA up to 10 µg/L (ENDS 2004).

Drinking water samples in Japan were contaminated at maximum concentration of 40 ng/L for PFOA in Osaka area (Saito et al. 2004) and at about same level for PFOS in Tokyo. Both authors indicated that the sources of tap water were from surface water which was contaminated at the same levels of PFOS and PFOA concentration. A study of surface water and tap water in Ruhr (Germany) (Skutlarek et al. 2006) found drinking water contamination up to 519 ng/L for PFOA and 22 ng/L for PFOS. Also there is published data to show that the concentrations found in drinking waters decreased with the concentrations of the corresponding raw water samples along the flow direction of the Ruhr river (from east to west) and were not significantly different from surface water concentrations. This indicates that perfluorinated surfactants are at present not successfully removed by water treatment steps. By measuring concentrations in tap water and surface water in an area of Germany, Skutlarek et al. revealed that perfluorinated surfactants are at present not successfully removed by water treatment steps (Skutlarek et al. 2006).

Dr Lien, a researcher worked with our research team also reported the same observation of similar PFOS levels in tap water and surface water in a given area. She reported that her case study in Kinki Region (Japan) and Istanbul (Turkey) had demonstrated similar levels of both PFOS and PFOA in tap water to those of water supply sources and these results suggested that PFOS and PFOA, at the levels of several ng/L to several tens ng/L were not effectively removed through water treatment steps.

2.7.2 Membrane filtration

Tang et al. (2006) investigated the feasibility of using reverse osmosis (RO) membranes for treating semiconductor wastewater containing PFOS. They reported that the RO membranes generally rejected 99% or more of the PFOS (feed concentrations 0.5 - 1500 ppm). Also they found that the rejection was better for tighter membranes, but was not affected by membrane zeta potential. Flux decreased with increasing PFOS concentration.

E. S. Darling and M. Reinhard (2008) measured the rejections of 15 perfluorochemicals (PFCs), five perfluorinated sulfonates, nine perfluorinated carboxylates, and one perfluorooctane sulfonamide (FOSA)s by four nano filtration membranes (NF270, NF200, DK, and DL). They reported that the rejections for anionic species were >95% for MW > 300 g/mol. FOSA (MW 499 g/mol), which is uncharged at the pH of deionized water (5.6), was rejected as

little as 42% (DL membrane). Lowering the pH to less than 3 reduces rejection by up to 35%. An alginate fouling layer increases transmission by factors of 4-8. Based on rejection kinetics and the extent of sorption, they suggested that two different sorption processes are significant: charged species adsorb quickly to the membrane surface, whereas the uncharged species adsorb within the membrane matrix in a much slower process.

2.7.3 PFCs adsorption

In 2007, our research group has investigated (Yong 2007) the adsorption characteristics of PFCs onto GAC by batch experiments and the results had been interpreted by the Freundlich equation and homogenous surface diffusion model (HSDM). Isothermal and kinetics experiments have implied that PFCs adsorption onto GAC was directly related with their carbon chain lengths. By ascending the carbon chain length, adsorption capacity for specific PFC had been increased, and diffusion coefficient (D_s) decreased. D_s of GAC adsorption had been decreased gradually in smaller GAC diameters. Coexisted natural organic matters (NOMs) have reduced adsorption capacities by mechanisms of competition and carbon fouling.

It was found that Carbon fouling reduces the adsorption capacity much more intensively than by organics. Acidic bulk solution was slightly helpful for adsorption of PFCs. However adsorption velocity or kinetics was affected by NOM and pH significantly. GAC from Wako Company has showed the best performance among four kinds of GACs, and Filtra 400 from Calgon Company has considered more suitable to removal all PFCs among the commercial GACs. The results implied that background organics broke through fixed GAC bed much earlier than trace level of PFCs. Medium-chained PFCs was found to be effectively removed by fixed bed filtration without concerning biological processes.

Valeria and Reyes (2008) have evaluated the three anionic PFC surfactants, i.e., perfluorooctane sulfonate (PFOS), perfluorooctanoic acid (PFOA) and perfluorobutane sulfonate (PFBS), for the ability to adsorb onto activated carbon. Additionally, the sorptive capacity of zeolites and sludge for PFOS was compared to that of granular activated carbon. They determined the adsorption isotherms at constant ionic strength in a pH 7.2 phosphate buffer at 30°C. They reported that the sorption of PFOS onto activated carbon was stronger than PFOA and PFBS, suggesting that the length of the fluorocarbon chain and the

nature of the functional group influenced sorption of the anionic surfactants. Among all adsorbents evaluated in their study, activated carbon (Freundlich K_f values = 36.7-60.9 [(mg PFOS/g sorbent)(mg PFAS/l)⁻ⁿ]) showed the highest affinity for PFOS at low aqueous equilibrium concentrations, followed by the hydrophobic, high-silica zeolite NaY (Si/Al 80, K_f = 31.8[(mg PFOS/g sorbent)(mg PFAS/l)⁻ⁿ]), and anaerobic sludge (K_f = 0.9-1.8[(mg PFOS/g sorbent)(mg PFAS/l)⁻ⁿ]). Activated carbon also displayed a superior sorptive capacity at high soluble concentrations of the surfactant (up to 80 mg /L). These findings indicate that activated carbon adsorption is a promising treatment technique for the removal of PFOS from diluted aqueous streams.

Qiang Yu et al., (2009) have investigated the feasibility of using powdered activated carbon (PAC), granular activated carbon (GAC) and anion-exchange resin (AI400) to remove PFOS and PFOA from water, with regard to their sorption kinetics and isotherms. They have reported that the adsorbent size greatly influenced the sorption velocity, and both the GAC and AI400 required over 168 hrs to achieve the equilibrium, much longer than 4 hrs for the PAC. They have adopted kinetic models to describe the experimental data, and the pseudo-second-order model well described the sorption of PFOS and PFOA on the three adsorbents. The sorption isotherms have showed that the GAC had the lowest sorption capacity both for PFOS and PFOA among the three adsorbents, while the PAC and AI400 possessed the highest sorption capacity of 1.04 mMol g/L for PFOS and 2.92 mMol g/L for PFOA according to the Langmuir equation. Based on the sorption behaviors and the characteristics of the adsorbents and adsorbates, they have concluded that ion exchange and electrostatic interaction as well as hydrophobic interaction were involved in the sorption, and some hemi-micelles and micelles possibly formed in the intraparticle pores.

But in real scale application it is reported that the usage of activated carbon to ensure the removal of perfluorinated surfactants is not effective. In some German water treatment plants with carbon filters has shown poor performances to eliminate PFCs. (Schaefer et al.,2006). **Table 2.3** and **Table 2.4** show the summary of studies done to evaluate different materials to eliminate PFCs, mainly PFOS and PFOA.

2.7.4 PFCs oxidation

PFCs are recalcitrant towards oxidation due to the complete substitution of fluorine (C-F bond) for hydrogen (C-H bond). Fluorine will retain its electrons at any cost. Fluorine is nearly always found in the (-1) valence state with the only exception being F₂ where its oxidation state is (0). The fluorine atom is the most powerful inorganic oxidant known with a reduction potential of 3.6 V (Eq. 1.1) (Wardman, 1989) and thus is thermodynamically unfavorable to create the fluorine atom with any other one-electron oxidant.



Perfluorination will also reduce the oxidizability of the ionic headgroup (SO₃⁻ for PFOS and CO₂⁻ for PFOA) since it inductively reduces headgroup electron density. Thus PFCs are quite resistant to oxidation as compared with their alkyl analogs.

2.7.4.1 Advanced oxidation processes (AOPs) - Oxygen-containing radicals

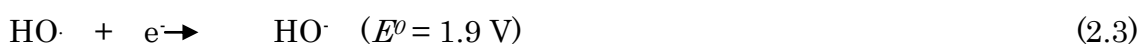
For particularly persistent organics, AOPs which utilize the hydroxyl radical, ozone, or O-atom are a viable solution (Oppenladter, 2003; Pera-Titus et al., 2004; Legrini, 1993). Hydroxyl radical can be generated through hydrogen peroxide photolysis (Kochyany, 1992), ozonation (Hoigne et al., 1983), photo-Fenton's (Zepp et al., 1992), sonolysis (Hua et al., 1997), and peroxone chemistry (Acero et al., 2001). Hydroxyl radical normally reacts with saturated organics through an H-atom abstraction to form water (Eq. (1.2)) and will react with unsaturated organics primarily via an addition reaction. The hydroxyl radical reacts with most aliphatic and aromatic organics at near diffusion-controlled rates (Buxton et al., 1988). At environmentally relevant pH levels, PFOS and PFOA contain no hydrogens to abstract, thus the hydroxyl radical must act through a direct electron transfer to form the less thermodynamically favored hydroxyl ion (Eq. (1.3)).

Table2.3 Summary of previous studies on materials to adsorb PFOS

Material	Condition mg L ⁻¹ of PFOS	Freundlich constants		Langmuir constants		Reference
		K _f	n ⁻¹	q _m	b	
GAC	20-250	0.43mmol ^(1-1/n) L ^{1/n} g ⁻¹	0.18	0.37mmol g ⁻¹	39Lmol ⁻¹	Qiang et al., 2009
PAC	20-250	1.27 mmol ^(1-1/n) L ^{1/n} g ⁻¹	0.18	1.04 mmol g ⁻¹	55 Lmol ⁻¹	Qiang et al., 2009
AI400(Ion exchange resin)	20-250	0.52 mmol ^(1-1/n) L ^{1/n} g ⁻¹	0.17	0.42 mmol g ⁻¹	69 Lmol ⁻¹	Qiang et al., 2009
GAC(Calgon F400)	15-150	960.90 mg ^(1-1/n) L ^{1/n} g ⁻¹	0.28	236.40 mg g ⁻¹	0.124Lmg ⁻¹	Ochoa-Herrera et al., 2008
GAC(Calgon F300)	15-150	38.50mg ^(1-1/n) L ^{1/n} g ⁻¹	0.332	196.20mg g ⁻¹	0.068Lmg ⁻¹	Ochoa-Herrera et al., 2008
GAC(Calgon URV-MODI)	15-150	36.70mg ^(1-1/n) L ^{1/n} g ⁻¹	0.371	211.60mg g ⁻¹	0.080Lmg ⁻¹	Ochoa-Herrera et al., 2008
NaY Zeolite	15-150	0.01mg ^(1-1/n) L ^{1/n} g ⁻¹	1.577	-	-	Ochoa-Herrera et al., 2008
13X Zeolite	15-150	0.73mg ^(1-1/n) L ^{1/n} g ⁻¹	0.507	12.00mg g ⁻¹	0.018Lmg ⁻¹	Ochoa-Herrera et al., 2008
NaY 80Zeolite	15-150	31.80mg ^(1-1/n) L ^{1/n} g ⁻¹	0.339	114.70mg g ⁻¹	0.218Lmg ⁻¹	Ochoa-Herrera et al., 2008
Anaerobic sludge	15-150	0.95mg ^(1-1/n) L ^{1/n} g ⁻¹	1.083	-	-	Ochoa-Herrera et al., 2008

Table2.4 Summary of previous studies on materials to adsorb PFOA

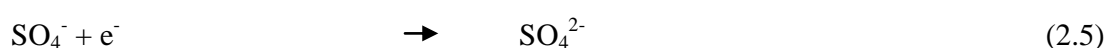
Material	Condition mg L ⁻¹ of PFOA	Freundlich constants		Langmuir constants		Ref
		K _f	n ⁻¹	q _m	b	
GAC	20-250	0.47mmol ^(1-1/n) L ^{1/n} g ⁻¹	0.28	0.39mmol g ⁻¹	18Lmol ⁻¹	Qiang et al., 2009
PAC	20-250	0.83 mmol ^(1-1/n) L ^{1/n} g ⁻¹	0.20	0.67mmol g ⁻¹	59Lmol ⁻¹	Qiang et al., 2009
AI400(Ion exchange resin)	20-250	3.35 mmol ^(1-1/n) L ^{1/n} g ⁻¹	0.13	2.92 mmol g ⁻¹	69 Lmol ⁻¹	Qiang et al., 2009
GAC(Calgon F400)	15-150	11.8 mg ^(1-1/n) L ^{1/n} g ⁻¹	0.443	112.1 mg g ⁻¹	0.038Lmg ⁻¹	Ochoa-Herrera et al., 2008



Thus the perfluorination or substitution of all of the organic hydrogens for fluorines in PFOS and PFOA renders these compounds inert to advanced oxidation techniques (Schroder et al., 2005). The addition of H₂O₂ is detrimental to the photolytic degradation of PFOA by competitively adsorbing photons (Hori et al., 2004). An upper limit for the second order rate constant of ‘HO· + PFOA’ has been determined to be $k_{\text{HO}\cdot + \text{PFOA}} \leq 10^5 \text{ L}\cdot\text{mol}^{-1}\text{s}^{-1}$, which is multiple orders of magnitude slower than the reaction of hydroxyl radical with most hydrocarbons (Buxton et al., 1988). The futility of conventional advanced oxidation for the degradation of PFOS and PFOA is noted in the use of perfluorinated compounds to enhance advanced oxidation of other organics. PFOS is used as an additive to increase aqueous solubility of PAHs (An et al., 2009) enhancing their degradation by UV-H₂O₂. PFOS has also been utilized as a TiO₂ surface coating to increase adsorption of PCBs (Hung et al., 2000) and chlorinated aromatics (Yuan et al., 2001) leading to enhanced oxidation rates. Biphasic water-perfluorocarbon systems have been utilized to increase organic ozonation rates (Gromadzka et al., 2007) by increasing dissolved ozone concentrations. Conventional advanced oxidation methods utilizing oxygen-based radicals are not practical methods for the decomposition of perfluorochemicals.

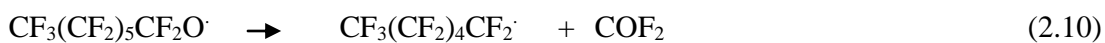
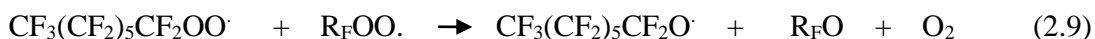
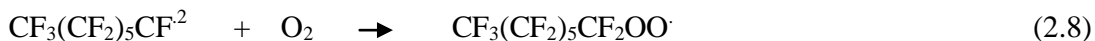
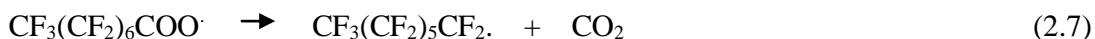
2.7.4 .2 Persulfate photolysis - Sulfate radical oxidation

Persulfate photolysis has been utilized for the oxidative degradation of a number of organics (Waldemar et al., 2007; Anipsitakis et al., 2004; Ball et al., 1956). Persulfate photolysis (Dogliott et al., 1967) or thermolysis (Kolthoff et al., 1956) generates two sulfate radicals, SO₄⁻, (Eq. (1.4)). The sulfate radical is an oxidizing radical that reacts by a direct one-electron transfer to form sulfate (Eq. (1.5)). The sulfate radical has a one-electron reduction potential of 2.3 V (Wordman, 1989), making it a stronger direct electron transfer oxidant than the hydroxyl radical.



Persulfate photolysis has been utilized to degrade a number of perfluoroalkylcarboxylates of various chain lengths (Chen et al., 2006.b; Hori et

al., 2005 1-2; Kutsuna et al., 2007). PFOA degradation by sulfate radical oxidation has achieved minimum half-lives on the order of 1 hr with fluoride accounting for 15% of the total fluorine over the same period of time. The existence of total fluorine as fluoride can be used as a measure of PFOA mineralization. A reaction mechanism for the sulfate radical mediated degradation of perfluoroalkylcarboxylates was proposed by Kutsuna and Hori (Kutsuna et al., 2007). The initial degradation is postulated to occur through an electron transfer from the carboxylate terminal group to the sulfate radical (Eq. (1.6)). The oxidized PFOA subsequently decarboxylates to form a perfluoroheptyl radical (Eq. (1.7)) which reacts quantitatively with molecular oxygen to form a perfluoroheptylperoxy radical (Eq. (1.8)). The perfluoroheptylperoxy radical will react with another perfluoroheptylperoxy radical in solution since there are no reductants present to yield two perfluoroalkoxy radicals and molecular oxygen (Eq. (1.9)). The perfluoroheptyloxy has two branching pathways: unimolecular decomposition to yield the perfluorohexyl radical and carbonyl fluoride (Eq. (1.10)) or an H-atom abstraction from an acid such as HSO_4^- to yield perfluoroheptanol (Eq. (1.12)). The perfluorohexyl radical formed in Eq. (1.10) will react with O_2 (Eq. (1.9)) and resume the radical ‘unzipping’ cycle. The COF_2 will hydrolyze to yield CO_2 and two HF (Eq. (1.11)). The perfluoroheptanol from Eq. (1.12) will unimolecularly decompose to give the perfluoroheptylacyl fluoride and HF (Eq. (1.13)). Perfluoroheptyl acyl fluoride will hydrolyze to yield perfluoroheptanoate (Eq. (1.14)).



During photolysis, Kutsuna and Hori have observed the pH decline to lower than 3 due to HF production (Eq. (1.12)). The produced shorter chain carboxylates will be just as recalcitrant as PFOA. Persulfate photolysis in liquid carbon dioxide/water mixtures (Hori et al., 2005) has been reported to be a good medium for the degradation of longer chain carboxylic acids normally

insoluble in water. Through kinetic modeling of batch reactions the second order rate constants of the sulfate radical with various chain-length perfluorocarboxylates have been determined to be on the order of $10^4 \text{ L}\cdot\text{mol}^{-1}\cdot\text{s}^{-1}$ (Katsuna et al., 2007) consistent with a flash photolysis study (Maruthamuthu et al., 1995) which measured sulfate radical reaction with trifluoroacetate to be $1.6 \cdot 10^4 \text{ L}\cdot\text{mol}^{-1}\cdot\text{s}^{-1}$. A relatively slow rate when compared to second order rates of the sulfate radical with hydrocarbons; short-chain alcohols and carboxylic acids are at the lower end with reaction rates on the order of $10^6 \text{ L}\cdot\text{mol}^{-1}\cdot\text{s}^{-1}$ and aromatic organics are at the upper end with reaction rates being diffusion-controlled, $10^9\text{--}10^{10} \text{ L}\cdot\text{mol}^{-1}\cdot\text{s}^{-1}$ (Neta et al., 1998). The presence of any other dissolved organic species with aqueous PFOA will competitively inhibit degradation. Persulfate photolysis would be a practical technique for the degradation of 'pure' aqueous PFOA. When other organics are present, significant PFOA degradation will only occur when the PFOA concentration greatly exceeds the total organic concentration ($[\text{PFOA}]/[\text{Org}]_{\text{total}} > 100$). Persulfate photolysis under the previously stated conditions would be a viable decomposition method for perfluoroalkyl carboxylates of all chain lengths, since they have similar second order kinetics with the sulfate radical (Katsuna et al., 2007).

2.7.4 .3 Direct Ultra Violet (UV) photolysis

Photolysis is chemical bond-breaking driven by light. UV light adsorption yields an electronically excited molecule. An electronically excited molecule has a bonding (molecular) or non-bonding (atomic) electron promoted to an anti-bonding orbital. An electronically excited molecule is more susceptible to chemical reaction and may open new chemical reaction pathways unavailable to the ground state species. Terrestrial solar-driven photolytic processes require utilization of 290–600 nm photons due to atmospheric absorption of higher energy light. Organics with large chromophores can be directly photolyzed by solar irradiation (Schwarzenbach et al., 2003). Simulated sunlight applied to aqueous solutions of PFOS, and N-EtFOSE 30 days had no effect on their concentrations ($[\text{FC}]_i = 100 \text{ mmol}\cdot\text{L}^{-1}$, $\lambda = 290\text{--}600 \text{ nm}$, 10W , $5\text{W}\cdot\text{L}^{-1}$). The 8:2 fluorotelomer alcohol have not significantly degraded under direct photolysis (Gauthier et al., 2005). Ultraviolet-C (UV-C, $\lambda < 300 \text{ nm}$) and vacuum ultraviolet (VUV, $\lambda < 200 \text{ nm}$) have been utilized for a number of disinfection and AOPs (Oppenlander, 2003). UV-C generated by a black or germicidal lamp ($\lambda = 250 \pm 10 \text{ nm}$) is primarily used for indirect photolyses (e.g., persulfate photolysis), disinfection and in some cases direct photolysis (Lee et al., 2005). VUV irradiation is of high enough energy to photodissociate water into an H-atom

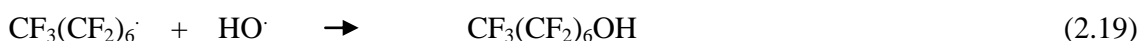
and HO· (Eq. (1.15)) with a quantum yield of 0.3 at 185 nm (Getoff et al., 1968; Fricke et al., 1936).



Vacuum Ultra Violet (VUV) has a very short liquid penetration depth (<100 mm) due to the strong adsorption by water yielding a strongly oxidizing region near the lamp surface. Organic degradation during VUV photolysis is primarily via HO oxidation (Oppenlander et al., 2000; Jakob et al., 1993; Quici et al., 2008). Hori et al. (2004) reported on the photolytic degradation of PFOA which occurred with a half-life of 24 hrs ($[\text{PFOA}]_i = 1.35 \text{ mmol.L}^{-1}$, 200W Xe-Hg lamp, 22 mL, 4.8 atm of O₂). The primary photoproducts have been shorter chain carboxylic acids with fluoride accounting for 15% of the decomposed PFOA fluorine after 24 hrs. Aqueous PFOA VUV photolysis (Chen et al., 2006; Hori et al., 2008) proceeds at a faster rate having a photolysis half-life of 90 min ($[\text{PFOA}]_i = 100 \text{ mmol.L}^{-1}$, $\lambda = 254 \text{ nm}$ with minor 185 nm, 15W, 800 mL, pH 3.7, 40°C, N₂) with fluoride accounting for 12% of the degraded PFOA fluorine. The gas-phase VUV photolysis of trifluoroacetic acid yields CO₂, CF₃, and H atom as predominant photoproducts (Eq. (16), Osborne et al., 1999). Aqueous PFOA will be dissociated into its ion products at pH 3.7 and direct photolysis will be of the PFOA anion (Eq. (1.17)), which may unimolecularly decompose to a perfluoro alkyl anion, CO₂, and an aqueous electron which will protonate under the experimental conditions (Eq. (1.18)).



The hydroxyl radical concentration in the region near the VUV lamp surface may be great enough to also lead to PFOA oxidation and perfluoroalkyl radical formation. Since the photolysis conditions are anoxic (i.e., N₂ atmosphere) the perfluoroalkyl radical will react at diffusion-controlled rates with HO· (Eq. (1.19)).



The overall degradation mechanism will occur through similar reactions as seen in persulfate photolysis (Eqs. (1.7)– (1.14)) to yield a perfluoroalkyl carboxylate (PFCA) one –CF₂– unit shorter than the initial species. The produced PFCA will undergo photolysis until the perfluorinated tail is completely unzipped. PFOS

photolytic degradation has also been reported (Yamamoto et al., 2007) and has a slower photolysis rate, half-life of 5.3 days, than PFOA under similar conditions ($[PFOS]_i = 40 \text{ mmol.L}^{-1}$, $\lambda = 254 \text{ nm}$, 32W, 750 mL, 36–40°C, N_2). Shorter chain perfluorocarboxylates and perfluoroalkyl alcohols were detected as reaction intermediates. After 50% of the PFOS is decomposed, fluoride accounts for 59% of the decomposed PFOS fluorine. The greater fluoride mass balance than observed with PFOA is likely due to faster photolysis rates of the PFCA intermediates than of the initial PFOS. Direct photolysis of PFOS and PFOA will be negligible under environmental conditions. Higher energy UV and VUV photolysis can degrade PFOX. Competitive UV light absorption by solvent and other matrix components will limit photolysis rates.

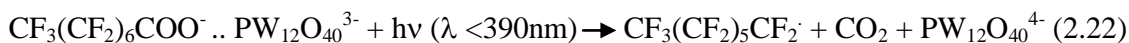
2.7.4 .4 Phosphotungstic acid photocatalysis

Phosphotungstic acid, $H_3PW_{12}O_{40}$, is a heteropolyacid or polyoxometalate that has been utilized for photocatalytic degradation of contaminants (Ozer et al., 2001; Fox et al., 1987) and as an electron shuttle (Lee et al., 2007; Weinstock, 1998; Akid et al., 1985). $PW_{12}O_3^{-40}$ is the predominant form when $pH < 2$ and absorbs light with $\lambda < 390 \text{ nm}$. Upon light adsorption, $PW_{12}O_40^{-3}$ enters a photo-excited state enhancing its oxidation strength (Eq. (1.20)).



PFOA (Hori et al., 2004-a) and PFPA (Hori et al., 2004-b) have been reported to be decomposed by $H_3PW_{12}O_{40}$ photocatalysis. PFOA has half-life of 24 hrs during phosphotungstic acid photolysis ($[PFOA]_i = 1.35 \text{ mmol.L}^{-1}$, $[H_3PW_{12}O_{40}] = 6.7 \text{ mmol.L}^{-1}$, $pH < 2$, 9000 W.L^{-1} , Xe-Hg lamp, 4.8 atm of O_2). After 24 hrs of photolysis when 50% of the PFOA is degraded, fluoride accounts for 20% of the total fluorine. The extent of fluoride production is similar to that observed during persulfate photolysis suggesting a similar degradation mechanism where the carboxylate headgroup is oxidatively removed and a shorter-chain perfluoroalkylcarboxylate is formed.

Hori et al. (2004-b) proposed that $PW_{12}O_{40}^{3-}$ photocatalytic PFOA decomposition involves a photo-Kolbe type mechanism. PFOA first complexes with $PW_{12}O_{40}^{3-}$ (Eq. (1.21)), and upon photon adsorption an electron is directly transferred from PFOA to $PW_{12}O_{40}^{3-}$ (Eq. (1.22) (Hori et al., 2004-b). Similar to the sulfate radical mechanism, PFOA will decarboxylate to form the perfluoroheptyl radical. Oxygen is essential to the photocatalytic cycle in that it accepts an electron from the reduced phosphotungstic acid, $PW_{12}O_{40}^{4-}$, (Eq. (1.23) returning it to its photoactive state.



The superoxide produced in Eq. (1.13) will protonate when $\text{pH} < 2$ to the hydroperoxy radical (Eq. (1.24)) which can act as a reductant for perfluoroalkylperoxy (Eq. (1.25)) and perfluoroalkoxy radicals (Eq. (1.26)). The perfluoroalkylhydroperoxide produced in Eq. (1.25) will likely photolyze to a perfluoroalkoxy radical and a hydroxyl radical (Eq. (1.27)).

Previous researches (Yong et al. 2007) in our group have found that the irradiation at UV_{254} nm and $\text{UV}_{254+185}$ nm can both degrade PFCAs and stepwise decomposition mechanism of PFCAs was confirmed by mass spectra analysis, and *consecutive* kinetics was proposed to simulate experimental data. It was also reported that PFASs can be degraded by $\text{UV}_{254+185}$ photolysis, although the products have not been identified yet. Coexisting NOMs have reduced performance of UV photolysis for PFCAs by competing for UV photons. Sample volume or irradiation intensity showed significant influence on degradation of PFCAs. They have recommended local river water polluted by PFOA to be cleaned up by $\text{UV}_{254+185}$ photolysis effectively. Ozone-related processes were also studied by them, but ineffective to degrade PFC molecules.

Table 2.5 Summary of previous studies on PFOA degradation

Technique	Condition	Power (W) & Volume(mL)	k	product	Energy (kJ)	Reference
UV direct photolysis	9.6 mgL ⁻¹ of PFOA $\lambda = 220\text{--}460$ nm	200 22	0.69 d ⁻¹ $\tau^{1/2} = 1440$ min	33% F ⁻ 38% CO ₂ 65% PFacids	792000	Hori et al. 2004
UV phosphotungstic photocatalysis	9.6 mgL ⁻¹ of PFOA $\lambda = 220\text{--}460$ nm 0.48 MPa of O ₂ 6.6 mmol · L ⁻¹ of PTA	200 22	2.0 d ⁻¹ $\tau^{1/2} = 500$ min	30% F ⁻ 25% CO ₂ 70% PF acids	276000	Hori et al. 2004
TiO ₂ photocatalysis	414 mgL ⁻¹ of PFOA $\lambda = 310\text{--}400$ nm pH = 2–3, 0.1 g of TiO ₂	75 50	0.69 d ⁻¹ $\tau_{1/2} = 1440$ min	50% F ⁻ 50% CO ₂	132000	Kutsuna et al. 2006
UV direct photolysis	20gL ⁻¹ of PFOA $\lambda = 185$ nm	23 1000	0.017 min ⁻¹ $\tau^{1/2} = 41$ min	10% F ⁻ 90% PFacids	49	Chen and Zhang 2006
UV persulfate photolysis	20gL ⁻¹ of PFOA $\lambda = 254$ nm 1.5 mmol · L ⁻¹ of S ₂ O ₈ ²⁻	23 1000	0.012 min ⁻¹ $\tau^{1/2} = 58$ min	5% F ⁻ 95% PFacids	69	Chen and Zhang 2006
UV persulfate photolysis	540gL ⁻¹ of PFOA $\lambda = 220\text{--}460$ nm, 0.48 MPa of O ₂ , 10 mmol · L ⁻¹ of S ₂ O ₈ ²⁻ , pH = 2–3, 10 mmol · L ⁻¹ of S ₂ O ₈ ²⁻	200 22	0.69 h ⁻¹ $\tau_{1/2} = 58$ min	12% F ⁻ 85% PFacids	33600	Hori et al. 2005

Table 2.5 Summary of previous studies on PFOA degradation (*Continued*)

Technique	Condition	Power (W) & Volume(mL)	k	product	Energy (kJ)	Reference
photocatalysis	20gL ⁻¹ of PFOA	23	0.0077 min ⁻¹	10 % F ⁻	500	Chen et al. 2006
TiO ₂ /Ni-Cu	λ = 254 nm	250	τ ^{1/2} = 90 min	90% PFacids		
photoelectrocatalysis	20gL ⁻¹ of PFOA	23	0.015 min ⁻¹	20% F ⁻	250	Chen et al. 2006
TiO ₂ /Ni-Cu	λ = 254 nm - 0.1 V	250	τ ^{1/2} = 45 min	80% PFacids		
persulfate photolysis	535mgL ⁻¹ of PFBA λ = 254 nm 50 mmol · L ⁻¹ of S ₂ O ₈ ²⁻	60 200	0.0096 min ⁻¹ τ ^{1/2} = 72 min		1300	Kutsuna and Hori 2007
hydrogen peroxide photolysis	2.5 mmol · L ⁻¹ of PFBA λ = 254 nm 250 mmol · L ⁻¹ of H ₂ O ₂	60 200	3.0e-5 min ⁻¹ τ ^{1/2} = 23100 min	n/a	420000	Kutsuna and Hori 2007
sonolysis	8.2 L ⁻¹ of PFOA f = 354 kHz	150 600	0.018 min ⁻¹ τ ^{1/2} = 39 min	95% F ⁻	670	Vecitis et al. 2008
sonolysis	82 μgL ⁻¹ of PFOA f = 354 kHz	150 600	0.047 min ⁻¹ τ ^{1/2} = 15 min	95% F ⁻	260	Vecitis et al. 2008
UV-KI photolysis	8.2 gL ⁻¹ of PFOA λ = 254 nm	1.5 30	0.0014 min ⁻¹ τ ^{1/2} = 500 min	10% F ⁻ gaseous fluoroalkanes	1500	Park et al. 2009

Table 2.5 Summary of previous studies on PFOA degradation (*Continued*)

Technique	Condition	Power (W) & Volume(mL)	k	product	Energy (kJ)	Reference
UV-KI photolysis	200 nmol·L ⁻¹ of PFOA λ = 254 nm	1.5 30	0.0025 min ⁻¹ τ ^{1/2} = 280 min	10% F ⁻ Gaseous fluoroalkanes	820	Park et al. 2009
Ferrophotolysis	14.3 gL ⁻¹ of PFBA 2.5 mmol·L ⁻¹ of Fe ₂ (SO ₄) ₃ λ = 220–460 nm	200 105	0.028 h ⁻¹ τ ^{1/2} = 1490 min	45% F ⁻ 55% short chains	89400	Hori et al. 2007

Table 2.6 Summary of previous studies on PFOS degradation

Technique	Condition	Power (W) & Volume(mL)	k	product	Energy (kJ)	Reference
sub-critical Fe(0)	185 mgL ⁻¹ of PFOS 0.5 g of Fe(0) 350°C, 20 MPa	0 10	0.013 min ⁻¹ τ ^{1/2} = 53 min	50% F ⁻	2000	Hori et al. 2006
UV direct photolysis	20 mgL ⁻¹ of PFOS λ = 254 nm	32 750	0.13 d ⁻¹ τ ^{1/2} = 7700 min	71% F ⁻ 90% SO ₄ ²⁻	17000	Yamamoto et al. 2007
UV alkaline IPA photolysis	20 mgL ⁻¹ of PFOS λ = 254 nm	32 750	0.93 d ⁻¹ τ ^{1/2} = 1070 min	NaF _(s)	2500	Yamamoto et al. 2007
sonolysis	10 mgL ⁻¹ of PFOS f = 354 kHz	150 600	0.011 min ⁻¹ τ ^{1/2} = 63 min	95% F ⁻ 100% SO ₄ ²⁻	945	Vecitis et al., 2008

Table 2.6 Summary of previous studies on PFOS degradation (*Continued*)

Technique	Condition	Power (W) & Volume(mL)	k	product	Energy (kJ)	Reference
UV-KI photolysis	10mgL ⁻¹ of PFOS $\lambda = 254 \text{ nm}$ [KI] = 10 mmol·L ⁻¹	1.5 30	0.002 min ⁻¹ $\tau^{1/2} = 350 \text{ min}$	50% F ⁻ 50% fluoroalkanes	960	Park et al. 2009
UV-KI photolysis	100mgL ⁻¹ of PFOS $\lambda = 254 \text{ nm}$ [KI] = 10 mmol·L ⁻¹	1.5 30	0.008 min ⁻¹ $\tau^{1/2} = 87 \text{ min}$	50% F ⁻ 50% fluoroalkanes	260	Park et al. 2009
Sonolysis	100mgL ⁻¹ of PFOS f = 354 kHz	150 600	0.023 min ⁻¹ $\tau^{1/2} = 30 \text{ min}$	95% F ⁻ 100% SO ₄ ²⁻	450	Vecitis et al. 2008

Chapter 3 Ferrate oxidation of PFCs

3.1 Introduction

Oxidation of PFCs (if it is possible) is an important technique as a treatment process, because both elimination and degradation of PFCs can be achieved. According to the available literature, PFCs level in tap water has showed a linear correlation to surface water suggesting the incapability of conventional disinfection agents to oxidize PFCs.

Advanced oxidation processes (AOPs) may be possible candidates to oxidize PFCs. Being involved in generation of hydroxyl radicals to enhance water treatment, this kind of process shows excellent performance to control micro pollutants in water and waste water. Most common processes of AOPs include O_3/H_2O_2 , O_3/UV and UV/H_2O_2 . UV/TiO_2 process and Fenton's reagent have also shown efficiency on specific wastewater (Gottschalk, et al., 2000). However, previous researches have showed that AOPs including O_3 , O_3/UV , O_3/H_2O_2 and Fenton process cannot degrade PFOS, but degrade PFOS precursors and partly fluorinated polymers effectively (Schröder and Meesters, 2005). Our research group too investigated on capabilities of AOPs to oxidize PFCs and deduced with four main conclusions (Yong 2007).

- (1) Mass spectra analysis on UV photolysis of PFCAs confirmed stepwise degradation mechanism of PFCAs. UV photolysis can also degrade PFAS, however, the velocity was very low and final products can not be identified yet.
- (2) Results of UV photolysis for PFCAs were successfully estimated by *consecutive* kinetics. Kinetic parameter for $UV_{254+185}$ irradiation on PFCAs was estimated as 2~6 hr^{-1} in pure water. Background absorbance can significantly reduce degradation of PFOA in wastewater, by which k was decreased from 2.5~3.5 hrs^{-1} in pure water to 0.9~1 hr^{-1} in sand filtration effluent.
- (3) PFOA polluted river water can be cleaned by UV photolysis process. $UV_{254+185}$ showed satisfactory performance to degrade more than 90% of 40 $\mu g/L$ PFOA in 4 hrs, with k value of 0.81 hr^{-1} . UV_{254} was ineffective to degrade PFOA because of strong background absorbance. UV wave length and sample volume showed significant influences on degradation kinetics.
- (4) For ozone-related processes, mass spectra and batch experiments proved inefficiency of O_3/H_2O_2 to degrade PFCs. Semi-batch experiments showed obvious removal of PFCs in first order kinetics, which was attributed to air-floating effect by aeration.

3.1.1 Ferrate Oxidation

Although the ferrate(VI) species were discovered a century ago, a renaissance of interest in ferrate(VI) application began in the 1970s, when a number of researches were carried out for the degradation of various organic pollutants including the emerging micro-pollutants such as endocrine disrupt chemicals (EDCs) and pharmaceuticals. Extensive studies on the ferrate(VI) are also due to its unique oxidation/coagulation capacity in the environmental remediation and it is a green chemical. Ferrate(VI) is a strong oxidizing agent, which can be seen from the reduction potentials of reactions (3.1) and (3.2) in acidic and alkaline solutions, respectively (Wood, 1958).



The spontaneous reduction of ferrate (VI) in water forms non-toxic by-products, molecular oxygen and iron(III) (Eq. (3.3)) (Sharma, 2002a), suggesting that ferrate(VI) is an environment-friendly oxidant.



Ferric(III) hydroxide, produced from ferrate(VI), acts as a coagulant for the removal of metals, non-metals, radionuclides, and organics (Potts and Churchwell, 1994; Sharma, 2002a). Ferrate(VI) has been proposed as an alternative to chlorine for the disinfection of water and wastewater (Sharma, 2002a, 2007b; Sharma et al., 2005a). **Table 3.1** shows the oxidation potential of common disinfectants currently used in water and wastewater industry.

Fe(VI) solutions are generally unstable; their decomposition by reduction to Fe(III) species occurs rapidly at room temperature. The instability may be retarded but not stopped at low temperatures or with careful control of solution concentrations. Hence, without steps of refrigeration or high purification, the solutions cannot be stored for use in practice. Solid ferrate(VI) salts are stable, but they are costly as they require multiple chemical reagents and long synthesis time. This makes it difficult to be used in industry. In order to solve the problems of instability and the high cost of using ferrate(VI), some researchers have suggested to generate ferrate in situ and apply the generated ferrate(VI) directly for water and wastewater treatment.

Table 3.1: Oxidation potentials of common oxidants

Disinfectant	Oxidant	Reaction Eo, V
Chlorine	$\text{Cl}_2(\text{g})+2\text{e} \rightleftharpoons 2\text{Cl}^-$	1.358
	$\text{ClO}^-+\text{H}_2\text{O}+2\text{e} \rightleftharpoons \text{Cl}^-+2\text{OH}^-$	0.841
Hypochlorite	$\text{HClO}+\text{H}^++2\text{e} \rightleftharpoons \text{Cl}^-+\text{H}_2\text{O}$	1.482
Chlorine dioxide	$\text{ClO}_2(\text{aq})+\text{e} \rightleftharpoons \text{ClO}_2$	0.954
Perchlorate	$\text{ClO}_4^-+8\text{H}^++8\text{e} \rightleftharpoons \text{Cl}^-+4\text{H}_2\text{O}$	1.389
Ozone	$\text{O}_3+2\text{H}^++2\text{e} \rightleftharpoons \text{O}_2+\text{H}_2\text{O}$	2.076
Hydrogen peroxide	$\text{H}_2\text{O}_2+2\text{H}^++2\text{e} \rightleftharpoons 2\text{H}_2\text{O}$	1.776
Dissolved oxygen	$\text{O}_2+4\text{H}^++4\text{e} \rightleftharpoons 2\text{H}_2\text{O}$	1.229
Permanganate	$\text{MnO}_4^-+4\text{H}^++3\text{e} \rightleftharpoons \text{MnO}_2+2\text{H}_2\text{O}$	1.679
	$\text{MnO}_4^-+8\text{H}^++5\text{e} \rightleftharpoons \text{Mn}^{2+}+4\text{H}_2\text{O}$	1.507
Ferrate(VI)	$\text{FeO}_4^{2-}+8\text{H}^++3\text{e} \rightleftharpoons \text{Fe}^{3+}+4\text{H}_2\text{O}$	2.20

3.1.2 Ferrate production

There are two basic methods for ferrate production: Chemical (Ockerman and Schereyer, 1951; Thompson et al., 1951) and electrochemical. The chemical methods are based on contacting iron compounds, such as iron(III) nitrate and iron oxide, with an oxidizing material in either an alkaline environment, the wet route, or under extreme temperatures in a controlled atmosphere, the dry route. The drawback of this method is that it requires additional processes and reagents to obtain high yield and purity which makes it expensive. On the other hand, the electrochemical method usually consists of a sacrificial iron anode in an electrolysis cell containing a strongly alkaline solution with an electric current serving to oxidize the iron to Fe(VI). The electrochemical method is more promising than the chemical for ferrate generation as it has a simpler process and does not require costly chemical reagents. The main elements that affect the electrochemical production of ferrate(VI) are the anode composition, the type and concentration of electrolyte, the current density and the cell design (Máková et al., 2009).

3.1.3 Application of ferrate oxidation in water and wastewater treatment

It has been shown that ferrate(VI) has a high efficient oxidation performance for the degradation of a number of compounds that could contaminate water such as inorganic oxysulfur compounds (Read et al., 2001), thiourea and thioacetamide (Sharma, 2002), and H_2S could be completely converted to sulphate with the ratio 2.5:1 of ferrate or more to the total hydrogen sulfide (Simon et al., 2002), sulfide mine tailings where ferrate reduces the potential of acid production and enhance the potential of toxic metal species from tailing by oxidizing tailing bounded sulfide to

sulphate (Mursheda et al., 2003), alachlor which could be totally eliminated from wastewater within 10 min under optimization conditions (Zhu et al., 2006), phenol and chlorophenol (Graham et al., 2004), endocrine disrupting chemicals (EDCs), which could be reduced to low levels ranging from 10 to 100 ng/L (Jiang et al., 2005), sulfamethoxazole (SMX) (Sharma et al., 2006) and cetylpyridinium chloride (CPC), which are mineralized after opening the pyridine ring by ferrate (Eng et al., 2006). Some organics such as methanol, ethanediol and phenol could be oxidized completely to CO₂ and H₂O even at room temperature (Denver and Pletcher, 1996 1,2). Ethionine was oxidized by ferrate to sulfoxide within 500 s and thiourea was oxidized to urea within 10 s (Read et al., 2004). The oxidation of seleno-DL-methionine by potassium ferrate to the selenoxide is complete within 7.5 ms to 2 s (Read and Wyand, 1998). The half-lives for hydrogen sulfide, thiourea, thioacetamide, cyanide and thiocyanate are 3.0 ms, 0.6 s, 0.8 s, 9.3 s and 180 s, respectively. The oxidation of pollutants and amino acids with Fe(V), which is formed as a result of the use of ionizing radiation and photocatalytic techniques in the presence of Fe(VI), is 3–5 order of magnitude faster than Fe(VI) (Sharma, 2004). Offensive odor of the compounds generated during sewage treatment were reduced immediately and to an acceptable level by stabilization with Fe(VI) (Lucas et al., 1996). Most toxic ion cyanide in aqueous wastewater can be oxidized in few minutes (Tiwari et al., 2007). The disinfection performance of ferrate (VI) was also intensively studied by several researchers; removing more than 99.9% of total coliform was reported by Waite (1979), Kato and Kazama (1991) and Jiang et al. (2007). It was shown that ferrate can reduce 30% more COD and kill three log more bacteria than ferric sulphate and aluminum sulphate at a similar or even smaller dose (Jiang et al., 2006 2). It was reported that ferrate could rapidly inactivate virus at pHs 6–8 (Schink and Waite, 1980; Kazama, 1994; Kazama, 1995). Such high disinfection performance is of utmost importance for the water industry. It was also shown that ferrate could enhance the coagulation of algae (Lui and Ma, 2002; Ma and Liu, 2002 1, 2) and that microcystin was easily decomposed by ferrate depending on the dosage of ferrate, the pH, and the contact time (Yuan et al., 2002). On the other hand, the effect of ferrate on the enhancement of photocatalytic degradation of microcystin was studied by Yuan et al. (2006) and showed that above 81% degradation can be achieved at ferrate concentration of 0.08– 0.17 mmol/L within 10 min. In addition to the oxidation and disinfection effect, ferrate(VI) generates a coagulant in a single dosing and mixing unit process as a result of reduction of ferrate ions to Fe(III) during the process of oxidation/disinfection (Jiang et al., 2001). The research progress of using ferrate as a coagulant, a disinfectant and an oxidant has been reviewed by Jiang (Jiang, 2007). Table 3.2 shows a

summary of previous work on Ferrate oxidation of various organic compounds.

Table 3.2 Ferrate oxidation of various organic compounds

Pollutants	pH	k (M ^{-1s-1})	t ^{1/2}	Reference
Thioacetamide	9	5.6×10 ³	0.36s	Sharma et al., 2000
Thiourea	9	3.4×10 ³	0.59s	Sharma et al., 1999
p-Toluidine	9	1.3×10 ³	1.5s	Sharma et al., 1995
Glyoxylic acid	8	7.0×10 ²	2.9 s	Carr et al., 1985
Thiodiethanol	8	7.0×10 ²	20.0s	Carr et al., 1985
Phenol	9	8.0×10 ¹	25.0s	Carr et al., 1985
p-Aminobenzoic acid	9	4.3 × 10 ¹	46.9s	harma et al., 1995
Methylamine	8	4.0×10 ¹	50.0s	Carr et al., 1985
Nitriloacetic acid	8	2.0×10	16.7min	Carr et al., 1985
Diethylamine	8	7.0×10 ⁻¹	47.6min	Carr et al., 1985
Neopentyl alcohol	8	1.0×10 ⁻¹	5.55h	Carr et al., 1985
Isopropyl alcohol	8	6.0×10 ⁻²	9.26h	Carr et al., 1985.

Note k = constant, t^{1/2} = half time

3.1.4 Ferrate oxidation of PFCs

Even though we have realized the strength of C-F bond and the resistance of PFCs to oxidize by our previous work (Yong 2007), this experiment was carried out as ferrate (VI) technology has not been tested for PFCs oxidation including PFOS and PFOA.

3.2 Aims

Major aim of this chapter is to study the oxidation characteristics of PFCs by ferrate techniques. A series of batch type experiments were conducted at room temperature (24°C) and pressure to reach the objectives. A control test was done with Cetylpyridinium chloride (CPC) to ensure the accuracy of the methodology adapted. Objectives in detail are listed below.

- (1) To conduct batch experiment with PFOA to identify the optimum Ferrate(VI):PFCs molar ratio for ferrate oxidation.
- (2) To conduct batch experiment with PFOA to understand the kinetic behavior of ferrate oxidation of PFCs.

- (3) To conduct batch experiment with a mixture of PFCs to understand the competitive ferrate oxidation of PFCs.
- (4) To conduct batch experiment with CPC to ensure the accuracy of the methodology adapted.

3.3 Experimental method

3.3.1.1 Chemicals

All PFCs standards, sodium sulfite, sodium phosphate and 0.5 M borate buffer having purity more than 98% were obtained from WAKO pure chemical industries, Japan. Potassium ferrate(VI) and CPC salt (98+ % purity) were obtained from Aldrich Company. All chemicals were used without further purification. Solutions were prepared in ultra pure water purified with 18.2 M Ω Milli-Q (Millipore SAS 67120) water purification system. Ferrate(VI) solution was freshly prepared by dissolving a desired amount of ferrate(VI) salts into a 1.7 mM borate / 8 mM phosphate buffer solution. The phosphate served as a complexing agent for the Fe(III) produced, which otherwise could precipitate as a hydroxide and would accelerate the decomposition of ferrate(VI).

3.3.1.2 Analytical equipments and methods

All PFCs were directly analyzed and measured using LC/MS/MS. Extract 10 μ L was injected to a 2.1 \times 100 mm (5 μ m) Agilent Eclipse XDB-C18 column. Mobile phase consisted of (A) 5 mM ammonium acetate in ultrapure water (LC/MS grade) and (B) 100% Acetonitrile (LC/MS grade). At a flow rate of 0.25 mL/min, the mobile phase started with an initial condition of 30% (B), increased to 50% (B) at 16.5 min, then to 70% (B) at 16.6, 75 held at 70% (B) for 3.4 min, went up to 90% (B) at 21 min, kept at 90% (B) for 1 min, and then ramped down to 30% (B). The total running time was 34 min for each sample. For quantitative determination, the HPLC was interfaced with an Agilent 6400 Triple Quadrupole (Agilent, Japan) mass spectrometer (MS/MS). Mass spectrometer was operated with the electrospray ionization (ESI) negative mode. Analyte ion was monitored by using multiple reaction monitoring (MRM) mode. Both parent ion (499m/z) and daughter ion (80m/z) were monitored with the retention time of 13.8min. A total organic carbon (TOC) analyzer, Shimadzu 5050 was used to measure the TOC content (in mg/L) of samples. The calibration curve of all PFCs gave good coefficient of determination ($R^2 > 0.995$).

3.3.1.3 Oxidation tests of PFC

Two kinds of batch type oxidation experiments were conducted for PFOA and a mixture of PFCs ((PFDA, PFOA, PFHpA, PFPeA, PFOS and PFHS).

In both cases, collected samples were centrifuged at 4000 rpm for 10 minutes to eliminate precipitant (Kubota ICE 61010-2-020). Then the samples were diluted by acetonitrile (LC/MS grade) to reach 40% acetonitrile level in the sample, which is required by LC/MS/MS. **Figure 3.1** shows the flow chart of batch experiments; **Figure 3.2** shows a schematic diagram of a batch experiment with the magnetic stirrer and **Table 3.3** summarizes experimental conditions.

3.3.2 Determination of optimum Molar ratio

In this experiment, four parallel batch tests (250 mL each) were conducted with ferrate(VI) to PFOA molar ratios of 10, 100, 1000, and 10,000 at room temperature (25°C). The PFOA concentration was kept fixed at 16 µg/L, while concentration of ferrate(VI) was changed to increase the molar ratio. In each oxidation test, samples were constantly mixed by magnetic stirrer (Figure 3.2) and samples were taken (1 mL) at distinct time intervals up to 24 hrs (Table 3.3). Sodium sulfite solution was added immediately to each sample upon removal from the reactor in order to quench the ferrate and stop any further oxidation.

Table 3.3 Summary of the conditions for experiments.

Exp No.	Chemicals	Concentration		Molar ratio	Contact time	Measurement items
		Chemicals, µg/L	Ferrate(VI), mg/L			
1	PFOA	16	0.071	10	1, 2, 3, 4, 5, 6, 7, 8, 9, 11, 14, 17, 24 (hrs)	Remaining PFOA
			0.710	100		
			7.100	1000		
			71.000	10000		
2	Mixture of PFOS, PFOA, PFDA, PFHpA, PFPeA, PFHS	0.10 0.50 1.0 5.0 10 25	0.030, 0.059, 0.089	100, 200, 300	24 (hrs)	Remaining PFCs
			0.150, 0.300, 44.000			
			0.300, 0.590, 0.890			
			1.480, 2.960, 4.440			
			2.960, 5.920, 8.880			
			7.4100, 14.800, 22.200			
3	CPC*	10,000	29.100	3	0, 5, 10, 20, 35, 50 (min)	TOC
	PFOA	10,000	23.900	3	0, 5, 15, 35, 50 (min)	

* References: Yong *et al.*. 2006

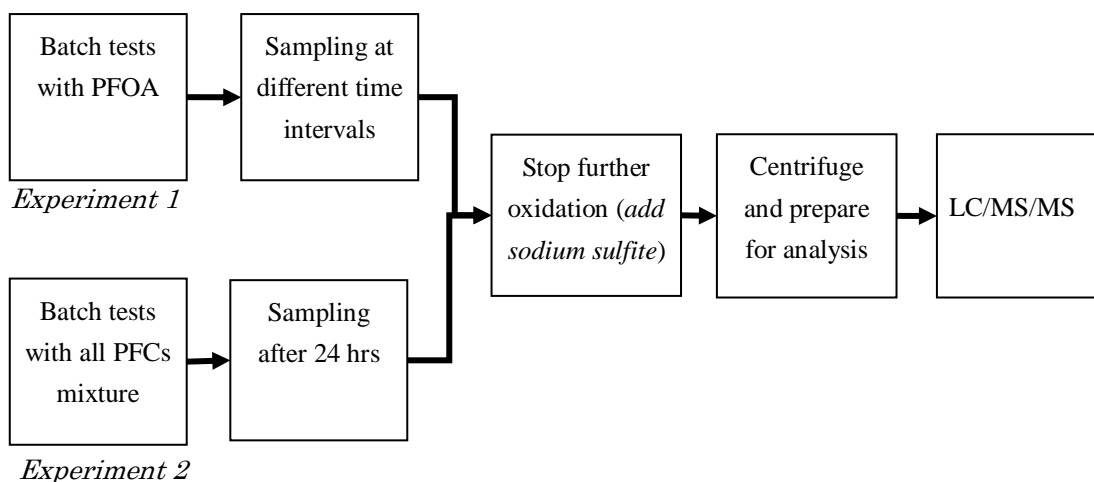


Fig. 3.1 Flow chart of the batch experiments

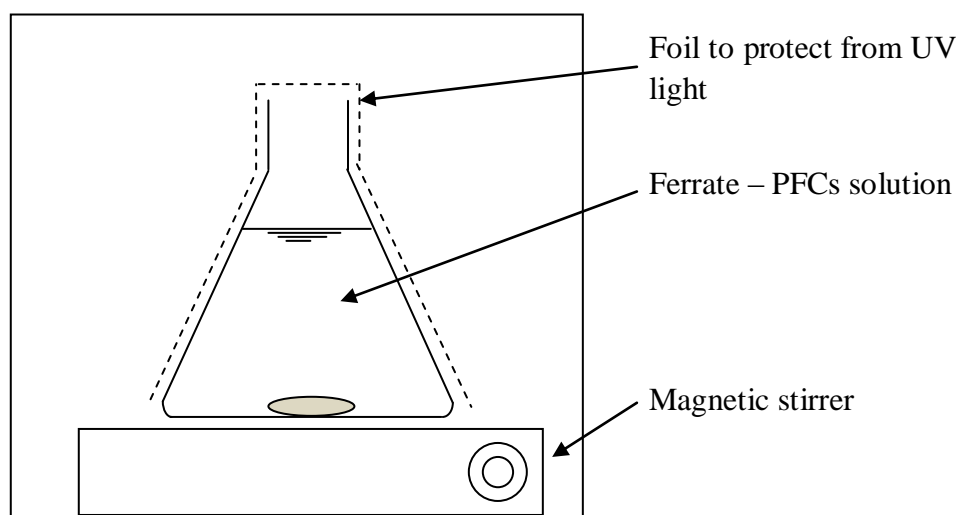


Fig. 3.2 schematic diagram for the batch experimental setup with magnetic stirrer

3.3.3 Mixture of PFCs oxidation by ferrate

In this experiment, six parallel batch experiments (250 mL each) were conducted with different initial PFC concentrations ($\mu\text{g/L}$) of 0.10, 0.50, 1, 5, 10 and 25. The experiment was repeated for 3 ferrate(VI) to PFCs molar ratios of 100, 200 and 300 and the reaction time was 24 hrs. Separate experiment was conducted to determine the reduction of TOC equivalent to PFOA by ferrate oxidation and the results were compared with the results of the same experiment for CPC.

3.4 Results and discussion

3.4.1 Oxidation test of PFOA in a ferrate solution

Figure 3.3 shows results of the Experiment 1. Maximum PFOA reduction of 10.0 % was obtained at the molar ratio 100, followed by 6.0 % reduction by molar ratio 1000, 0.3 % reduction by molar ratio 10. It was noticed that PFOA concentration was kept unchanged at 10000 molar ratio.

It was also noticed that the reaction with high ferrate(VI) to PFOA molar ratios (>1000) gave more fluctuating readings over the reaction time, whereas less molar ratio of 10 gave less fluctuation. One possible phenomenon to describe this fluctuation is adsorption. Temporary adsorption and desorption process of PFOA in to ferrate(VI) and ferrite(III) (solid particles) can cause fluctuation of the reading.

Previous studies have shown that five times higher concentration of ferrate(VI) than the concentration of target pollutant is good enough to oxidize most of other pollutants than PFCs, and observed that most pollutants are quick to react with ferrate. (Li et al., 2008; Yong et al., 1995; Srarma et al., 1995; Sharma et al., 2000; Carr et al., 1985). However, our results showed that the PFOA was not oxidized by ferrate(VI) even at very high molar ratio (10,000) and longer reaction time (24 hrs) (**Figure 3.3**).

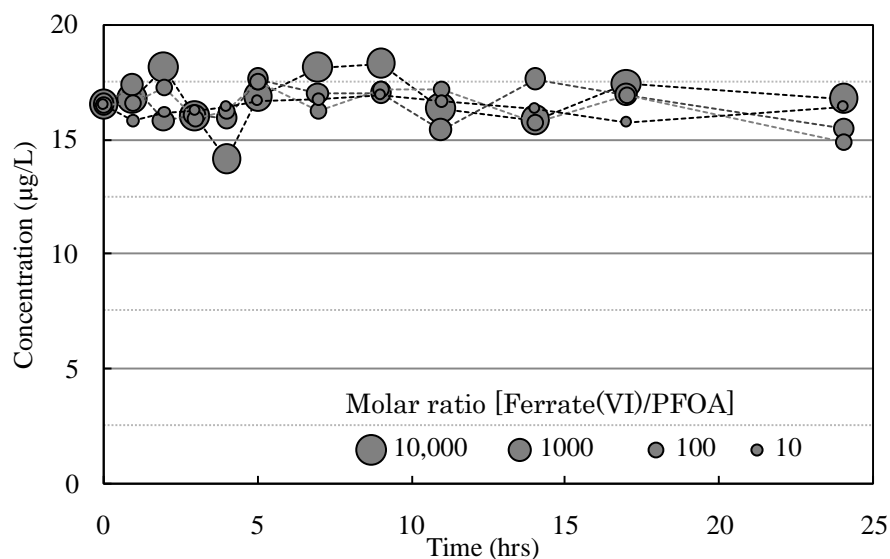
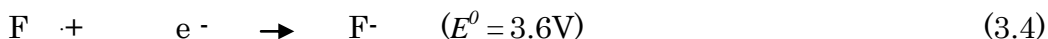


Fig. 3.3 Ferrate(VI) degradation of PFOA with time

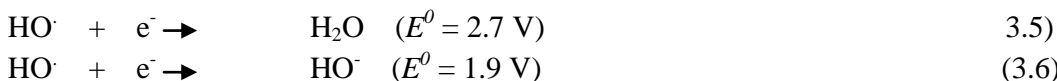
3.4.1.1 Stability of PFOA chain

As mentioned in the introduction of this chapter, PFOA is recalcitrant towards oxidation due to the complete substitution of fluorine (C-F bond) for hydrogen (C-H bond). Fluorine will retain its electrons (i.e., will resist oxidation) at any cost. Fluorine is nearly always found in the (-1) valence

state with the only exception being F₂ where its oxidation state is (0). The fluorine atom is the most powerful inorganic oxidant known with a reduction potential of 3.6 V (Eq. 3.4) (Wardman, 1989) and thus is thermodynamically unfavorable to create the fluorine atom with any other one-electron oxidant.



Perfluorination will also reduce the oxidizability of the ionic headgroup of CO₂⁻ for PFOA, since it inductively reduces headgroup electron density. The other important characteristic of PFOA is absence of C-H bonds which is important to initiate oxidation process. Particularly persistent organics such as PFOA hydroxyl radical normally reacts with saturated organics through an H-atom abstraction to form water (Eq. (3.6)) and will react with unsaturated organics primarily via an addition reaction. The hydroxyl radical reacts with most aliphatic and aromatic organics at near diffusion-controlled rates (Buxton et al.,1988). At environmentally relevant pH, PFOA contains no hydrogens to abstract, thus the hydroxyl radical must act through a direct electron transfer to form the less thermodynamically favored hydroxyl ion (Eq. 3.6).



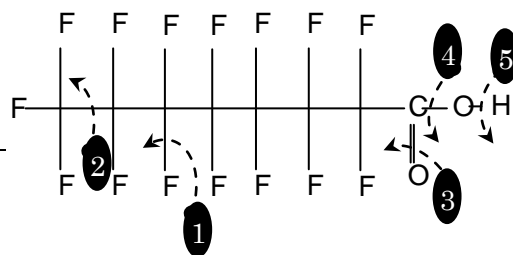
Thus the perfluorination or substitution of all of the organic hydrogens for fluorines in PFOA renders these compounds inert to advanced oxidation techniques (Schroder et al.,2005). Table 3.4 shows bond energy of each bond in the PFOA molecule.

3.4.1.2 Oxidation of PFOA by Ferrate

Oxidation can be defined as the loss of at least one electron when two or more substances interact. Carbon can take the oxidation numbers of -4, -3, -2, -1, +1, +2, +3 and +4. Fluorine has only one oxidation number of -1. **Figure 3.4** shows oxidation numbers of each atoms of PFOA chain. According to this figure two carbon atoms at the end of the chain have same oxidation number of +3 and the interior carbon atoms have oxidation number of +2.

Table 3.4 Bond energies in PFOA molecule

Bond no	Bond	Standard Bond Energy (kcal/mole)	Bond length (pm)
1	C-F	116	135
2	C-C	83	154
3	C=O	179	120
4	C-OH	110	143
5	O-H	111	96



R.T.Sanderson, Chemical Bonds and Bond Energy, 1976

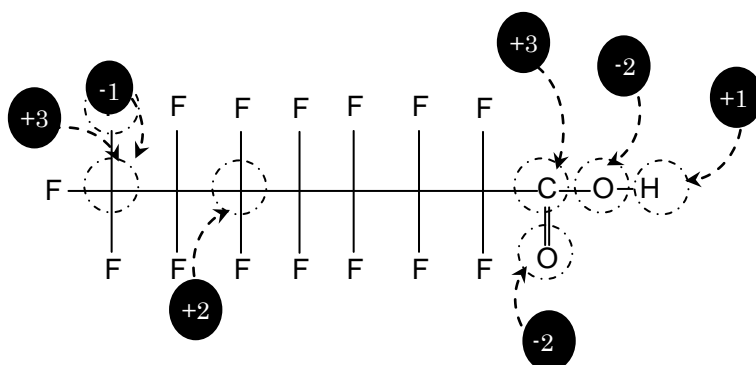


Fig 3.4 Oxidation numbers in PFOA chain

It is obvious that the PFOA molecule has positive oxidation numbers except fluorine and oxygen. It has some possible oxidations such as Carbon in the PFOA chain in to +4 (CO₂). This reaction may take place at high temperature and pressure, but not by the strong oxidants at room temperature and pressure.

3.4.2 CPC oxidation by ferrate - reference study

Yong et al (2006) have studied the oxidation of CPC by ferrate. It was the first report to show that ferrate technique can open the pyridine ring and mineralize the aliphatic chain of the organic molecule resulting inorganic ions. They have demonstrated the unique property of ferrate(VI) to degrade almost completely the cationic surfactant, CPC. The decrease in total organic carbon (TOC) from CPC was more than 95%; suggesting mineralization of CPC to carbon dioxide. In order to check the reliability of the methodology adapted for this experiment, a part of ferrate oxidation test for CPC was imitated.

3.4.2.1 Kinetics of TOC reduction by ferrate oxidation.

In this experiment the ferrate to CPC molar ratio (beginning of the experiment) was kept at 3, which ensures the availability of excess ferrate for the reaction during entire reaction time. Yong et al (2006) has reported that the CPC can be completely oxidized by ferrate and this can be explained by the rate law as shown in Eq 3.7(Yong et al., 2006).

$$d[\text{Fe(VI)}]/dt = k[\text{Fe(VI)}][\text{CPC}]^2 \quad (3.7)$$

The reaction has taken only few minutes and molar consumption of ferrate(VI) has been nearly equal to the oxidized CPC. Also they have suspected the mineralization of CPC to carbon dioxide as they observed more than 95% TOC reduction in this experiment.

Figure 3.5 a and b show the rate of change of TOC with prevailing TOC concentration in the mixing flask. From our study the kinetic of TOC oxidation can be expressed as (Figure 3.5 a),

$$d(\text{TOC})/dt = 0.1187x \quad R^2 = 0.8034 \quad (3.8)$$

and according to the published data same oxidation can be written as (Figure 3.5 b)

$$d(\text{TOC})/dt = 0.1249x \quad R^2 = 0.7732 \quad (3.9)$$

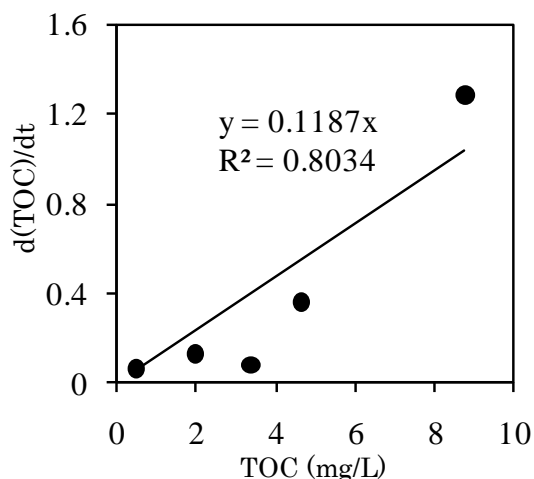


Fig 3.5a The changing rate of TOC with remaining TOC level. (This study)

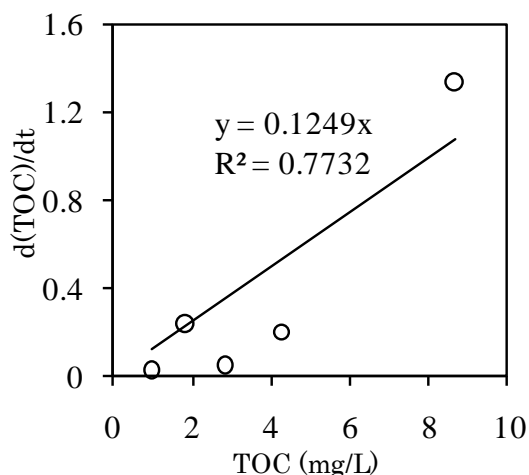


Fig 3.5b The changing rate of TOC with remaining TOC level (Yong et al (2006))

According to Eq 3.8 and 3.9 the kinetic constant for TOC reduction by ferrate for this study and the previous study were 0.1187 and 0.1249 respectively.

Our reading just deviated by 5% from the published reading and it is quite reasonable to conclude that the methodology adapted in this experiment is acceptable.

3.4.2.2 TOC reduction at the ferrate oxidation of PFOA and CPC

Figure 3.6 shows the percentage TOC reduction with time for PFOA and CPC. It was found that the TOC removal was 14% for PFOA, but for the control test with CPC the TOC reduction was more than 95% after one hour. This totally agrees with the previous results of this experiment, where PFOA was not oxidized by ferrate. Since process of mineralization was not started to reduce PFOA in to CO₂, the levels of TOC remain unchanged. The main reason to reduce TOC by 14% in this experiment could be the temporary adsorption of PFCs onto ferrite (III). Since the concentrations used in this experiment was in mg/L level and ferrite to PFOA molar ratio was 3, there is a high possibility for the PFOA to attach with ferrite (III), which have been settled in the centrifuge process, reducing the TOC in the final analysis.

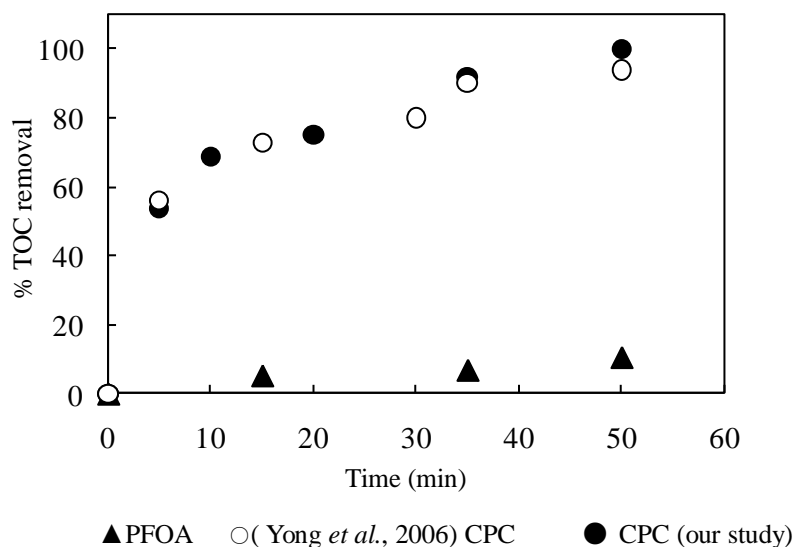
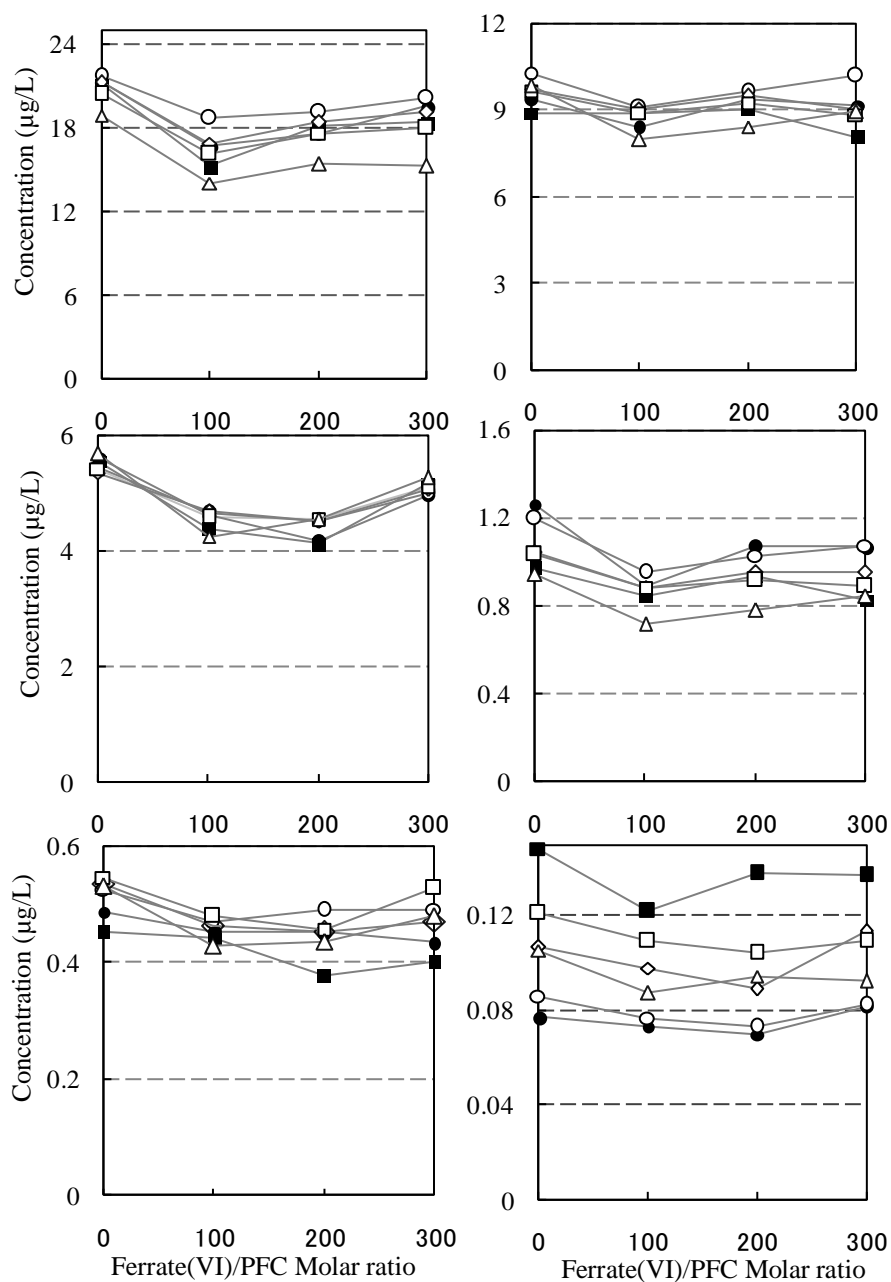


Fig 3.6 Percentage TOC reduction with time for CPC and PFOA

3.4.3 Ferrate oxidation of a mixture of PFCs

It is expected to understand the ability of ferrate to oxidize other PFCs with this experiment. Also the effect of initial concentration of PFCs on ferrate oxidation was studied in this experiment. **Figure 3.7** shows the results of six individual batch tests of experiment No. 2 (table 3.3). It was observed that all PFCs were behaving in a similar pattern in each individual batch test for different PFCs concentrations. In the case of 25 µg/L batch experiment, molar ratio of 100 gave the best performance of about 15% reduction of overall PFCs and the performance was reduced as the molar ratio was

increased. Similar pattern was noticed for the 10 $\mu\text{g/L}$ batch experiment. For the 5 $\mu\text{g/L}$ batch experiment, ideal molar ratio was 200 which also gave about 15% overall PFCs reduction. For the concentrations of 0.5 $\mu\text{g/L}$ and 0.1 $\mu\text{g/L}$, ideal molar ratio was 100 for one set of PFCs and 200 for another set of PFCs. High ferrate(VI) to PFC concentration seems to be discouraging PFCs removal. The reason may be coagulation effect of ferrate(VI), which may flocculate ferrite(III) particles reducing the adsorption process.



Δ PFPeA(C5) \square PFHpA(C7) \diamond PFOA(C8) \circ PFDA(C10) \blacksquare PFHS(C6) \bullet PFOS(C8)

Fig 3.7 Ferrate(VI) degradation of PFCs with different initial concentrations and molar ratios

Table 3.5 Summarized results of ferrate oxidation of PFCs

PFCs	Max removal	Optimum molar ratio	Optimum initial concentration
PFBA(213)C4	26	100	20
PFPeA(263)C5	23	100	20
PFHxA(313)C6	31	100	20
PFHpA(363)C7	20	100	20
PFOA(413)C8	28	100	20
PFNA(463)C9	19	100	1
PFDA(513)C10	27	100	1
PFA(563)C11	21	100	1
PFBuS(299)C4	21	100	20
PFHS(399)C6	17	100	1
PFOS(499)C8	18	100	1

Table 3.5 shows the summarized results of ferrate oxidation of PFCs. We tested different reaction combinations of initial PFCs concentrations and molar ferrate to PFCs molar ratios. The maximum PFCs reduction among all the combinations studied was 31.26%, which was given by PFHxA with molar ratio 100 and initial PFHxA concentration of 20 µg/L.

It was observed in this experiment that the percentage reduction of PFCs with sulfonate functional group is lower than that of PFCs with acid functional group. Higher polarity of the acid functional group may be the reason for this phenomenon. It is suspected that the main removal mechanism is adsorption rather than oxidation which is encouraged by higher surface charges.

This result totally agrees with the previous experiment done for PFCs oxidation with other oxidants. Yong Qiu et al. (2007) reported that PFCs cannot be decomposed by O_3/H_2O_2 . Occurrence of PFCs in drinking water is an example of ineffectiveness for PFCs oxidation by the common oxidants used in water purification process.

3.5 Summary

Ferrate(VI) technique has been identified as an emerging water purification technique and has proved its effectiveness to treat many organic and inorganic pollutants even at trace level. We tested the ferrate technique to oxidize PFCs at trace concentrations (from 0.1 to 25 μ g/L).

1. The best ferrate to PFCs molar ratio to reach maximum PFCs reduction was identified as 100.
2. It was noticed that the average elimination of PFCs with sulfonane functional group is 18% and acid functional group is 24%.
3. PFCs reduction by ferrate(VI) technique might occur due to adsorption than oxidation. It was also found that high ferrate(VI) to PFC molar ratio discouraged PFC removal. Coagulation property of ferrate(VI), which flocculate ferrite(III) particles might be reducing the adsorption effect.
4. It was concluded that ferrate technique alone is not sufficient to oxidize PFCs at environmental pressure and temperature.
5. Since the ferrate(VI) can oxidize many pollutants in water except PFCs, it might be useful in methodology development in PFCs determination, especially to degrade organic matrices in wastewater samples.

Chapter 4 PFCs adsorption (batch experiment)

4.1 Introduction

In 1970s, synthetic resin sorbents became available as an alternative to GAC. One of the major advantages of these resins over GAC is their on-site regeneratability through steam stripping, solvent extraction, or microwave irradiation. The ability to regenerate resins on-site potentially offers economic advantages over GAC, which typically requires off-site high-temperature incineration for regeneration. In addition, because the manufacturing process of synthetic resins is a controlled process, resins can have specially designed functional groups and pore size ranges that can be manipulated to optimize their performance for specific applications. Currently, synthetic resin sorbents are used in a variety of industrial applications such as purification processes in the food and drug industry, odor control, and industrial wastewater treatment. They have also been used in a number of groundwater remediation applications (e.g., removal of halogenated organic compounds) and landfill leachate purification (Melin, 1999)

The higher unit costs of resins compared to the more traditional sorbent GAC has been mainly responsible for the limited applications of resin sorbents. The recent developments have suggested that synthetic resin sorbents may be economically competitive with other more established treatment technologies (AOPs, and GAC) for removing some organic compounds.

Improvements in resin regeneration processes such as steam regeneration, solvent regeneration, and microwave regeneration may make the life cycle cost of a resin system competitive or, perhaps, more economical than other options. Also the resins (unlike AOPs) do not produce oxidation by-products. The effectiveness of resin sorbents for PFCs removal is evaluated in this chapter.

4.1.1. Process principle

Synthetic resins, like the widely used GAC, rely on sorption processes to remove organic compounds from water. In the context of water treatment, the process of interest generally involves the sorption of contaminants, such as certain ions or organic compounds from water by porous solid or semi-solid sorbent particles. The sorption of compounds by such sorbents occurs because of two primary driving forces: the hydrophobic character of the sorbate and/or the high affinity of the sorbate for the sorbent. For the majority of systems encountered in water and wastewater treatment systems, sorption results from the net effect of the combined interaction of these two driving forces (Weber, 1972). The hydrophobicity of a compound is inversely proportional to its solubility in water. An extremely hydrophobic compound has a low aqueous solubility and, thus, may prefer to adsorb onto

a solid surface or into an amorphous matrix rather than remain surrounded by water molecules. On the other hand, hydrophilic compounds tend to be stable in aqueous solutions and will leave the solution only if the sorbent provides an attractive force sufficient to overcome the strong bonds between the compound and water molecules. This attractive force, or affinity of the compound for the sorbent, can result from physical or chemical mechanisms. Physical mechanisms include dipole-dipole interactions and Vander-Waals interactions. This intermolecular interaction results in a net attraction between the two molecules (Montgomery, 1985). When two neutral molecules that lack permanent dipoles approach each other, a weak polarization is induced in each because of quantum mechanical interactions between their charge distributions. As a general rule, Vander-Waals interactions increase with increasing size or surface area of the molecules involved (Schwarzenbach et al., 1993). Vander-Waals interactions are generally weaker than dipole-dipole interactions.

4.1.2 Synthetic Polymer Production and application

Non ion-exchange resins and ion-exchange resins are manufactured through very similar processes and are often created from the same base material or polymer backbone. The main difference between the two products is that ion-exchange resins contain charged functional groups, which can form chemical bonds with ions in the solution while non ion-exchange resins rely on physical or non-ionic interactions to remove contaminants from water. In addition to their chemical composition, resins are differentiated on the basis of their pore size distributions. As a matter of convention, micropores are defined as pores less than 20 angstroms (\AA) (2×10^{-9} m) in diameter, mesopores are between 20 to 500 \AA (2×10^{-9} to 5×10^{-8} m) in diameter, and macropores have diameters greater than 500 \AA . Synthetic resins generally have a more controlled and even distribution of pore sizes than GAC. In order to be useful for sorptive applications in water treatment, resins have an extensive network of micropores, similar to GAC, which creates high surface areas and abundant sorption sites.

To produce superior kinetics over GAC, resins are also designed with a significant percentage of pores in the mesopore and macropore size range, which can provide access to the inner surfaces of resins (Melin, 1999).

Similar to GAC, granular synthetic resins also can be used in fixed bed filters, particularly to eliminate organic pollutants. In the real applications, the process flow configuration of synthetic resin systems is very similar to that of GAC systems. The main difference between two systems is the provision for a regeneration process for resin systems as resins can be regenerated on-site (Melin, 1999). Sorbent columns can be operated in series, in parallel, or as a combination of the two configurations depending on a number of factors, including the need for

continuous operation, space constraints, effluent criteria, service cycle time constraints, operation logistics, and requirements for multi-barrier treatment. (Weston, 1995). However, the higher unit costs of resins compared to the more traditional sorbent GAC has been mainly responsible for the limited applications of resin sorbents in drinking water treatment scenarios (Melin, 1999).

4.1.3 Non ion-exchange Resins

Non ion-exchange polymeric resins are typically based on cross-linked polymers having polystyrene, phenolformaldehyde, or acrylate matrices (Faust and Aly, 1998). Most commercial macroporous polymeric sorbents are based on polystyrene-divinylbenzene copolymers (Neely, 1982) in which the divinylbenzene serves as a cross-linking agent that makes the styrene insoluble and confers physical strength to the resin (DeSilva, 1995). Although they can be based on the same matrices, polymeric resins differ from traditional ion-exchange resins in their lack of ionic functional groups.

4.1.4 Ion-exchange resins

4.1.4.1 Fundamentals of Ion-Exchange

Ion-exchange is the reversible interchange of ions between a solid (ion exchange material) and a liquid in which there is no permanent change in the structure of the solid. Ion-exchange is used in water treatment and also provides a method of separation in many non-water processes. It has special utility in chemical synthesis, medical research, food processing, mining, agriculture and a variety of other areas.

Ion-exchange occurs in a variety of substances and it has been used on an industrial basis since 1910 with the introduction of water softening using synthetic zeolites. Sulfonated coal, developed for industrial water treatment, was the first ion-exchange material that was stable at low pH. The introduction of synthetic organic ion-exchange resins in 1935 resulted from the synthesis (Adams et al., 1935) of phenolic condensation products containing either sulfonic or amine groups which could be used for the reversible exchange of cations or anions. A variety of functional groups have been added to the condensation or addition polymers used as the backbone structures. Porosity and particle size have been controlled by conditions of polymerization and uniform particle size manufacturing technology. Physical and chemical stability have been modified and improved. As a result of these advances, the inorganic exchangers (mineral, greensand and zeolites) have been almost completely displaced by the resinous types except for some analytical and specialized applications. Synthetic zeolites are still used as molecular sieves.

4.1.4.2 Cation Exchange Resins

Weak acid cation exchange resins are based primarily on acrylic or methacrylic acid that has been crosslinked with a di-functional monomer (usually divinylbenzene [DVB]). The manufacturing process may start with the ester of the acid in suspension polymerization followed by hydrolysis of the resulting product to produce the functional acid group. Weak acid resins have a high affinity for the hydrogen ion and are therefore easily regenerated with strong acids.

4.1.4.2 Anion Exchange Resins.

Strong base anion resins are classed as Type 1 and Type 2. Type 1 is the reaction of trimethylamine with the copolymer after chloromethylation. The Type 1 functional group is the most strongly basic functional group available and has the greatest affinity for the weak acids such as silicic acid and carbonic acid, which are commonly present during a water demineralization process. However, the efficiency of regeneration of the resin to the hydroxide form is somewhat lower, particularly when the resin is exhausted with monovalent anions, such as chloride and nitrate. The regeneration efficiency of a Type 2 resin is considerably greater than that of Type 1. Type 2 functionality is obtained by the reaction of the styrene-DVB copolymer with dimethylethanolamine. This quaternary amine has lower basicity than that of the Type 1 resin, yet it is high enough to remove the weak acid anions for most applications. The chemical stability of the Type 2 resins is not as good as that of the Type 1 resins, the Type 1 resins being favored for high temperature applications (Wheaton and Lefevre 2000).

4.1.4.3 Resins Capacity

Ion exchange capacity may be expressed in a number of ways. Total capacity, i.e., the total number of sites available for exchange, is normally determined after converting the resin by chemical regeneration techniques to a given ionic form. The ion is then chemically removed from a measured quantity of the resin and quantitatively determined in solution by conventional analytical methods. Total capacity is expressed on a dry weight, wet weight or wet volume. The ion exchange capacities relevant with the resins used in this study is tabulated in **Table 4.2**.

4.2 Objectives

The aim of this study is to investigate on different potential granular materials to identify optimum adsorbent to eliminate PFCs. Two ion-exchange resins and four non ion-exchange resins were tested.

The specific objectives of the study explained in this chapter are listed below

1. To optimize the methodology for bottle point experiment.
2. To determine the PFCs sorption capacities of ion-exchange polymers, non ion-exchange polymers and activated carbon by fitting the bottle point experimental data into a suitable sorption model.
3. To determine the PFCs sorption kinetic characteristics of ion-exchange polymers, non ion-exchange polymers and activated carbon.
4. To check the suitability of new materials with actual wastewater

4.3 Experimental Description

4.3.1 Materials

Four kinds of non ion-exchange polymers, two kinds of ion-exchange polymers and one kind of GAC were studied in details. Some physical properties of these materials are shown in the **Tables 4.1, 4.2 and 4.3**. All granular materials were purchased from WAKO Company (Japan). Almost all the granular materials are specifically produced for water and wastewater treatment particularly to eliminate organic compounds in water.

Table 4.1 Physical properties of non ion-exchange polymers

Adsorbent	Matrix*	Surface area* (m ² /g)	Specific gravity	Physical form	Diameter (mm)
Dow V493	Styrene-DVB, macroporous	1025	>1	orange to Brown spheres	0.8
Dow L493	Styrene-DVB, macroporous	1100	>1	orange to brown spheres	0.8
Dow V503	Styrene-DVB, macroporous	2003	<1	orange to brown spheres	0.85– 1.1
Amb XAD 4	Macroreticular crosslinked aromatic polymer	>750	>1	white translucent beads	0.35-1.18

*Provided by the supplier

Table4.2 Physical properties of ion-exchange polymers

Adsorbent	Matrix	Exchange capacity	Functional group	Diameter (mm)
Amb IRA-400	Styrene-DVB	3.0-3.5 (eqkg ⁻¹)	-N ⁺ R ₃ (Cl)	0.8
Dow MarathonA	Styrene-DVB	1.3 (eqL ⁻¹)	Quaternary Amine	0.57

Table 4.3 Physical properties of GAC (Filtersorb 400, coal based)

Total pore volume	0.61 cm ³ /g
Macropores (>500 A)	0.04 cm ³ /g
Mesopores (20-500 A)	0.09 cm ³ /g
Micropores (<20A)	0.48 cm ³ /g
Surface area	900-1100 m ² /g
Matrix	Stacked layers of fused hexagonal ring of C atoms
Diameter	0.25-0.50 mm

4.3.2 Material cleaning - Synthetic polymer materials.

Prior to the use in the sorption experiment, the resins were first washed in deionized water to remove dirt and then dried at 50°C (Qiang Yu, 2009). After draining, the materials were washed with MeOH (LC/MC grade) to ensure the materials are free of PFCs. Then the materials are again washed with deionized water and dried at 50°C till the weight is constant. Dried materials are stored in airtight container to prevent contamination of prepared material from external PFCs and moistures.

Above procedure was applied for both ion-exchange polymers of Dow MarathonA, Amb IRA-400 and non ion-exchange polymers of Dow V493, Dow L493 and Dow V503. The process was little changed for gel type non ion-exchange polymer of AMB XAD-4 as it was observed that the sorption capacity of this polymer is drastically reduced by drying at 50°C and the drying temperature was changed to 30°C. In order to make the correction for the moisture content at the material comparison, a separate experiment was carried out to determine the moisture content of AMB XAD4 at 50°C.

4.3.3 Material cleaning - Cleaning of GAC.

The GAC were first boiled in deionized water for one hour to remove fine particles and preloaded organics. Floating impurities and grease were readily removed from water surface during boiling. Right after boiling, GAC was flushed with abundant pure water to cool and clean carbons. After intensive washing, carbons were submerged in pure water and stored in room temperature overnight to equilibrate surface properties. The water was discarded and GAC was moved into an oven and dried up at 105°C for around two days to completely remove moisture inside pores (Kimura 2007). In order to obtain GAC in required diameters, dried GAC was firstly pulverized in a mortar by a pestle. Then the crushed GAC was separated by sieving in required ranges of diameters. The fine particles or powders attached on the surface of crushed GAC during pulverization should be

removed before experiments. Therefore, sieved GAC was washed again by deionized water, and used water with fine particles is poured out carefully. The washing step was repeated for several times until the water over GAC granules was clean and clear. The washed GAC was again dried in oven at 105°C for around two days and stored in airtight bottles. Benefited from former cleaning process, granular materials can be precisely weighed before experiments. After weighing, dried granular materials were moved into PP sampling valves (2mL) and soaked in small amount of pure water (1mL) to pre-wet inner pores by Applying a vacuum for 24 hrs. This step is important and necessary because air inside pores might adversely reduce adsorption capacity and velocity (Nicholas and Paul 1993). After pre-wetted, excessive water was discarded by pipette and the materials are added to the bottles which were filled with PFCs solutions.

4.3.4 Preparation of PFCs solutions

PFCs solutions were prepared from stock solutions by diluting them in MilliQ water or wastewater matrix. Since the working maximum PFCs concentration was not exceeding 10 μ Mol/L, pH was not significantly changed (6.4 – 6.9) and did not add any buffer solutions to control pH. Mainly two types of PFCs solutions were prepared for the batch experiment. First kind of PFCs solutions were prepared by dissolving individual PFCs in MilliQ water to determine isotherm and kinetic characteristics of each granular materials tested in this study. A series of individual PFCs solution with different concentration was prepared by adding required volume of stock solution in to MilliQ water and thoroughly mixing it (manual mixing and ultra-sonication).

The applicability of the real wastewater was examined in this study with batch test experiment with effluent wastewater from a PFCs related industry. The effluent wastewater was directly applied for the test without any pre preparation. The PFCs concentration of the wastewater was not changed by spiking PFCs solutions.

4.4 Experimental methods

4.4.1 Experimental apparatus

The batch test experiment was carried in a thermo-stat shaker with shaking speed of 140 rpm at 25°C. In the shaker, the prepared sample bottles were horizontally packed and clamped to the shaking basin. The arrangement is schematically shown in **Figure 4.1**. The volume of the sample bottle was 125mL and the screw type lid tightly closed the bottle. The temperature in the bottle was controlled by controlling the water bath temperature at 25°C.

4.4.2 Experimental conditions

Three series of batch experiments were carried out to meet the objectives with the apparatus shown in **Figure 4.1**. Details of each batch test are explained by following paragraphs.

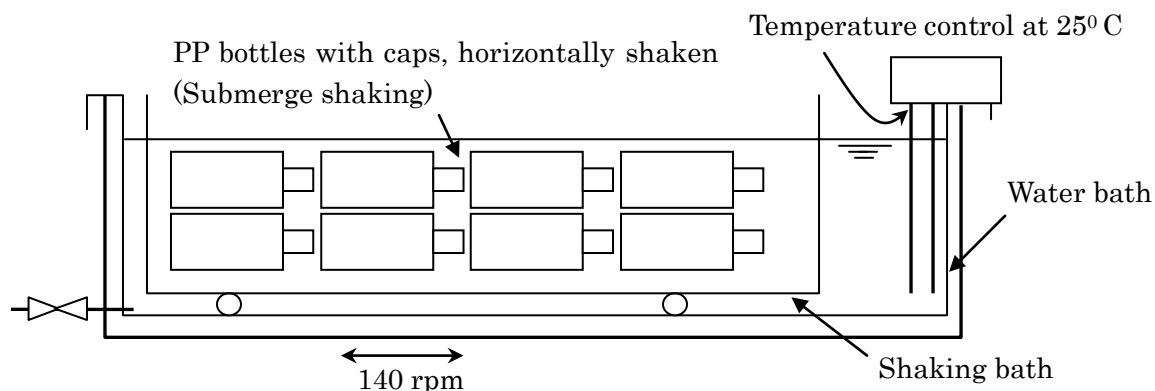


Fig 4.1 Schematic diagram of batch test experiment to understand isotherm and kinetic characteristics of different granular materials

4.4.2.1 Isotherm experiments with different changing parameters

In the isotherm experiment sorption capacity was calculated with respect to different equilibrium concentrations. The shaking duration was 100 hrs and it was ensured that all the granular materials reached their equilibrium concentration within this shaking time. Different equilibrium concentrations could be reached by two methods, i.e. by changing initial sorbate concentration, while keeping the sorbent concentration constant and by changing the sorbent concentration, while keeping the sorbate concentration constant.

Sorption isotherm of GAC was tested by both methods and the experimental conditions are listed in **Table 4.4**.

4.4.2.2 Batch test to determine isotherm characteristics of individual PFCs

Adsorption isotherm characteristics of individual PFCs on different granular materials were studied by constant sorbent concentration method. For the known PFCs of PFOA, PFHxA and PFOS, ion-exchange, non ion-exchange and GAC were tested and other selected PFCs only non ion-exchange and GAC materials were tested. **Table 4.5** shows the individual combinations studied in this experiment. The conditions of the experiment are shown in **Table 4.6**.

Table 4.4 Experiment condition for sorption isotherm experiment

Parameter	Constant sorbate concentration	Constant sorbent concentration
Adsorbate concentration ($\mu\text{g/L}$)	2000	30, 60, 120, 250, 800, 2000, 5000
Selected adsorbent	F-400 (GAC)	F-400 (GAC)
Selected adsorbates	PFOA, FFHpA	PFOA, FFHpA
Adsorbant concentration (g/L)	0.05, 0.1, 0.3, 0.8, 1.0, 1.5, 2.0	1 ± 0.05
Shaking time (hrs)	100	100
Volume (mL)	100	100
Temperature ($^{\circ}\text{C}$)	25	25
Shaking speed (rpm)	150	150
pH	$6.4 < \text{pH} < 6.6$	

4.4.2.3 Batch test to examine the applicability of new materials to real wastewater

Treated wastewater was collected from the wastewater treatment plant in a PFCs related industry. This wastewater has been identified as one of a major PFCs polluter in Okayama prefecture (Okamoto, 2010) it was measured that the level of POFA in this wastewater is more than $4 \mu\text{g/L}$. Since the level of PFCs in this wastewater was kept unchanged the sorbent concentration was changed in this experiment to get different equilibrium concentrations. The experimental conditions are tabulated in **Table 4.7**.

Table 4.5 Different sorbent-sorbate combinations considered for individual batch experiments to determine the characteristics of sorption isotherms kinetics

	PFBA	PFHxA	PFHpA	PFOA	PFDA	PFOS
Dow V493	√	√	√	√	√	√
Dow L493	√	√	√	√	√	√
Dow V503	√	√	√	√	√	√
Dow V503	√		√		√	√
Amb XAD 4	√	√	√	√	√	√
Amb IRA-400		√		√		√
Dow MarathonA		√		√		√
F400(GAC)	√	√	√	√	√	√

Table 4.6 Experiment condition for sorbent-sorbate combination (Table 4.4) for the sorption isotherm experiment-2

Parameter	Set value
Adsorbate concentration ($\mu\text{g/L}$)	10, 30, 60, 120, 250, 500, 1000, 2000, 5000
Shaking time (hrs)	100
Volume (mL)	100
Temperature ($^{\circ}\text{C}$)	25
Shaking speed (rpm)	150
Adsorbant concentration (g/L)	1 ± 0.05
pH	$6.4 < \text{pH} < 6.9$
Sampling	
<i>Before shaking (one sample from each bottle)</i>	<i>1*9</i>
<i>After shaking (two samples from each bottle)</i>	<i>2*9</i>

Table 4.7 Experiment condition for sorption isotherm for industrial wastewater

Parameter	Set value
Adsorbate concentration ($\mu\text{g/L}$)	PFCs related industrial wastewater-PFOA is dominant ($\approx 4 \mu\text{g/L}$)
Selected adsorbent	Dow V493, Dow L493, Amb XAD 4, Amb IRA-400, Dow MarathonA, F400(GAC)
Adsorbant concentration (g/L)	0.01, 0.02, 0.05, 0.08, 0.1
Shaking time (hrs)	100
Volume (mL)	100
Temperature ($^{\circ}\text{C}$)	25
Shaking speed (rpm)	150
pH	7
Sampling	
<i>Before shaking</i>	<i>1*6*5</i>
<i>After shaking</i>	<i>2*6*5</i>

4.4.2.4 Batch test to determine kinetic characteristics.

A series of experiments were carried out to determine kinetic characteristics for different sorbent-sorbate combinations. Similar to the second experiment of isotherm test, separate batch tests were carried out for each sorbent-sorbate combination as tabulated in Table 4.5. Contrasting to the sorption test, the sampling was done at different time intervals. The experiment conditions are summarized in **Table 4.8**.

Table 4.8 Experiment condition for sorbent-sorbate combinations (Table 4.5) for the sorption kinetic experiment

Parameter	Set value
Adsorbate concentration ($\mu\text{g/L}$)	500, 5000
Sampling intervals (hrs)	0, 1.5, 4.5, 21, 72, 100
Shaking time (hrs)	100
Volume (mL)	100
Temperature ($^{\circ}\text{C}$)	25
pH	6.4-6.8
Shaking speed (rpm)	150
Adsorbant concentration (g/L)	1 ± 0.05

4.5 Modeling and simulation

4.5.1 Adsorption isotherms models

An adsorption isotherm describes the equilibrium of the sorption of a material at a surface (more general at a surface boundary) at a constant temperature. It represents the amount of material bound at the surface as a function of the material present in the solution. Sorption isotherms are often used as empirical models (Atkin 1998). Yong (2007) has summarized some of these equations as tabulated in **Table 4.9**.

Even though a number of isotherm equations are suggested based on different assumptions Freundlich equation and Langmuir equation are widely applied in water and wastewater treatment. Especially for the low equilibrium concentrations, Freundlich equation is the only possible isotherm equation to model the experimental data.

Table 4.9 summary of adsorption isotherm models developed with various assumptions

Assumption	Name	Equations	Conditions	Comments
Single layer local site	<i>Generalized Langmuir</i>	$\frac{q}{q_m} = \left[\frac{(Kc)^n}{1 + (Kc)^n} \right]^{m/n}$	$n=m=1$	Langmuir
			$0 < n = m < 1$	Langmuir-Freundlich
			$n=1, 0 < m < 1$	General. Freundlich
			$m=1, 0 < n < 1$	Tóth
Multilayer adsorption	<i>B.E.T.</i>	$\frac{q}{q_m} = \frac{1}{1-x} \cdot \frac{Kx/(1-x)}{1 + Kx/(1-x)}, x = \frac{c}{c_s}$		Hüttig
				Sircar
				Lopez-Gonzalez&Dietz
Micropore filling	<i>Dubinin- Astakhov</i>	$\frac{q}{q_m} = \exp \left[-B(RT)^n \ln^n \frac{C_s}{C} \right]$	$n=1$	Freundlich
			$n=2$	Dubinin-Raduskevich
			$n=i, \sum$	Exponential Jaroniec
Empirical	<i>Freundlich</i>	$q = Kc^n$		Narrow c range, but large range for GAC
	<i>Radke-Prasunitz</i>	$q = \frac{AKc}{1 + (Kc)^n}$		Combine Henry ($q=Kc$) and Freundlich ($q=Kc^m$), better performance than either
	<i>Jossens</i>	$Kc = q \cdot \exp(B \cdot q^m)$		Exponentially depend on isosteric heat
	<i>Tiemkin</i>	$q = A + B \log c$		Suitable for gas catalyst

Note: q is adsorbent loading rate, q_m is maximum loading rate, c is bulk concentration, c_s is saturated bulk concentration, K , A and B are adsorptive coefficients, n , m and R are constants, T is temperature.

Freundlich equation is an empirical relationship describing the adsorption of solutes from a liquid surface to a solid surface. It is widely applied to describe adsorption process for many compounds on to heterogeneous surfaces, including activated carbon, metals and polymers in dilute solutions (Bruce et al., 1997; Robert et al., 2000; Sirinivasan et al., 2008).

The Freundlich equation is defined by

$$q_c = K_f C_e^{1/n} \quad 4.1$$

the equation can be rewritten as

$$\text{Log}(q_c) = \text{Log}(K_f) + 1/n \text{Log}(C_e) \quad 4.2$$

where q_c ($\mu\text{g/g}$) is the concentration in the solid phase, C_e ($\mu\text{g/L}$) is the equilibrium concentration of solute in solution, K_f ($\mu\text{g/g})(\mu\text{g/L})^{-1/n}$ is the Freundlich adsorption constant or capacity factor and n is the Freundlich exponent.

Parameters of K_f and n in Freundlich equation were determined by least square fitting of experiment data on q and C_e , as shown in **Eq. (4.2)**.

According to the **Eq 4.1** adsorption capacity of a given sorbent (given sorbent concentration) is a constant for a given equilibrium concentration of a given sorbate (at given temperature).

The Freundlich isotherm is known to be operative only within certain concentration limits. This is because, given an exponential distribution of binding sites, the number of sites increases indefinitely with a decreasing association constant, implying that there are infinite number of sites. But the Freundlich isotherm will be a more accurate approximation at lower concentrations (Robert et al., 2001).

Most of the polymers tested in this study are widely used in water and wastewater treatment, particularly for organics. The adsorptive capacities of tested polymers at low concentrations (1 ng/L – 1 $\mu\text{g/L}$) were calculated with the Freundlich constants determined by the experiment.

In the case of unit equilibrium concentration (in this study $C_e = 1 \mu\text{g/L}$) the effect of power n can be neglected and the amount of PFCs adsorbed in to the polymer at this equilibrium concentration is given by K_f

4.5.2 Kinetics models

To further understand the sorption kinetics, the pseudo second-order model was selected to fit the kinetic data. The model assumes that the sorption rate is controlled by chemical sorption and the sorption capacity is proportional to the number of active sites on the sorbent (McKay 1999).

The concept is mathematically expressed in the **Eq 4.3**.

$$\frac{\delta q_t}{\delta t} \propto (q_e - q_t)^2 \quad 4.3$$

or

$$\frac{dq_t}{dt} = k_2 (q_e - q_t)^2 \quad 4.4$$

Where q_e and q_t are the sorption capacity at equilibrium and at time t , respectively and k_2 is the rate constant of the pseudo-second order sorption. For the boundary conditions $t = 0$ to $t = t$ and $q_t = 0$ to $q_t = q_t$, the integrated

form of **Eq 4.4** becomes:

$$\frac{1}{q_e - q_t} = \frac{1}{q_e} + k_2 t \quad 4.5$$

Which is the integrated rate law for a pseudo-second order reaction. **Eq 4.5** can be rearranged to obtain

$$q_t = \frac{1}{\frac{1}{k_2 q_e^2} + \frac{t}{q_e}} \quad 4.6$$

Which has a linear form:

$$\frac{1}{q_t} = \frac{1}{k_2 q_e^2} + \frac{1}{q_e} \quad 4.7$$

4.6 Results and Discussion

4.6.1 Time required to reach the equilibrium concentration

In the sorption experiment, it is essential to reach all the sorbate in the bottles into the equilibrium concentration with the sorbent added in each bottle. **Figure 4.2** shows the variations of material sorption capacities with time for PFOS and PFHxA. It was clearly identified that ion-exchange polymers and GAC reached their equilibrium concentrations much earlier than non ion-exchange polymers. Since a comparative study was to be done with work, a common shaking duration of 100 hrs was selected. It was ensured with **Figure 4.2** that all kinds of granular materials had reached their equilibrium concentrations during this shaking period.

4.6.2 Determination of isotherm characteristics with different methodologies

In order to determine the sorption isotherms, it is required to determine different sorption capacities at different equilibrium concentrations. In the experiment, actual equilibrium concentration was measured and based on which, material adsorption capacity was calculated with known values of initial sorbate and sorbent concentrations.

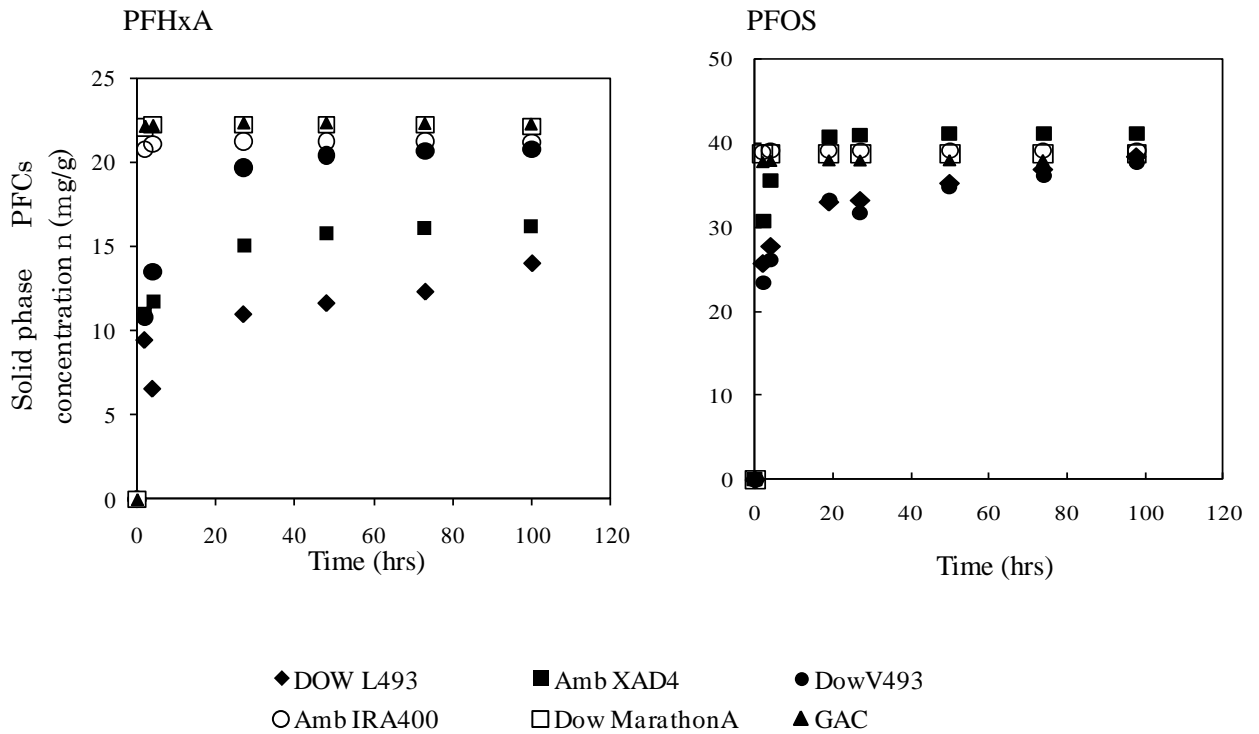


Fig 4.2 Time requirement for different granular materials to reach equilibrium concentration

Different initial concentrations can be achieved by two methods, i.e. by changing initial sorbate concentration while keeping the sorbent concentration constant, or changing sorbent concentration while keeping the sorbate concentration constant. Isotherm characteristics of GAC were checked with both methods and the Freundlich isotherm curves drawn with different methods are shown in **Figure 4.3**. It was found that the Freundlich curves given by two methodologies were not same. The Freundlich coefficient given by constant sorbate method was 7.10 and same coefficient given by constant sorbent method was 24.51.

The experiment was repeated with different PFCs and found that constant sorbent method was better than constant sorbate method for isotherm experiments. It was noticed several times that unrealistic results were given by constant sorbate method. In this experiment, granular materials were shaken for 100 hrs in a 120 mL horizontally mounted PP bottles. It was assumed that the sorbate and sorbents are homogeneously mixed in the bottles during the shaking experiment. But in the real application it was noticed that heavy granular materials were confined into channels along with the hydraulic eddies, which are created by the constant shaking speed.

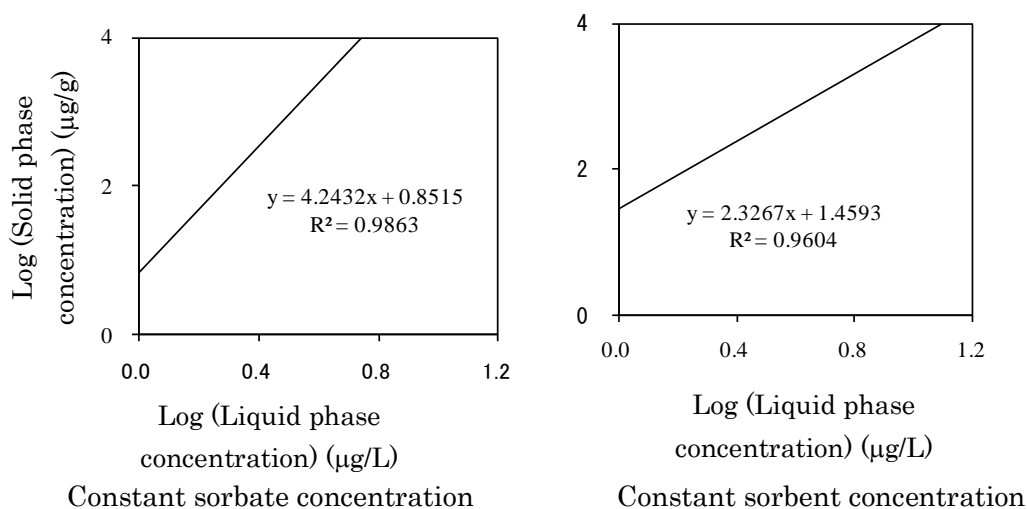


Fig 4.3 Freundlich isotherm curve drawn with different experimental methods

Due to this reason, changing of initial sorbent concentration seems not effective compared with the constant sorbent method, where initial PFCs concentration is changed. Constant sorbent method was selected for the determination of isotherm characteristics in this chapter as discussed below.

4.6.3 Isotherm experiment for individual coagulants with individual PFCs

4.6.3.1 Non Ion-Exchange polymers

The values determined for the Freundlich constants are listed in **Table 4.10**. It was found that isotherms of all non ion-exchange granular medias were nicely fixed with Freundlich isotherm ($R^2= 0.76-0.99$). Freundlich exponent (n) is an indicator of nonlinearity of Freundlich curve. Nonlinearity can occur due to many reasons including the sorption site heterogeneity and sorbate-sorbate interactions (Cheung, 2001). In this study GAC gave comparatively higher nonlinearity. It might be due to the sorption site heterogeneity of GAC is higher than that of synthetic polymers. **Table 4.3** shows physical properties of GAC which could be calculated that more than 78% of total pore volume in GAC was occupied by micro pores, 14% meso pores and the rest was occupied by macro pores (Table 4.3). Pores in the GAC with different sizes occurred when it was prepared under controlled pressure and temperature.

Even though pore size distribution is comparatively uniform for synthetic non ion-exchange polymers there is a procedure to add some macro pores to enhance kinetic characteristics. To produce macroporous polymeric resins, the polymerization process was carried out in the presence of an inert material. Small amount of an inert material yields a non-macroporous,

three-dimensional network while a high inert material content leads to the formation of microstructures, or nuclei. As the polymerization progresses, the nuclei agglomerate and crosslink to form microspheres. Aggregates of microspheres form irregularly shaped particles, which constitute the resin beads (Malley et al., 1993). The pore size distribution of polymeric resins can also be controlled during their manufacture by varying the amount of extender used in the polymerization reaction; this governs the degree of cross-linking and the ultimate pore structure created (Weber and van Vliet, 1981).

In the case of unit equilibrium concentration (in this study $C_e = 1 \mu\text{g/L}$) the effect of power n can be neglected and the amount of PFCs adsorbed into the polymer at this equilibrium concentration is given by K_f . It was noticed that K_f was increased with the length of the carbon chain for all adsorbents suggesting longer chain PFCs can be easily adsorbed. Same results have been obtained in a previous research (Yong, 2007). However in actual situation PFCs in discharge water should be in ng/L level. Calculated q_c values for 3 different equilibrium concentrations (1, 10 and 100 ng/L) with Freundlich equation are tabulated in **Table 4.10**. It was interesting to notice that synthetic polymer materials show better sorption capacities than GAC at low equilibrium concentrations. This might be the reason of failure for application of GAC to eliminate PFCs in German drinking water treatment plants (Schaefer, 2006).

Figure 4.4 shows the PFDA adsorption curves for synthetic non ion-exchange polymers and GAC. For the long chain PFCs of PFDA, highest K_f was given by Amb XAD 4 (2965) followed by Dow L493 (434.51), Dow V493 (415.91) and GAC (121.89).

Table 4.10 Freundlich constants for different sorbent/ sorbate combinations and calculated q_c for different C_e (ng/L) based on K_f and n values

Adsorbate	Adsorbent	Freundlich Isotherm parameter			q_c^{*2}		
		K_f^{*1}	n	R^2	C_e^{*3} =1	C_e^{*3} =10	C_e^{*3} =100
PFBA	Dowexoptopore V493	4.61	0.872	0.89	0.011	0.083	0.619
	Dowexoptopore V503	0.62	1.020	0.99	0.001	0.006	0.059
	Dowexoptopore L493	1.70	0.984	0.99	0.002	0.018	0.176
	Amberlite XAD 4	5.23	0.953	0.99	0.007	0.065	0.583
	Filtrisorb 400 (GAC)	13.36	0.979	0.98	0.015	0.147	1.402
PFHxA	Dowexoptopore V493	176.36	0.663	0.97	1.809	8.325	38.318
	Dowexoptopore L493	20.66	0.659	0.95	0.218	0.993	4.530
	Amberlite XAD 4	62.82	0.516	0.96	1.779	5.836	19.147
	Filtrisorb 400 (GAC)	344.03	1.023	0.94	0.293	3.095	32.628
PFHpA	Dowexoptopore V493	71.88	1.174	0.99	0.022	0.323	4.815
	Dowexoptopore V503	1.95	0.835	0.99	0.006	0.042	0.285
	Dowexoptopore L493	35.16	0.686	0.99	0.308	1.493	7.245
	Amberlite XAD 4	78.27	0.977	0.89	0.092	0.870	8.253
	Filtrisorb 400 (GAC)	53.26	1.924	0.90	0.000	0.008	0.634
PFOA	Dowexoptopore V493	998.45	0.404	0.80	61.281	155.355	393.846
	Dowexoptopore L493	208.26	0.500	0.94	6.586	20.826	65.857
	Amberlite XAD 4	554.50	0.541	0.93	13.201	45.888	159.514
	Filtrisorb 400 (GAC)	602.42	1.672	0.76	0.006	0.273	12.829
PFDA	Dowexoptopore V493	415.91	2.619	0.91	0.000	0.002	1.000
	Dowexoptopore V503	8.43	0.926	0.99	0.014	0.119	1.000
	Dowexoptopore L493	434.51	0.371	0.98	33.497	78.705	184.927
	Amberlite XAD 4	2965.00	1.418	0.86	0.165	4.325	113.246
	Filtrisorb 400 (GAC)	121.89	0.968	0.87	0.152	1.412	13.121

*¹Freundlich isotherm constants [$(\mu\text{g PFCs/g sorbent})(\mu\text{g PFCs/L})^{-n}$]

*²PFCs adsorbed on the adsorbent at equilibrium at equilibrium concentrations of 1,10 and 100 ng/L ($\mu\text{g/g}$)

*³Equilibrium concentration (ng/L)

PFDA adsorption by non ion-exchange polymers

But in further low concentrations of equilibrium concentration Dow L493 performed better than other polymers.

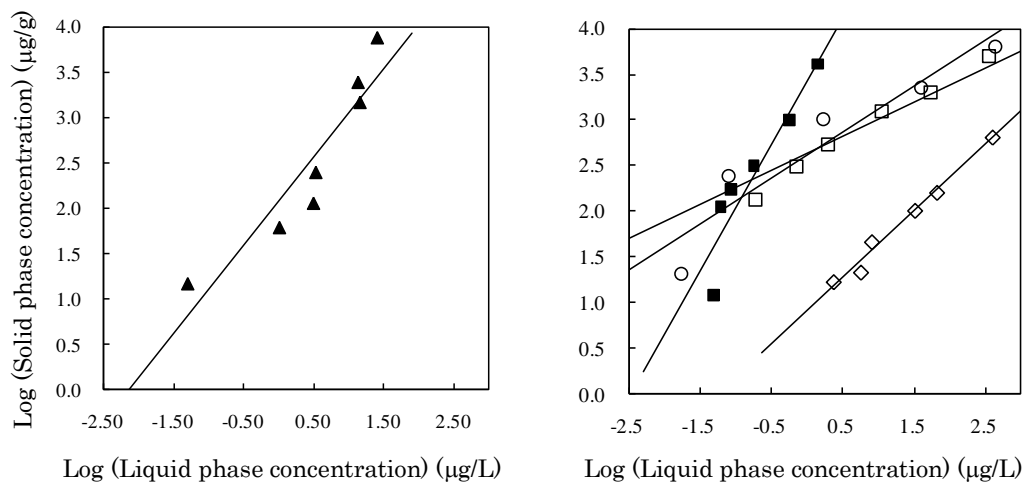


Fig 4.4 Adsorption isotherm of PFDA onto GAC(F400 - ▲), and non ion-exchange polymers (AmbXAD4 - ■ , Dow L493-□, Dow V493 - ○ and Dow V503 ◇)

PFOA adsorption by non ion-exchange polymers

Three kinds of synthetic non ion-exchange resins (Dow V493, Dow L493, Amb XAD4 and F400 (GAC)) were selected for this experiment. In the experiment, PFOA was identified as easily adsorbed PFCs like PFDA. Sorption capacity at unit equilibrium concentration of 1 µg/L, GAC showed higher sorption capacity of 602 µg/g which was the second best performance after Dow V493. But it was noticed that the sorption capacity at further low equilibrium concentrations of 100 ng/L and 10 ng/L of Amb XAD 4 showed better performances than GAC. **Figure 4.5** shows the variation of sorption capacity of each granular materials at equilibrium concentrations.

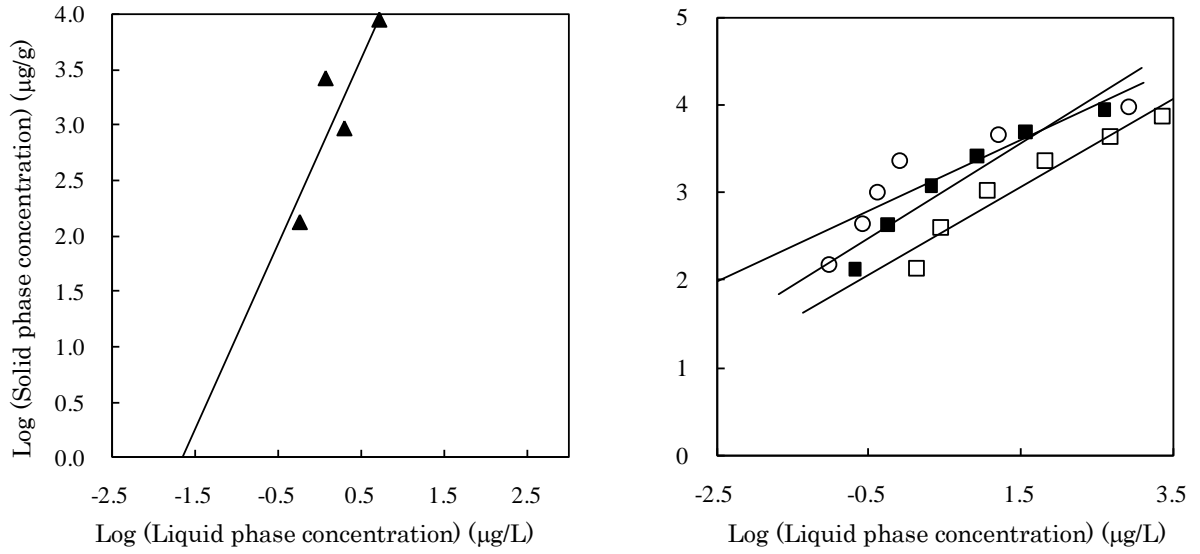


Fig 4.5 Adsorption isotherm of PFOA onto GAC(F400 - ▲) and non ion-exchange polymers (AmbXAD4 - ■ , Dow L493-□, Dow V493 - ○)

PFHpA adsorption by non ion-exchange polymers

PFHpA adsorption by four kind of synthetic non ion-exchange resins of Dow V493, Dow L493, Dow V503 and amb XAD4 and GAC were tested and

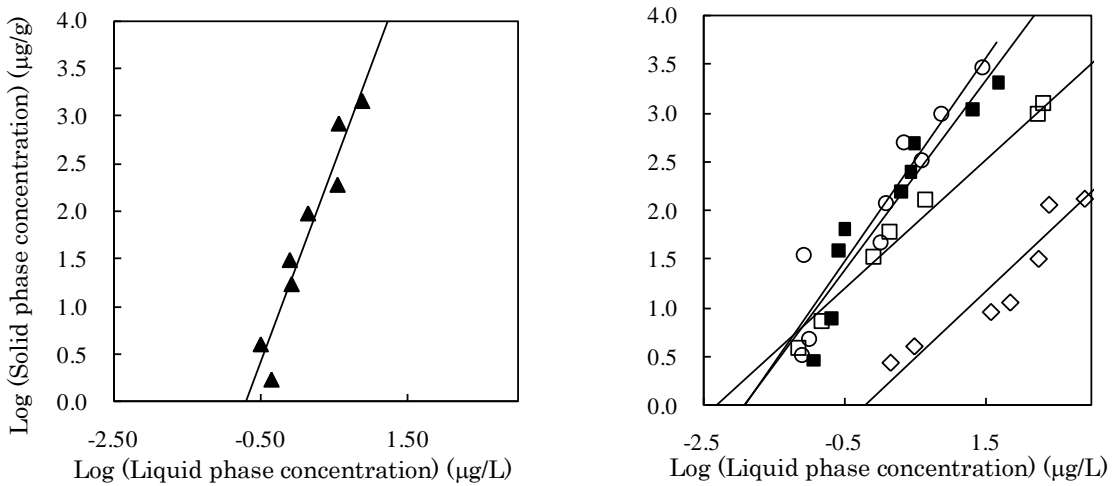


Fig 4.6 Adsorption isotherm of PFHpA onto GAC(F400 - ▲) and non ion-exchange polymers (AmbXAD4 - ■ , Dow L493-□, Dow V493 - ○, ◇ - Dow V503)

Figure 4.6 shows the adsorption isotherms determined for them. With the comparison of capacity factors determined for PFDA and PFOA, clear reduction was observed. Amb XAD4 was identified as the best candidate material to eliminate PFHpA from water.

PFHxA adsorption by non ion-exchange polymers

PFHxA dominates as a problematic PFCs, because some industries use it as an alternative for PFOS/PFOA. Three kind of synthetic non ion-exchange resins of Dow V493, Dow L493, Amb XAD4 and F400 (GAC) were selected for this experiment. GAC clearly showed the best sorption capacity at unit equilibrium concentration of 1 $\mu\text{g/L}$, but it was noticed that the other non ion-exchange polymers of Dow V493 and Amb XAD4 showed better sorption capacities at further low equilibrium concentrations. Ion-exchange resins showed the best performance for PFHxA elimination and it will be discussed later in this chapter.

Figure 4.7 shows the variation of sorption capacity of each granular material at equilibrium concentrations.

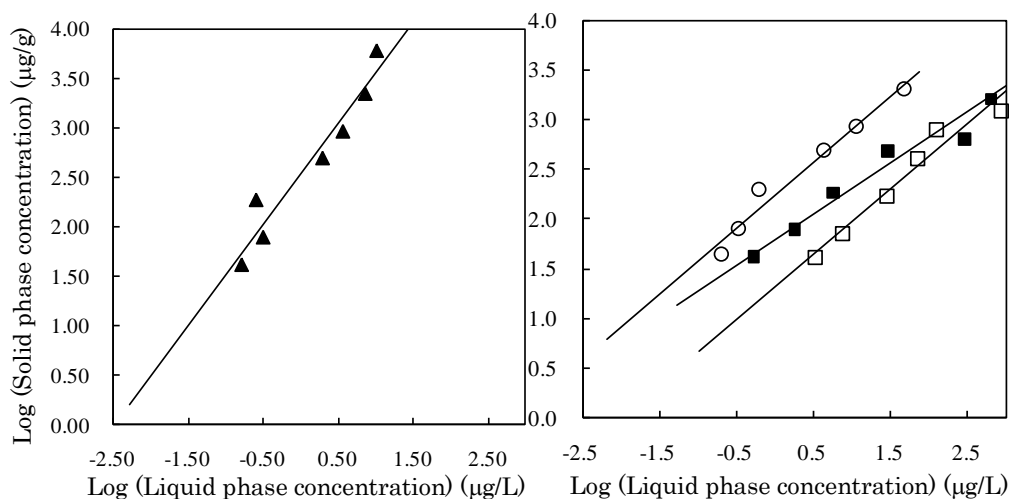


Fig 4.7 Adsorption isotherm of PFHxA onto GAC(F400 - ▲), and non ion-exchange polymers (AmbXAD4 - ■ , Dow L493-□, Dow V493 - ○)

PFBA adsorption by non ion-exchange polymers

PFBA is the shortest PFCs tested in this chapter. It is said that the level of toxicity for PFBA is not high as other long chain and medium chain PFCs because the retention time of PFBA is much lower than that of long chain and medium chain PFCs (verbal communication with US EPA). For this batch experiment, four kinds of synthetic non ion-exchange resins of Dow V493, Dow L493, Dow V503, Amb XAD4 and F400 (GAC) were selected. The sorption capacities determined by the results of the experiment clearly showed that the only possible non ion-exchange granular material to be

used for PFBA is GAC. This was valid even for the less equilibrium concentrations of 100ng/L, 10ng/L and 1 ng/L.

Figure 4.8 shows the variation of sorption capacities of each granular material at equilibrium concentrations.

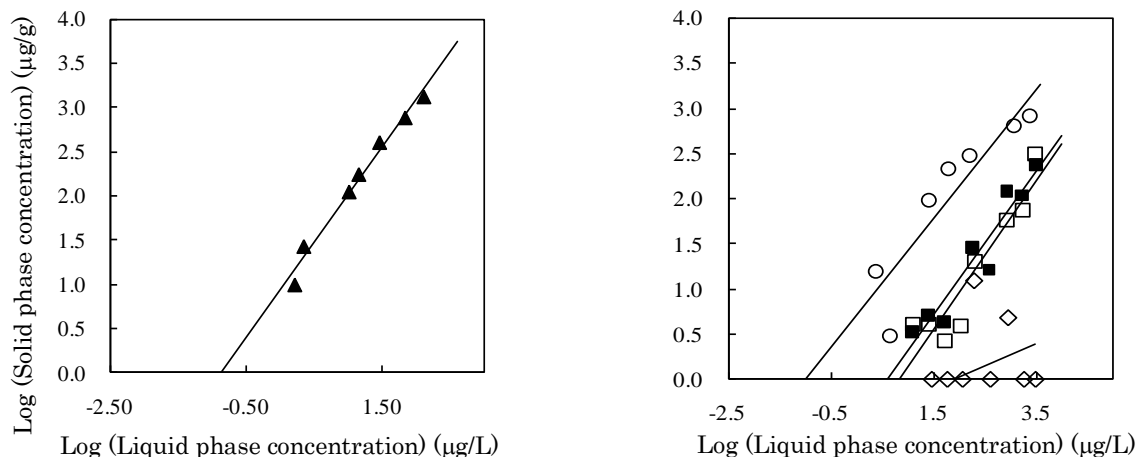


Fig 4.8 Adsorption isotherm of PFBA onto GAC(F400 - ▲), non ion-exchange polymers (AmbXAD4 - ■, Dow L493-□, Dow V493 - ○ and Dow V503 ◇)

4.6.3.2 Adsorption by ion-exchange polymers

Figure 4.9 and **4.10** show the isotherm curves of Amb IRA 400 and Dow Marathon A drawn for PFHxA and PFOA. Same materials were tested also with PFOS and the results are discussed under PFOS adsorption. The results of the experiment were modeled with Freundlich isotherm and the determined coefficients are shown in **Table 4.11**.

Comparing the same coefficient determined for GAC and non ion-exchange polymers, ion-exchange polymers showed excellent adsorption capacities for both PFCs at any equilibrium considered in the experiment. For PFOA adsorption, both ion-exchanges showed over 5000 µg/g of sorption capacity and unit equilibrium concentration, which is ten times higher than that of non ion-exchange polymers including GAC. Dow Marathon A showed the best performance to eliminate PFHxA.

Table 4.11 Freundlich constants for different sorbent/ sorbate combinations and calculated q_c for different C_e (ng/L) based on K_f and n values

Adsorbate	Adsorbent	Freundlich Isotherm parameter			q_c^{*2}		
		K_f^{*1}	n	R^2	C_e^{*3} =1	C_e^{*3} =10	C_e^{*3} =100
PFH A	Amb IRA-400	340.96	0.836	0.94	1.059	7.256	49.740
	Dow MarathonA	503.5	0.810	0.94	1.871	12.078	77.983
PFOA	Amb IRA-400	5154.23	0.712	0.73	37.633	193.983	999.917
	Dow MarathonA	6356.00	1.487	0.99	0.219	6.736	206.911

*¹Freundlich isotherm constants $[(\mu\text{g PFCs/g sorbent})(\mu\text{g PFCs/L})^{-n}]$

*²PFCs adsorbed on the adsorbent at equilibrium at equilibrium concentrations of 1, 10 and 100 ng/L ($\mu\text{g/g}$)

*³Equilibrium concentration (ng/L)

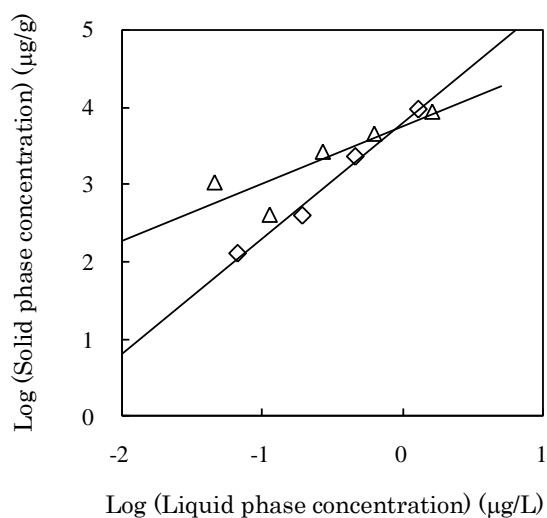


Fig 4.9 Adsorption isotherm of PFOA onto ion-exchange polymers (Amb IRA400 - Δ , Dow MarathonA- \diamond)

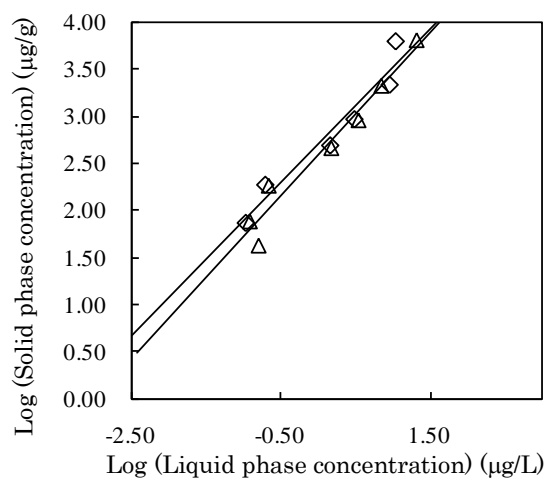


Fig 4.10 Adsorption isotherm of PFHxA onto ion-exchange polymers (Amb IRA400 - Δ , Dow MarathonA- \diamond)

4.6.3.3 PFOS adsorption

PFOS is the latest POPs categorized by the Stockholm Convention in May 2009. Many researchers work on the treatment of PFOS with different strategies and adsorption has been identified as a possible method. Ion-exchange resins, non ion-exchange resins and GAC were tested for PFOS adsorption and the isotherm curves drawn onto various adsorbents separately. The determined Freundlich constants are listed in **Table 4.12**. The shaking duration of isotherm experiment is 100 hrs and which ensures that all filter materials have reached their equilibrium concentrations. It was found that isotherms of all granular medias were nicely fixed with Freundlich isotherm ($R^2=0.92 - 0.99$).

Similar to the other PFCs in this chapter, Freundlich equation was used to calculate PFOS adsorption capacities onto various filter materials at further low equilibrium concentration of 100ng/L. Some possible errors can be expected with this calculation. Even though it is assumed in the calculation that all the materials follow Freundlich equation, practically all data points do not coincide with Freundlich curve ($R^2 \neq 1$). Also it should be emphasized that the minimum equilibrium concentration received in this experiment is 150ng/L.

4.6.3.3.1 Adsorption of PFOS onto Granular Activated Carbon

Granular activated carbons are commonly used adsorbent materials to eliminate organic compounds in water. It has been identified that F400 (coal based) is the best type of GAC to eliminate PFOS (Valeria et al., 2008).

Same type of GAC was used in this experiment with the physical properties as tabulated in Table 4.3.

In this study too, GAC gave comparatively a higher Freundlich exponent (n) than other polymer materials. n is an indicator of nonlinearity of Freundlich curve. Nonlinearity can occur due to many reasons including the sorption site heterogeneity and sorbate–sorbate interactions (Cheung, 2001). The reason for higher n for GAC may be the sorption site heterogeneity of GAC, which is higher than that of synthetic polymers. More than 78% total pore volume in GAC is occupied by micro pores, 14% meso pores and the rest is occupied by macro pores (Table 4.3).

With the isotherm experiment, it was determined that the PFOS adsorption of GAC (F400) at unit equilibrium concentration (1 $\mu\text{g/L}$) is 28.4 $\mu\text{g/g}$ (Figure 4.11). Valeria et al. (2008) reported that the amount of PFOS adsorbed onto GAC (F400) at unit equilibrium concentration (mg/L) is 25.9 mg/g. According to the available literature data, 2.6 $\mu\text{g/g}$ of Methyl Tertiary Butyl Ether (MTBE) detected in GRC-22 (coconut based GAC) at 1 $\mu\text{g/L}$ of equilibrium concentration (Melin 1999). Hydrophobicity of PFOS than MTBE may be the reason to have higher K_f than MTBE.

Among the six materials tested in this study, GAC showed lowest sorption capacities at 1 $\mu\text{g/L}$ (K_f) and 0.1 $\mu\text{g/L}$ equilibrium concentrations suggesting its incapability at low equilibrium concentrations ($< 1 \mu\text{g/L}$). It has been reported that the application of GAC to eliminate PFOS in German drinking water treatment plants was not effective (Schaefer, 2006).

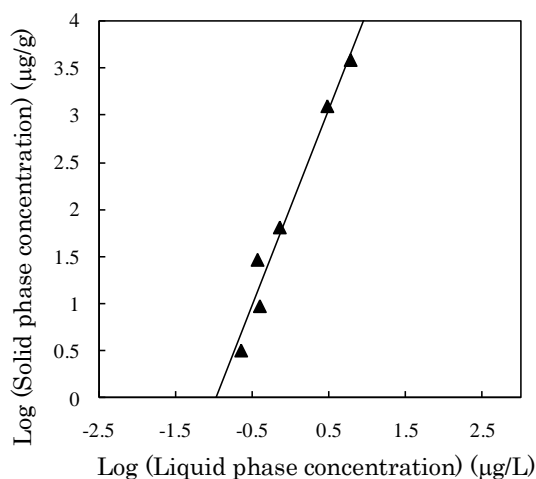


Fig 4.11 Adsorption isotherm of PFOS onto GAC(F400 - \blacktriangle)

4.6.3.3.2 Adsorption of PFOS onto ion-exchange polymers

PFOS is a fully fluorinated compound, which commonly appear as a salt with a functional group of sulfonate attached at the end of the molecule. The carbon–fluorine bond length is shorter than any other carbon–halogen bond, and shorter than carbon–nitrogen and carbon–oxygen bonds. Short bond length and the high electronegativity of fluorine give the carbon–fluorine bond a significant polarity/dipole moment. The electron density is concentrated around the fluorine, leaving the carbon relatively electron poor. This introduces ionic character to the bond through partial charges ($C\delta+—F\delta-$) (O'Hagan, 2008). Negatively charged molecular saturate of PFOS suggests higher adsorption onto anion-exchange polymers.

Among the all polymers tested in this experiment, anion-exchange polymers of Amb IRA-400 and Dow MarathonA showed the highest K_f of 108.8 and 95.9 $(\mu\text{g/g})(\mu\text{g/L})^{-n}$ respectively (Figure 4.12). Some characteristics of these polymers are tabulated in Table 4.2. Quang et al. (2008) investigated Amb IRA 400 for PFOS adsorption and reported that K_f is 250 for high equilibrium concentration of 1 mg/L.

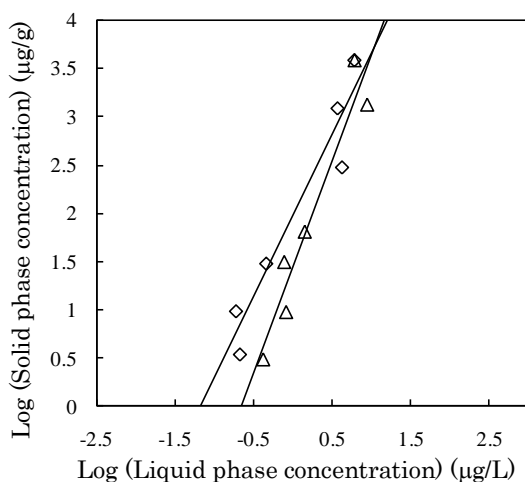


Fig 4.12 Adsorption isotherm of PFOS onto ion-exchange polymers(Amb IRA400 - Δ , Dow MarathonA- \diamond)

Among the two ion exchange polymers tested, Dow MarathonA showed smaller n (1.68) giving flatter Freundlich curve than Amb IRA-400 ($n = 2.8$), which indicated better performance of Dow MarathonA at equilibrium concentrations in ng/L level. Calculated adsorption capacity for Dow Marathon400 is 2.01 $\mu\text{g/g}$ whereas for Amb IRA-400 it is 0.9 $\mu\text{g/g}$.

4.6.3.3 Adsorption of PFOS onto non ion-exchange polymers

A significant aspect of the non ion-exchange polymer adsorption is that, the bonding forces between the adsorbent and the adsorbate are usually weaker than those encountered in activated carbon adsorption. Regeneration of the resin can be accomplished by simple, nondestructive means, such as solvent washing, thus providing the potential for solute recovery (Busca et al., 2008; Lin and Juang, 2009).

Dow L493, Dow V493 and Amb XAD 4 were tested for PFOS adsorption. Amb XAD4 and Dow V493 showed sorption capacities of 79.1 $\mu\text{g/g}$ and 81.3 $\mu\text{g/g}$ respectively at unit equilibrium concentration (1 $\mu\text{g/L}$) (**Figure 4.13**). These values are approximately in the range of 80% of sorption capacity determined for ion-exchange polymers and 250% of sorption capacity determined for GAC at 1 $\mu\text{g/L}$ equilibrium concentration. Distribution of homogeneous pore size in the surface of synthetic non-ion exchange polymers may be the reason for higher K_f than GAC. Also it was noticed that the adsorption capacities of Dow V493 and Dow L493 at 100 ng/L (calculated values) were better than ion-exchange polymers. Comparing with ion-exchange polymers and GAC, adsorption capacity of non ion-exchange polymers showed a linear (comparatively) correlation to equilibrium concentration ($n = 0.84, 1.61$ and 0.94) (**Table 4.12**).

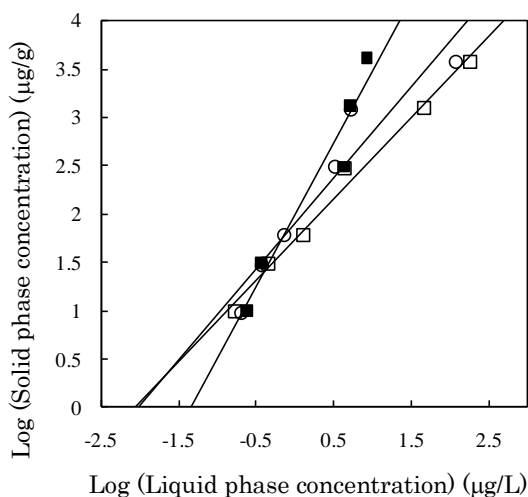


Fig 4.13 Adsorption isotherm of PFOS onto non ion-exchange polymers (AmbXAD4 -■ , Dow L493-□, Dow V493 - ○)

Table 4.12 Freundlich constants for PFOS with different adsorbents and calculated q_c for different C_e (ng/L) based on K_f and n values

Adsorbate	Adsorbent	Freundlich Isotherm parameter			q_c^{*2}		
		K_f^{*1}	1/n	R^2	C_e^{*3} =1	C_e^{*3} =10	C_e^{*3} =100
PFOS	Dowexoptopore V493	81.30	0.94	0.92	0.123	1.072	9.334
	Dowexoptopore L493	54.60	0.84	0.99	0.165	1.141	7.892
	Amberlite XAD 4	79.10	1.61	0.94	0.001	0.048	1.942
	Filtrisorb 400 (GAC)	28.40	2.20	0.93	0.000	0.001	0.179
	Amb IRA-400	95.90	1.68	0.92	0.001	0.042	2.004
	Dow MarathonA	28.40	2.20	0.93	0.000	0.001	0.179

*¹Freundlich isotherm constants $[(\mu\text{g PFCs/g sorbent})(\mu\text{g PFCs/L})^{-n}]$

*²PFCs adsorbed on the adsorbent at equilibrium at equilibrium concentrations of 1,10 and 100 ng/L ($\mu\text{g/g}$)

4.6.3.3 Sorption kinetics of PFOS

Figure 4.14 shows the amount of PFOS adsorption onto each adsorbent with time (with 5000 $\mu\text{g/L}$ initial concentration). Two ion-exchange polymers and GAC reached the equilibrium concentration within 4 hours.

Non ion-exchange polymer materials of Amb XAD4 reached it within 10 hours and Dow L493 and Dow V493 took 90 hours to reach the equilibrium concentration.

To further understand the sorption kinetics, the pseudo second-order model (Equation 4.7) was selected to fit the kinetic data. It was observed that our kinetic data of non ion-exchange polymers fixed well with the equation 2 ($R^2 = 0.99-1.00$) suggesting the dominance of the chemisorption at adsorption process.

Since ion-exchange polymers and GAC reached the equilibrium concentration within a very short time (< 4 h), the number of kinetic data was not sufficient to check with pseudo second-order kinetic model.

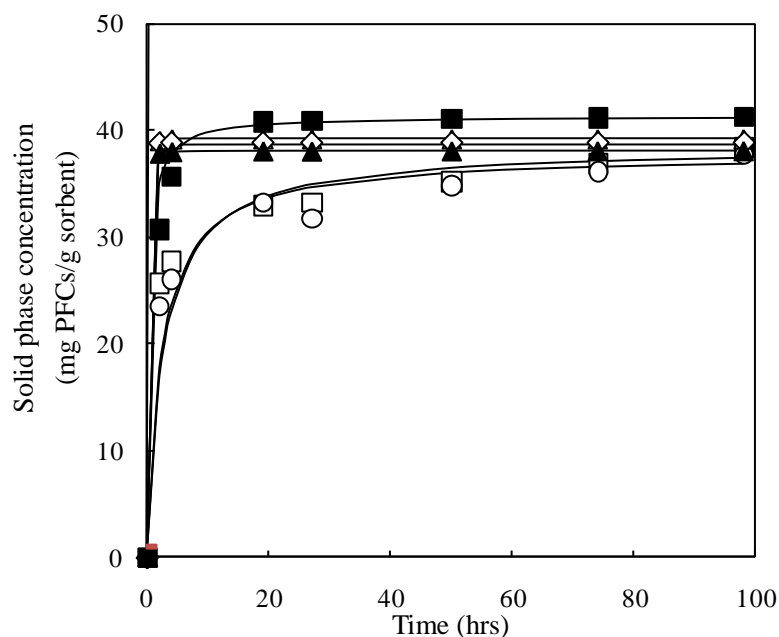


Fig 4.14 Adsorption Kinetics of PFOS onto GAC(F400 - ▲), ion-exchange polymers(Amb IRA400 - △, Dow MarathonA-◇) and non ion-exchange polymers (AmbXAD4 - ■ , Dow L493-□, Dow V493 - ○) and pseudo second-order kinetic curve —

4.6.4 Adsorption kinetics of non ion-exchange polymers

Figure 4.15 shows the sorption kinetics for three PFCs on the selected adsorbents for two initial concentrations of 500 µg/L and 5,000 µg/L. We observed that our kinetic data fixed well with the pseudo second order kinetic model (Equation 4.7) ($R^2=0.89-1.00$) suggesting the dominance of the chemisorption at adsorption processes. Table 4.13 shows the k and the q_e values calculated with the initial concentrations of 5000µg/L. Chemisorption is based on functional chemical group interactions. The principal difference between physical sorption and chemisorption is that the former is less specific with respect to which compounds sorb to which surface sites, has weaker forces and lower energies of bonding, and operates over longer distances between sorbate molecules and sorbent sites (Montgomery, 1985). In chemisorption, the attraction between sorbent and sorbate approaches by a covalent or electrostatic chemical bond between atoms, with shorter bond length and higher bond energy.

The sorption capacities observed in the kinetic experiment supported the results of isotherm experiment. The sorption capacities were increased with the length of the carbon chain of PFCs.

Sorbates bound by chemisorption to a surface generally cannot accumulate more than one molecular layer (monolayer) because of the specificity of the bond between the sorbate and the surface. The location of the sorption sites tends to be very specific since only certain functional groups on a sorbate molecule are able to form these chemical bonds.

In general, synthetic resins designed as sorbents for organic compounds have lower densities and varieties of chemical functional groups than activated sorbents such as GAC, and sorbate interactions with their surfaces are, thus, primarily through physical, rather than chemical, mechanisms.

Another important phenomenon observed in the kinetic experiment is the time required to reach equilibrium concentration for non ion-exchange polymers, which increased with the length of the carbon chain. This may be due to the lack of macro pores and meso pores in synthetic polymer surface which deaccelerates the access of long carbon PFCs in to inner microspores and ultimately it requires longer time to reach equilibrium concentration.

Kinetic characteristics of PFCs on selected adsorbents were also examined with a low concentration of 500 $\mu\text{g/L}$. Medium chain (PFHpA and PFOS) and long chain (PFDA) PFCs well obeyed with the Eq 2 but for PFBA only GAC and Dow V493 behaved according to the kinetic model at low concentration of 500 $\mu\text{g/L}$.

The graphs marked with b, d, and f of **Figure 4.15** Show adsorption kinetics of PFCs with initial concentration of 500 $\mu\text{g/L}$ and graphs marked with a, c and e show the results with 5,000 $\mu\text{g/L}$. It was obvious that an increase in initial PFCs concentration leads to an increase in adsorption capacity of PFCs on polymers. It was observed that GAC reached the equilibrium concentration within 4 hrs whereas Amb XAD 4 took less than 10 hrs for all PFCs except PFOS. Other polymers took more than 80 hrs to reach the equilibrium concentrations.

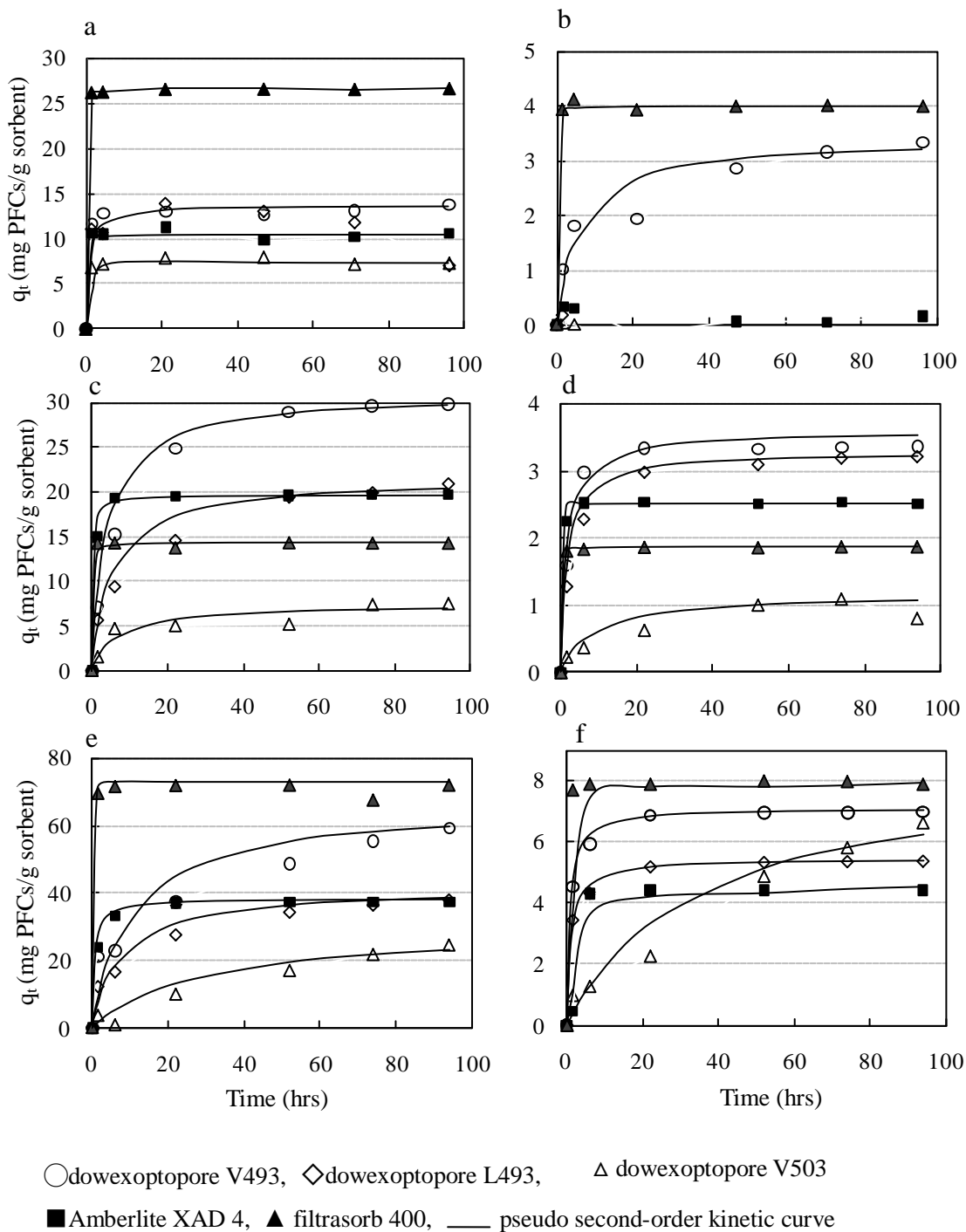


Fig. 4.15 Adsorption kinetics (for initial concentrations 500µg/L and 5000µg/L) for the PFCs of (a) PFBA 5000µg/L, (b) PFBA 500µg/L, (c) PFHpA 5000µg/L, (d) PFHpA 500µg/L, (e) PFDA 5000µg/L, (f) PFDA 500µg/L, and modeling using the pseudo second- order equation.

Table 4.13 Pseudo-second-order kinetic parameters for different non ion-exchange sorbent/ sorbate combinations

Adsorbate	Adsorbent	Pseudo-second-order kinetic parameter		
		q_e^{*2}	k^{*1}	R^2
PFBA	Dowexoptopore V493	13.7	0.091	0.998
	Dowexoptopore V503	7.3	-	0.998
	Dowexoptopore L493	8.1	-	0.994
	Amberlite XAD 4	10.4	1.024	0.998
	Filtrisorb 400 (GAC)	27.0	1.369	1.000
PFHpA	Dowexoptopore V493	31.0	0.008	0.997
	Dowexoptopore V503	7.5	0.020	0.953
	Dowexoptopore L493	21.5	0.009	0.992
	Amberlite XAD 4	19.7	0.214	1.000
	Filtrisorb 400 (GAC)	14.37	0.457	0.999
PFDA	Dowexoptopore V493	66.6	0.001	0.983
	Dowexoptopore V503	30.3	0.001	0.885
	Dowexoptopore L493	41.6	0.003	0.995
	Amberlite XAD 4	38.4	0.039	1.000
	Filtrisorb 400 (GAC)	72.9	16.900	1.000

*¹Sorption rate constant [g sorbent(mg PFCs)⁻¹(h)⁻¹]

*²PFCs adsorbed on the adsorbent at equilibrium(mg/g)

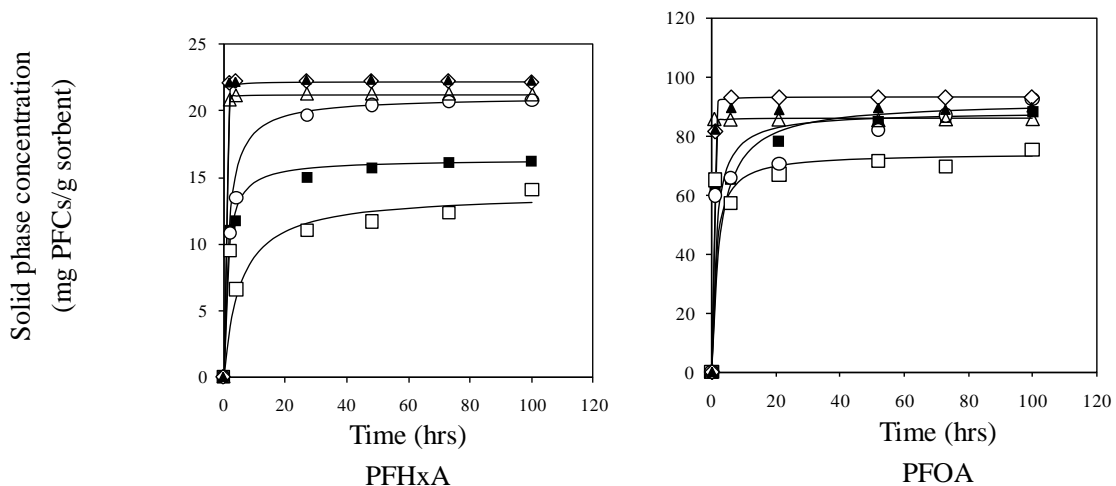


Fig 4.16 Adsorption Kinetics of PFHxA and PFOA onto GAC(F400 - ▲), ion-exchange polymers(Amb IRA400 - △, Dow MarathonA-◇) and non ion-exchange polymers (AmbXAD4 - ■ , Dow L493-□, Dow V493 - ○ and pseudo second-order kinetic curve —

4.6.5 Adsorption kinetics of ion-exchange polymers

Figure 4.16 shows the variation of adsorbed PFCs concentration with time. Comparing with non ion-exchange polymers, adsorption kinetics for ion-exchange polymers and GAC were high. Among the materials tested AmbIRA 400 (ion-exchange resin) gave the highest sorption constant (k) for all three PFCs tested (Table 4.14). Both GAC and Dow MarathonA showed similar kinetic profiles.

Table 4.14 Pseudo-second-order kinetic parameters of PFHxA, PFOA and PFOS with different ion-exchange, non ion-exchange and GAC

Adsorbate	Adsorbent	Pseudo-second-order kinetic parameter		
		q_e ^{*2}	k ^{*1}	R ²
PFHxA	Dowexoptopore V493	21.097	0.032	0.99
	Dowexoptopore L493	13.831	0.014	0.98
	Amberlite XAD 4	16.340	0.052	0.99
	Filtrisorb 400 (GAC)	22.321	2.230	1.00
	Amb IRA-400	21.231	2.773	1.00
	Dow MarathonA	22.173	1.071	1.00
PFOA	Dowexoptopore V493	91.743	0.004	0.99
	Dowexoptopore L493	74.074	0.012	0.99
	Amberlite XAD 4	88.495	0.008	0.99
	Filtrisorb 400 (GAC)	90.09	0.136	1.00
	Amb IRA-400	86.206	0.448	1.00
	Dow MarathonA	93.457	0.286	1.00
PFOS	Dowexoptopore V493	37.736	0.009	0.99
	Dowexoptopore L493	38.462	0.010	0.99
	Amberlite XAD 4	41.322	0.063	1.00
	Filtrisorb 400 (GAC)	38.168	2.288	1.00
	Amb IRA-400	38.760	13.313	1.00
	Dow MarathonA	39.216	8.128	1.00

^{*1}Sorption rate constant [g sorbent(mg PFCs)⁻¹(h)⁻¹]

^{*2}PFCs adsorbed on the adsorbent at equilibrium(mg/g)

4.6.6 Batch test with PFCs related industrial wastewater

Characteristics of wastewater

Collected wastewater from a discharge point of PFCs related industrial wastewater treatment plant was initially analyzed and found that pH was

6.9 and the TOC was 15.2 mg/L. The initial PFCs concentration of the wastewater was measured as shown in **Table 4.15**.

Table 4.15 Initial PFCs concentration of the wastewater

Date	PFOA ($\mu\text{g/L}$)	PFOS ($\mu\text{g/L}$)	PFHxA ($\mu\text{g/L}$)	PFHpA ($\mu\text{g/L}$)
2009-4	0.72	-	1.80	0.25
2009-5	2.60	-	4.20	1.40
2009-09	10.00	-	2.90	2.20
2010-02	4.35	0.02	0.75	0.33

Contrasting with individual PFCs in MilliQ water, it was difficult to get a good isotherm relationship with this experiment ($0.079 < R^2 < 0.99$) (**Figure 4.17**). The isotherm coefficient determined by the experiment and the calculated sorption capacities at further low concentrations of 1, 10 and 100 ng/L is tabulated in **Table 4.16**. It was observed in the experiment that AmbXAD4 can effectively remove PFOA, but negative isotherm coefficients were received.

According to the batch test results actual wastewater from PFCs related industry, GAC seems better for unit equilibrium concentration of 1 $\mu\text{g/L}$. For the low equilibrium concentrations (10 – 1 ng/L) synthetic resins seem to be more attractive than GAC in terms of sorption capacity. Especially DOW L493 gave best sorption capacity at ng/L level equilibrium concentrations.

The amount of research carried out with actual wastewater is not enough to come to a concrete solution, but the process of adsorption was identified as a possible method to eliminate PFCs in this wastewater. Long run column experiment is to be carried out with earmarked candidate materials and actual wastewater to understand the process clearly.

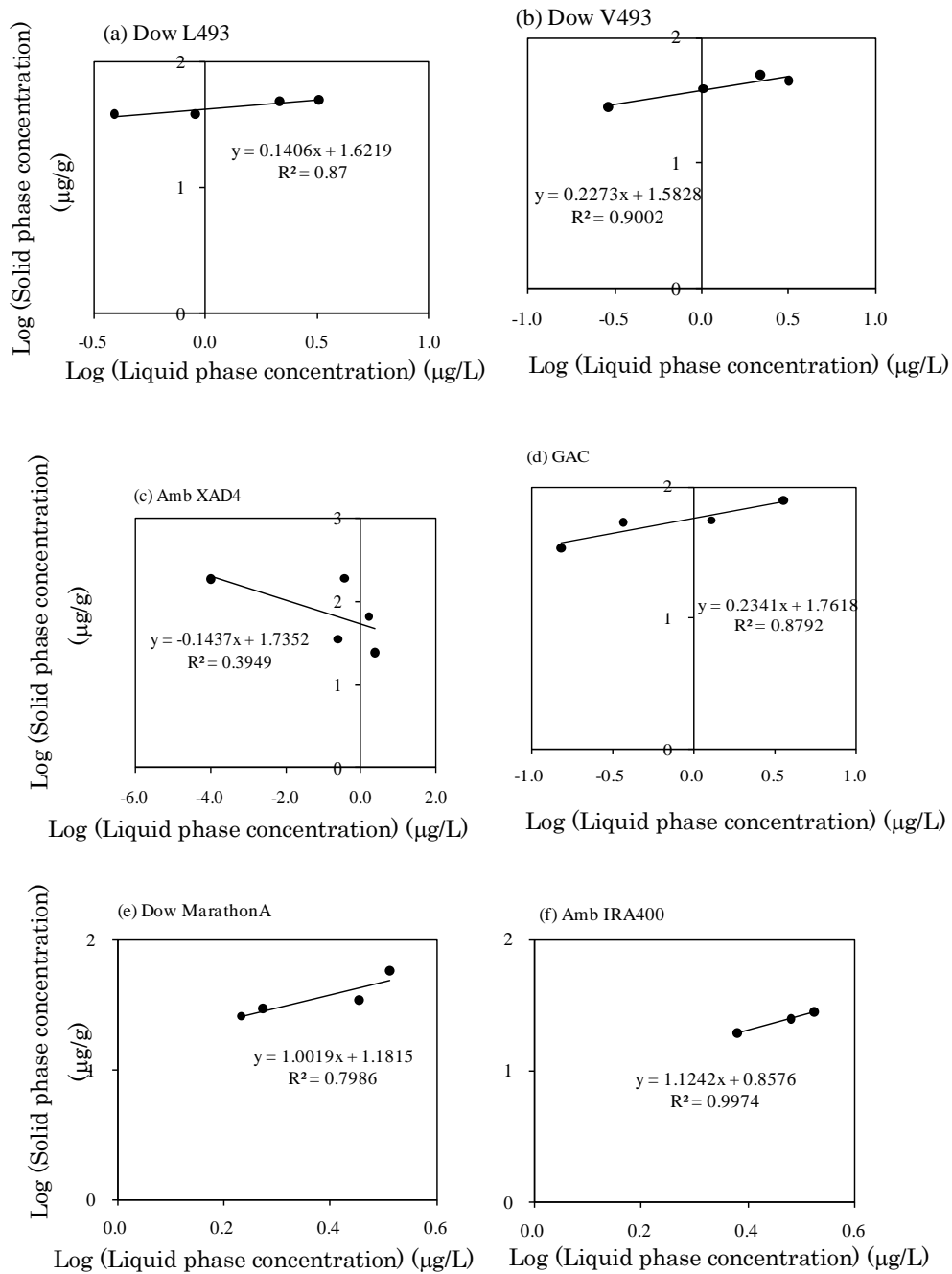


Fig 4.17 Adsorption isotherm of PFOA occurred in PFCs related industrial WW onto ion-exchange polymers, non ion-exchange polymers and GAC

Table 4.16 adsorption characteristics of different filter materials with PFCs related industrial wastewater

Adsorbate	Adsorbent	Freundlich Isotherm parameter			q_c^{*2}		
		K_f^{*1}	n	R^2	Ce^{*3} =1	Ce^{*3} =10	Ce^{*3} =100
PFHxA	Dowexoptopore V493	9.795	0.809	0.616	0.037	0.236	1.519
	Dowexoptopore L493	22.999	3.225	0.817	0.000	0.000	0.014
	Amberlite XAD 4	3.831	0.329	0.303	0.395	0.842	1.796
	Filtrisorb 400 (GAC)	3147.748	1.266	0.838	0.503	9.264	170.765
	Amb IRA-400						
	Dow MarathonA	4.756	0.650	0.125	0.054	0.239	1.066
PFHxA	Dowexoptopore V493	7.658	0.371	0.970	0.591	1.388	3.261
	Dowexoptopore L493	5.829	0.285	0.658	0.815	1.570	3.026
	Amberlite XAD 4						
	Filtrisorb 400 (GAC)	204.644	0.842	0.787	0.608	4.229	29.417
	Amb IRA-400	25.375	1.209	0.956	0.006	0.097	1.567
	Dow MarathonA	15.470	0.927	0.724	0.026	0.216	1.830
PFOA	Dowexoptopore V493	38.265	0.227	0.900	7.976	13.452	22.688
	Dowexoptopore L493	41.870	0.141	0.870	15.809	21.873	30.262
	Amberlite XAD 4						
	Filtrisorb 400 (GAC)	57.783	0.234	0.880	11.476	19.670	33.713
	Amb IRA-400	7.204	1.124	0.990	0.003	0.041	0.542
	Dow MarathonA	15.188	1.002	0.800	0.015	0.150	1.512

*¹Freundlich isotherm constants [$(\mu\text{g PFCs/g sorbent})(\mu\text{g PFCs/L})^{-n}$]

*²PFCs adsorbed on the adsorbent at equilibrium at equilibrium concentrations of 1,10 and 100 ng/L ($\mu\text{g/g}$)

*³Equilibrium concentration (ng/L)

4.7 Conclusion

1. Constant sorbent method was identified as the best method to determine sorption isotherm, where sorbent concentration is kept constant and sorbate concentration is changed.
2. Ion-exchange resins and GAC showed faster adsorption characteristics than non ion-exchange polymers. To reach the equilibrium concentration for all kind of granular materials, at least 100 hrs shaking is needed.
3. Synthetic polymer materials were identified as better filter materials (in terms of adsorption capacity) to eliminate PFCs in water at low concentration (1 $\mu\text{g/L}$). The magnitude of K_f decreases in the following order for most of long chain and medium chain PFCs tested: Ion-exchange polymers > Non ion-exchange polymers > GAC, but some cases at further low equilibrium concentration (100 ng/L) non ion-exchange polymers showed higher adsorption capacity than other adsorbents.
4. Amb IRA- 400 was identified as the best filter material to eliminate PFOS at equilibrium concentration > 1 $\mu\text{g/L}$. considering both adsorption isotherm and adsorption kinetics, Amb XAD 4 and Dow MarathonA can be recommended for eliminating PFOS at ng/L equilibrium concentrations.
5. Further studies are to be done to understand the sorption mechanisms of PFOS, but it can be suspected that the chemisorption is the dominant process.

Chapter 5 - PFCs coagulation

5.1 Introduction

Coagulation can be defined as the reactions and mechanisms involved in the chemical destabilization of particles in the formation of large particles through perikinetic flocculation. Coagulant is the chemical that is added to destabilize the colloidal particle in water so that floc formation can result. (Wastewater Engineering, Treatment and Reuser – Metcalf & Eddy). In the coagulation/flocculation process, very fine suspended particles are caused to come together to form larger particles that can be settled and filtered out of the water.

During coagulation, the coagulant is added to the water to be treated. The water is stirred vigorously in a fast mixer to assure quick, uniform dispersion of the coagulant. In the conventional treatment method, the coagulant may react rapidly with compounds in the water that contain carbonates, bicarbonates and hydroxides to produce a jelly-like substance that absorbs impurities. At the same time, coagulants can neutralize the charges on the particle surface.

5.1.1 Inorganic Coagulants

Most of the conventional inorganic coagulants are salts of aluminum or iron. These inorganic salts neutralize the charge on the particles causing raw water turbidity, and also hydrolyze to form insoluble precipitates, which entrap particles. **Table 5.1** lists few common inorganic coagulants with some physical and chemical properties.

5.1.2 Organic Polymers

Organic Polymers are categorized as natural organic polymers and synthetic organic polymers. In this study, only synthetic polymers are considered. Organic coagulants are used in a wide variety of municipal and industrial applications to enhance the coagulation, flocculation and removal of impurities in water.

Synthetic long chain organic coagulants consist of simple monomers that are polymerized into high molecular weight substances. Depending on their charge, when placed in water, are negative, positive or neutral. These polymers are classified as anionic, cationic and nonionic respectively. The action of polymeric coagulants also classified as charge neutralization, polymer bridge formation and combine charge neutralization-polymer bridge formation process.

Table 5.1 Commonly used inorganic coagulants

Name	Typical Formula	Typical Strength	Typical Forms Used in Water Treatment	Density
Aluminum sulfate	$\text{Al}_2(\text{SO}_4)_3 \cdot 14 \text{ to } 18 \text{ H}_2\text{O}$	17% Al_2O_3	lump, granular, or powder	60-70 lb/ft ³
Aluminum chloride	$\text{AlCl}_3 \cdot 6\text{H}_2\text{O}$	35% AlCl_3	liquid	12.5 lb/gal
Ferric sulfate	$\text{Fe}_2(\text{SO}_4)_3 \cdot 9\text{H}_2\text{O}$	68% $\text{Fe}_2(\text{SO}_4)_3$	granular	70-72 lb/ft ³
Ferric chloride	FeCl_3	60% FeCl_3 , 35-45% FeCl_3	crystal, solution	60-64 lb/ft ³ 11.2-12.4 lb/gal
Sodium aluminate	$\text{Na}_2\text{Al}_2\text{O}_4$	38-46% $\text{Na}_2\text{Al}_2\text{O}_4$	liquid	12.3-12.9 lb/gal

5.1.3 Uses and benefits of organic polymers in water Treatment

In general water soluble organic polymers are highly efficient contributors of cationic charge and molecular weight when applied in specific applications. The process of coagulation is made highly efficient by the proper application of chemistry and dosage. Sometimes organic coagulants are used most efficiently in combination with inorganic coagulants such as polyaluminum chloride and other aluminum and iron salts. The use of organic polymers offers several advantages over the use of inorganic coagulants:

1. Less sludge production.
2. The resulting sludge contains a less amount of chemically bound water and can be more easily dewatered.
3. Polymeric coagulants do not affect pH. Therefore, the need for supplemental alkalinity, such as lime, caustic, or soda ash, is reduced or eliminated.

5.1.4 Coagulation of anionic particles by cationic polymer coagulants

The basic reaction expected with anionic particles and cationic polymers is schematically shown in the **Figure 5.1**. The first expected reaction is the columbic attraction between opposite charge molecule and active site in the organic polymer. It is expected that this reaction is faster at the beginning of the experiment because of the availability of higher concentrations of opposite charges and it will decrease with time when

vacant sites and remaining anions decrease with the progression of the experiment. Also the coagulated polymers can combine with each other and make bigger particles. This bridging may be leading to floc formation.

Apart from the main two reactions mentioned above, there is a possibility for more reactions. Especially in this experiment, PFCs concentrations were in $\mu\text{g/L}$ level, but the coagulant dose is in mg/L level. There is a chance for some coagulant polymers to not to have any PFCs during the coagulation process. In such case the polymer chain can be fold back and settle within the chain or can be attached with other coagulated polymers.

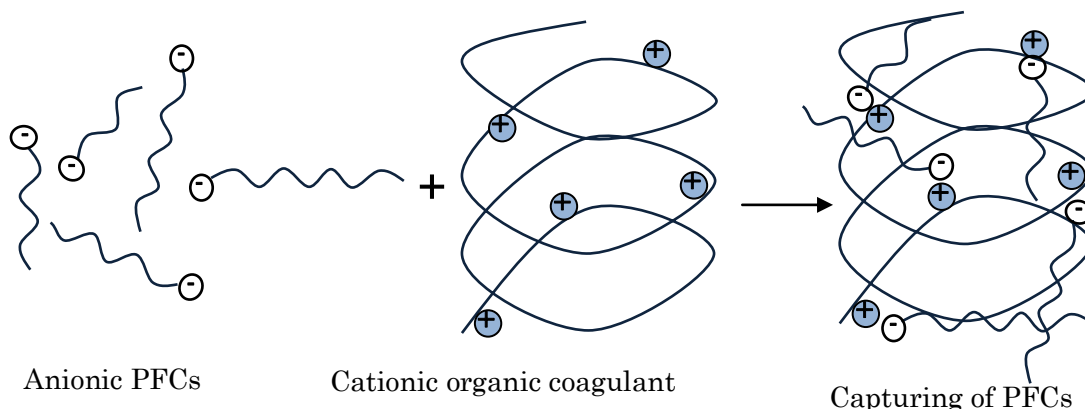


Fig 5.1 A diagram to explain conceptual mechanism of PFCs elimination by organic coagulants

5.2 Aims and Objectives

Major aim of this study is to identify possible candidate coagulants to eliminate PFCs for wastewater treatment process. Both inorganic coagulants and organic coagulants were tested by a series of jar test experiments. Coagulants were tested with both MilliQ water and effluent wastewaters from different WWTPs. The specific objectives of this chapter are listed below.

1. To determine the optimum coagulant dose to eliminate PFCs by jar tests.
2. To compare the performances of different coagulants (inorganic and organic) to coagulate PFCs by jar test.
3. To observe the individual coagulation of each PFCs when it appears as a mixture of PFCs in the initial solution.
4. To check the effect of other organic matters presence in water on PFCs coagulation.
5. To check the possibility of coagulation process to eliminate PFCs in the actual industrial water treatment process.

5.3 Materials and Method

5.3.1 Materials

All cationic organic coagulants (FL2250, FL2749, FL3050, FL4440, FL4620, FL4820) were received from SNS, Inc (Japanese agent). SNF, Inc. is one of the world's leading manufacturers of water-soluble polymeric organic coagulants. Inorganic coagulants (Iron(III) chloride, Sodium aluminate and Aluminum sulfate) were purchased from Wako chemicals (Japan). Some physico chemical properties of tested coagulants are tabulated in the **Table 5.2 and Table 5.3**

Table 5.2 Physico chemical properties of organic coagulants used in the experiment

Coagulant	Specific gravity	Viscosity	Color	Mol Wt/1000	Remarks
FL2250	1.12-1.16	25-35	Clear/ yellow	10	Low molecular weight, highly cationic
FL2749	-	-	Clear/ off white	120	Medium molecular weight, highly cationic
FL3050	1.12 – 1.16	1,000- 4,000	Clear/ off white	500	High molecular weight, highly cationic
FL4440	1.05-1.10	1,000- 3,000	Clear/ yellow	3,000	Medium molecular weight, homopolymer of diallyldimethylammonium chloride.
FL4620	1.02-1.07	700- 1,000	Clear/ off white	1,400	High molecular weight, homopolymer of diallyldimethylammonium chloride.
FL4820	1.02-1.07	1000- 3000	Clear/ off white	1,800	High molecular weight, homopolymer of diallyldimethylammonium chloride.

Table 5.3 Physico chemical properties of inorganic coagulants used in the experiment

Coagulant	Mol wt	Molecular structure	Color	Physical form
Ferric Chloride	162.20	Fe(Cl) ₃	Shining black	Granular
Sodium Aluminate	163.936 (without water)	Na ₂ Al ₂ O ₄	White	Powder
Aluminium Sulfate	342.15 (without water)	Al ₂ (SO ₄) ₃ .nH ₂ O (n=14-18)	White	Powder

5.3.2 Jar test

Coagulation and flocculation experiments were performed in a jar test apparatus (JMD6E-Osaka Miyamoto Riken Ind, Japan). Each sample (1.0 L) was rapidly mixed at 80 revolutions per minute (rpm) for 4min, slowly mixed at 25rpm for 30 min, and then settled (0 rpm) for 60 min. In the beginning of rapid mixing, inorganic and organic coagulants were added using the mechanism provided with the Jar test apparatus.

For the jar test with MilliQ water, 1 mL sample was collected from each jar prior to adding coagulant and was analyzed to determine initial PFCs level. The dosage of organic polymer coagulant ranged from 0 to 1000 µL/L in the first experiment, which was carried out to decide the optimum coagulant dosage. 200mg/L (for solid coagulant) or 200 µL/L (for liquid coagulant) was applied for other jar test experiments. Two duplicate jars were used for each condition. At the end of each jar test, the samples were filtered through membrane filters (GF/F; pore size. 0.45µm, and 0.2µm Millipore) and analyzed for remaining PFCs in the filtrate. Each steps involved with the jar test are schematically shown in **Figure 5.2**.

5.3.3 Methodology - Experiment 1- Optimum doze

This experiment was carried out to determine the minimum effective organic coagulant doze to eliminate PFCs. One selected PFCs of PFOA was tested with different dozes of selected coagulant of FL2250 by a Jar test.

PFOA stock solution was added to MilliQ water to yield the initial PFOA concentration of 10 µg/L and the prepared solution was filled in to 6 jars (1 L each). Five dozes of coagulants ranging from 0 µL/L to 1,000µL/L were added to five jars and the sixth one was kept with zero dose as the control. Then the jar test was conducted as described in **Figure 5.2**. In the jar test the coagulants were added after three seconds from starting the rapid

mixing by the facility provided by the jar test apparatus. **Table 5.4** shows the summary of experimental conditions. Since the MilliQ water was used in this experiment, filtered samples after the jar test were directly analyzed with LC/MS/MS after diluting with acetonitrile to ensure 40% acetonitrile content in the analyzed samples.

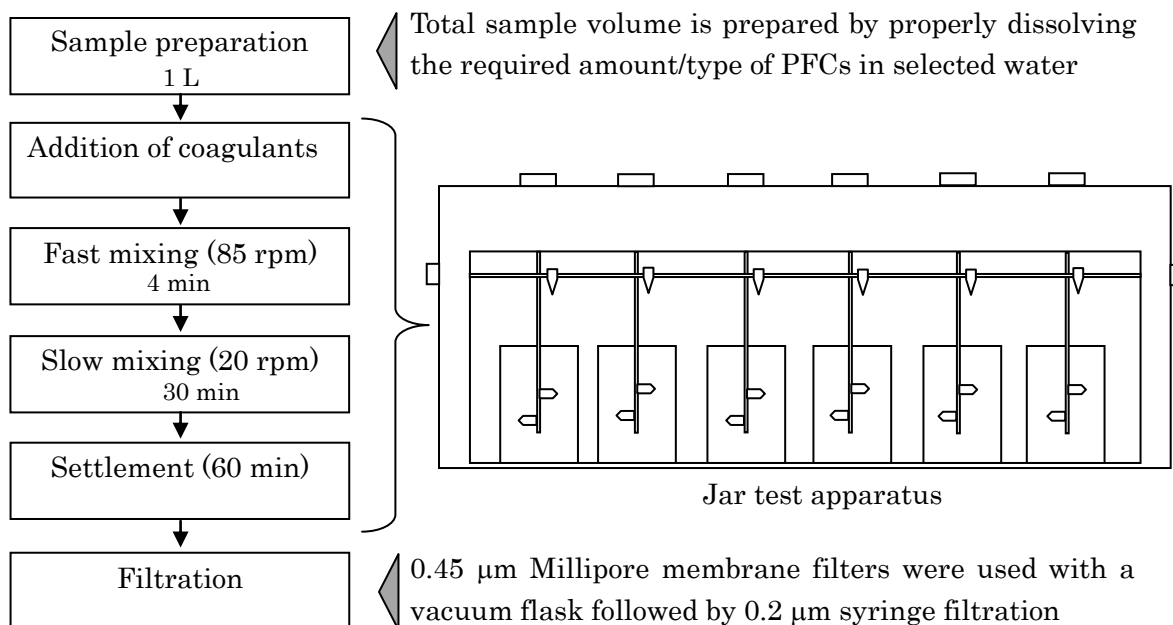


Fig5.2 Basic steps involved with Jar test

5.3.4 Methodology Experiment 2 – Comparison of coagulants

This experiment was designed to study the PFOA coagulation efficiencies by organic and inorganic coagulants. Three inorganic coagulants (Iron(III) chloride, Sodium aluminate and Aluminium sulfate) and six organic coagulants (FL2749, FL3050, FL2250, FL4620, FL4820 and FL4440) were tested with PFOA by a series of jar tests to determine the degree of coagulation. The optimum coagulant doze determined by the experiment 1 was applied in this experiment. The PFOA solution (10 μg/L) was prepared by adding PFOA stock solution into Milli Q to yield required concentration. Similar to the experiment 1, filtered samples were directly analyzed with LC/MS/MS after the dilution with acetonitrile. The experimental conditions of this test are summarized in the **Table 5.4**.

5.3.5 Methodology Experiment 3- Mixture of PFCs

This experiment was designed to investigate the PFCs coagulation as a mixture. A mixture of eight PFCs, which consist of long chain, medium chain, and short chain PFCs, and also different functional groups of acid and sulfonate was spike into MilliQ water to prepare the initial solution for the jar test. The rest of experiment was similar to experiment 2 . Filtered samples after the jar test were diluted with acetonitrile and analyzed with LC/MS/MS for remaining PFCs. The summary of the experimental conditions is shown in **Table 5.4**.

5.3.6 Methodology Experiment 4 – Wastewater spiked with PFCs

This experiment was designed to observe the effect of the presence of the organic matters in water on PFCs coagulation. Actual wastewater collected at a discharge point of a WWTP was spiked with a mixture of PFCs stock solution to prepare the initial solution for the jar test. The main steps of the jar test are shown in **Figure 5.2**. Since wastewater was used in this experiment, remaining organics other than PFCs had to be eliminated before analyze with LC/MS/MS. A measured volume of 50 mL from the filtered samples after jar test was sent through a Precip-C Agri cartridge by using the concentrator (flow rate 5mL/min). Then the cartridge was air dried for 1 hr using a vacuum manifold and then eluted it with organic solvents (methanol 3 mL + acetonitrile 3 mL). Eluted solution was completely dried by a flow of nitrogen gas at 60° C. then dried tube was reconstituted with 40% ACN. Final solution was analyzed and measured using LC/MS/MS.

5.3.7 Methodology Experiment 5 –Coagulation of industrial wastewater

This experiment was designed to check the applicability of inorganic and organic coagulants tested in previous experiments in the PFCs related industrial wastewater. Three inorganic coagulants and six organic coagulants shown in Table 5.3 were tested with the wastewater, which was collected at the discharge point of PFCs related industrial wastewater treatment plant. Collected wastewater samples were stored at 4 °C and the temperature was adjusted to 25°C before the experiment.

The jar test was carried out according to the main steps shown in Figure 5.2 since the remaining organics other than PFCs in the wastewater used in this experiment had to be eliminated before analyze with LC/MS/MS. 100 mL of the filtrate from the filtered samples after the jar test was sent

through a Precip-C Agri cartridge by using the concentrator (flow rate 5mL/min). Then the cartridge was air dried for 1 hr using a vacuum manifold and was eluted with organic solvents (methanol 3 mL + acetonitrile 3 mL). Eluted solution was completely dried by a flow of nitrogen gas at 60° C. Then dried samples were reconstituted with 40% ACN solution. Final solution was analyzed and measured using HPLC/MS/MS.

Table 5.4 Summary of the experimental conditions

Exp. No	PFCs	Coagulants	Type of water used
1	PFOA	FL2250	MilliQ
2	PFOA	Iron(III) chloride, Sodium aluminate, Aluminium sulfate FL2749, FL3050, FL2250, FL4620, FL4820 and FL4440.	MilliQ
3	PFPeA, PFHxA, PFOA, PFNA, PFDA, PFHS, PFOS	Iron(III) chloride, Sodium aluminate, Aluminium sulfate FL2749, FL3050, FL2250, FL4620, FL4820 and FL4440.	MilliQ
4	PFHxA, PFHpA, PFOA, PFNA, PFDA, PFHS, PFOS	Iron(III) chloride, Sodium aluminate, Aluminium sulfate FL2749, FL3050, FL2250, FL4620, FL4820 and FL4440.	Effluent wastewater
5	PFPeA, PFHxA, PFHpA, PFOA, PFNA, PFDA, PFOS	Iron(III) chloride, Sodium aluminate, Aluminium sulfate FL2749, FL3050, FL2250, FL4620, FL4820 and FL4440.	Effluent Wastewater

Note. The experiments were carried out at 20 °C. pH was around 6.5 with the addition of PFCs (10µg/L) and it was not adjusted. The initial TOC level of wastewater was measured as 10.5 mg/L

5.4 Results and discussion

5.4.1 Optimum dosage of organic coagulants

Figure 5.3 shows the percentage PFOA removal by coagulation plotted against the coagulation dosage. Since the concentration of the target compound (PFOA) is 10 µg/L, higher doses of coagulations were applied to get better results. This is a common situation at low concentration of target polar contaminant.

It was observed that the percentage PFOA removal was drastically increased up to 86% with the coagulant dosage. The corresponding coagulant dose at this point was 200 μ L/L. The additional dose after 200 μ L/L seems ineffective as there is no significant improvement in percentage PFOA removal. It was assumed that the effective coagulant dose is 200 μ L/L and it was applied for the rest of the experiments in this chapter. Martial Pabon(2007) has reported that he could remove 81% PFOA by coagulation with same coagulant of FL2250 at a dosage of 1.4g/L, but, with different initial PFOA concentration of 280 mg/L.

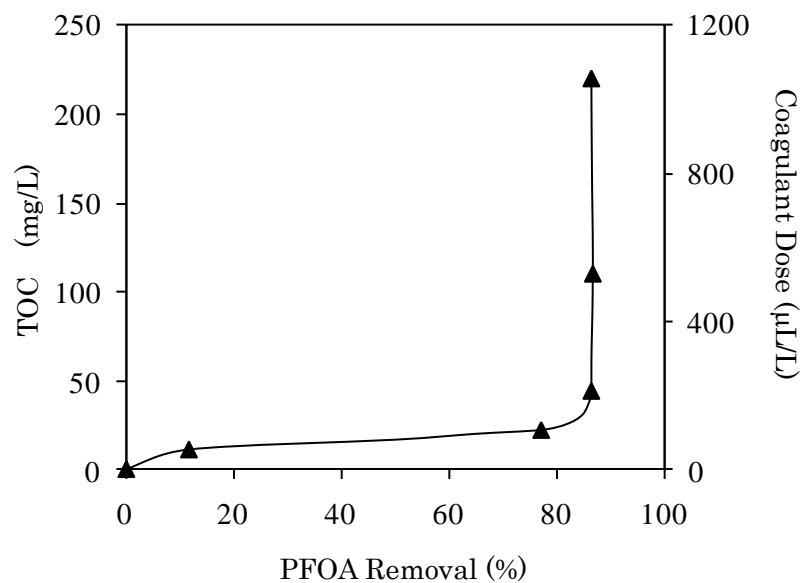


Fig 5.3 percentage PFOA removal with different dose of coagulants

5.4.2 Experiment 2- Performance of organic and inorganic coagulants

Experiment 2 was designed to understand the possibility of PFCs coagulation by inorganic and organic coagulant. **Figure 5.4** shows the percentage removal of PFOA by each organic and inorganic coagulant. Initial PFOA concentration was 10 μ g/L and the optimum dosage of coagulant (200 μ L/L) determined by the experiment 1 was applied in this experiment.

Organic coagulants showed better performance than inorganic coagulants to coagulated PFOA. The average coagulation efficiency of organic coagulant was 78%, which is 40% higher than that of inorganic coagulants. Among the organic polymers, FL2749, FL3050 and FL2250 showed more than 80% coagulation efficiency. It was interesting to notice that the last

three organic coagulants with least performance were consisted of homopolymer of diallyldimethylammonium chloride suggesting a mixture of multipolymers are better coagulants for PFCs.

In the case of inorganic coagulants experiment, high coagulant dose of 200 mg/L was applied, which is comparable with the dosage of organic coagulants. It was noticed that Ferric Chloride showed almost 80% PFOA elimination, which dominated among all inorganic coagulants. In the process of coagulation by inorganic coagulants, it is difficult to differentiate coagulation and adsorption. Inorganic coagulants may not fully dissolve in the solution and some PFOA molecules can be adsorbed onto surface of the coagulants especially at the flocculation (slow mixing) process. Filtration was carried out (0.45 μ m and 0.2 μ m) to eliminate the particle remain in the solution before analysis for PFOA. Both adsorbed PFOA and coagulated PFOA were eliminated in this step. One explanation for higher performance of Ferric Chloride is that the PFOA component eliminated by adsorption is high, so that the overall percentage of PFOA removal reached 80%.

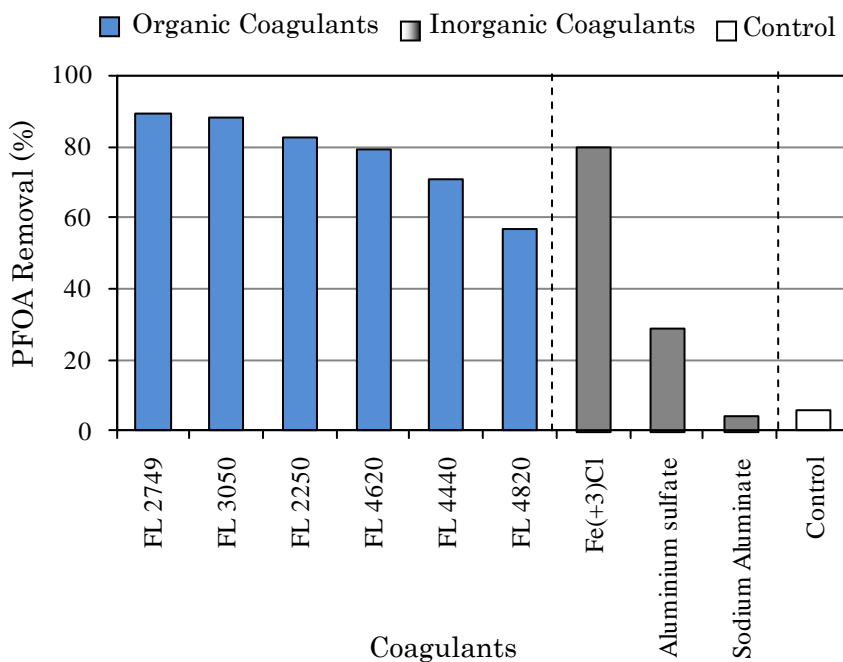


Fig 5.4 Percentage PFOA removal with different type of coagulants

5.4.3 Experiment 3 - PFCs coagulation as a mixture

Figure 5.5 shows the percentage removal of each PFCs in the mixture by various coagulants. Consolidating the results of experiment 2, organic coagulants showed better performances than conventional inorganic coagulants. Considering three inorganic coagulants and eight PFCs used in the experiment it can be figured out that an average PFCs removal by an inorganic coagulant is about 30% where as for organic coagulants same calculation gives 72%. In the first glance, it can be concluded that the PFCs coagulation efficiency by organic coagulants are double than that of inorganic coagulants for MilliQ water.

It was noticed for both organic and inorganic coagulants that there is no single coagulant to show the maximum performance for all PFCs. Different PFCs had different coagulants for maximum coagulation suggesting case by case consideration at the real application. Among the tested coagulants, FL 2749 was identified as the best material with average overall PFCs removal of 86%. For the inorganic coagulants, Aluminum sulfate was the best candidate with overall PFCs removal of 54% followed by Ferric Chloride with 36% overall removal.

It was clearly identified that short chain PFCs are difficult to coagulate than long chain PFCs. **Figure 5.6** shows different PFCs (with different chain lengths) removal by organic and inorganic coagulants. Given removal percentages are average values of organic (six coagulants) and inorganic (two coagulants, Sodium aluminates was not considered because its elimination is almost zero) coagulants.

In this experiment, PFCs were spiked into MilliQ water and it can be assumed that the competition to attach with sites in the coagulant chain is only among PFCs molecules. Long chain PFCs seems to be more effective than short chain PFCs for attachment with active sites in the polymer chain. One possible reason for high efficiency is molecular charge. Longer the carbon chain, higher the number of Fluorine attached and which ultimately increase the negative charge in the molecule, which can beat the weakly charged short chain PFCs at the competition to attach with cationic coagulants. The second possible mechanism is enmeshment, in which long chain PFCs can be trapped easily than smaller short chain PFCs.

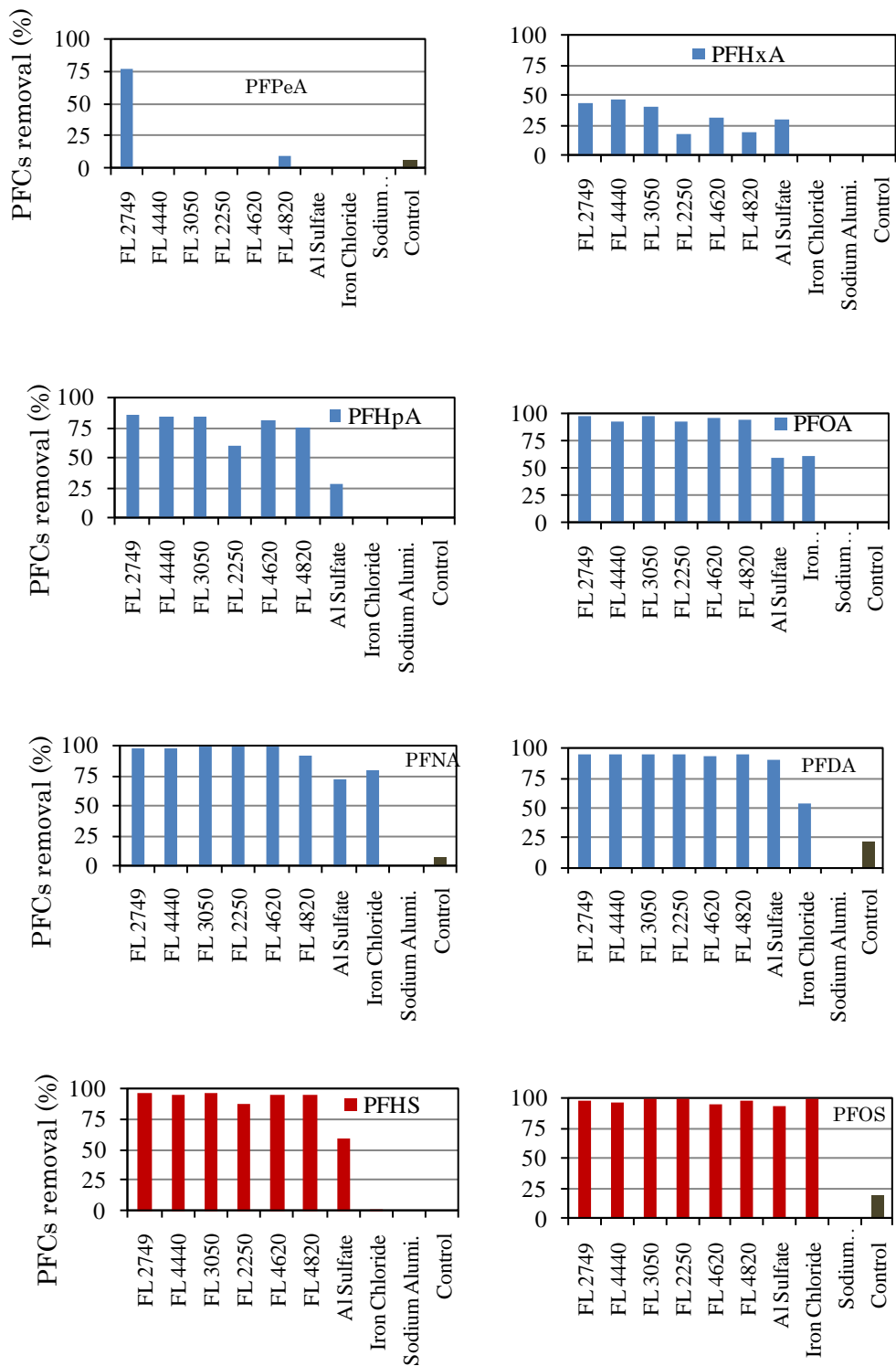


Fig. 5.5 Percentage reduction of each PFCs by various organic and inorganic coagulants for MilliQ water spiked with a mixture of PFCs

5.4.3.1 PFCs coagulation by organic coagulants

This comparative study clearly showed that the organic coagulants are much effective than conventional inorganic coagulants to eliminate PFCs. Also it should be highlighted that this study was carried out for MilliQ water spiked with a mixture of PFCs solution. Especially for well known PFCs of PFOS and PFOA, some organic coagulants showed more than 98% removal efficiencies. **Figure 5.7** shows the average PFCs removal for different molecular weights of coagulants. an organic coagulant (positively charged) with molecular weight around 100,000 seems to be ideal to eliminate PFCs of all chain lengths by coagulation/filtration process.

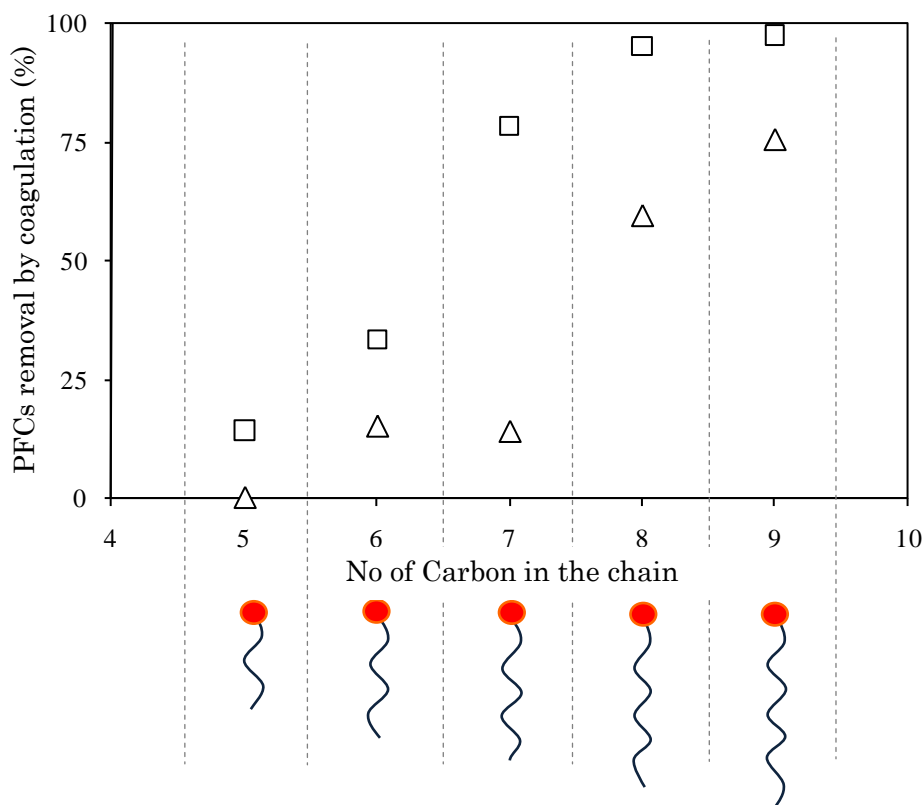


Fig. 5.6 PFCs with different chain lengths removal by coagulation

□ organic coagulation △ inorganic coagulation

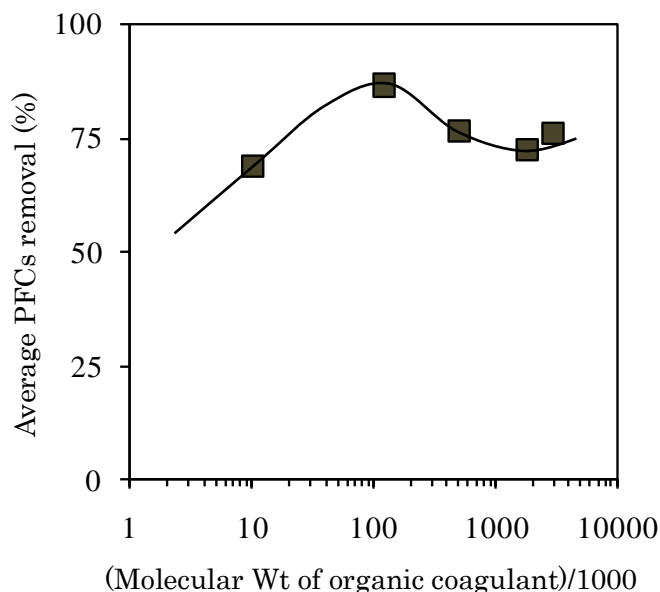


Fig. 5.7 the effect of molecular Wt on PFCs coagulation for organic coagulants

5.4.4 Experiment 4 – Coagulation of wastewater spike with a mixture of PFCs

Figure 5.8 shows the percentage removal of each PFC by various organic and inorganic coagulants in wastewater, which has been contaminated with a mixture of PFCs. In the same figure, the results of the experiment 3 have also been shown for the easy comparison. The TOC level is high in experiment 4 than experiment 3 because actual wastewater is used in this experiment. Measured TOC of the wastewater was 10.5 mg/L in this experiment whereas for MilliQ water measured TOC was zero.

It was clearly observed for all organic coagulants that the MilliQ spike with PFCs showed better removal percentage than that of wastewater spike with PFCs for short chain PFCs (PFHxA, PFHpA and PFHS). In case of medium chain and long chain PFCs, it was observed that a slight improvement of PFCs removal with the presence of other organics. These observations can be explained by charges of the PFCs molecules. For short chain PFCs, with less charge (negative) cannot compete with other organics to attach with coagulant polymer, so that their removal efficiencies were adversely affected. In the case of long chain PFCs (PFOS, PFOA and PFDA) with higher molecular charge, PFCs can compete with other organic matter and attach with the coagulant polymers. The process of coagulation for long chain PFCs seems to be accelerated by the presence of the other organic matter in the water. Some of the long chain PFCs may first attach

with organic matter in the water and then get attached with the coagulant polymer improving the overall removal efficiency.

5.4.5 Experiment 5 – Experiment with real waste water

Actual discharge wastewater from PFCs related industry was tested with organic and inorganic coagulants in this experiment. Collected wastewater was initially analyzed. The pH was 6.9 and the TOC was 15.2 mg/L.

The initial PFCs concentration of the wastewater was measured as shown in **Table 5.5**.

Table5.5 Levels of PFCs in the wastewater used in this study

Month of analysis	PFOA $\mu\text{g/L}$	PFOS $\mu\text{g/L}$	PFHxA $\mu\text{g/L}$	PFHpA $\mu\text{g/L}$
2009-4	0.72	-	1.80	0.25
2009-5	2.60	-	4.20	1.40
2009-09	10.00	-	2.90	2.20
2010-02 (This study)	4.35	0.02	0.75	0.33

Figure 5.9 shows removal percentage of each PFC by inorganic and organic coagulants. It should be emphasized that this wastewater is mainly polluted with PFOA (Table 5.5). Whatever the treatment technique applied in this wastewater must be essentially reduce the effluent PFOA level.

It was observed in the previous experiments in this chapter that the average PFCs removal by coagulation was more than 70%. Particularly in the experiments 3 and 4, the removal by some organic coagulants was more than 90%. But this experiment gave different results and none of the coagulants except ferric chloride reached 90% removal efficiency. Especially in PFOA removal, ferric chloride gave the best performance with 91% of removal efficiency followed by FL 2749, FL 3050 with removal efficiencies of 67% and 66% respectively. This observation clearly indicated that the behavior of PFCs in a solution of wastewater spiked with PFCs stock solution and the real wastewater from a PFCs related industry is not same. Another important observation is that the coagulation of short chain PFCs did not show much difference for MilliQ water spiked with PFCs, wastewater spiked with PFCs or actual wastewater from PFCs related industries.

PFCs, particularly long chain PFCs appeared in industrial wastewater seems to be attached to other polar particles. Most probably the negatively charged long chain PFCs may attach with positively charge matters appeared in the industrial wastewater as it has enough mixing and retention time before collecting wastewater sample. The story is different for wastewater spiked with PFCs stock solution, because the retention time is minimum and mixing is provided only to get homogenous solution. This explanation is further consolidated by the results of inorganic coagulants.

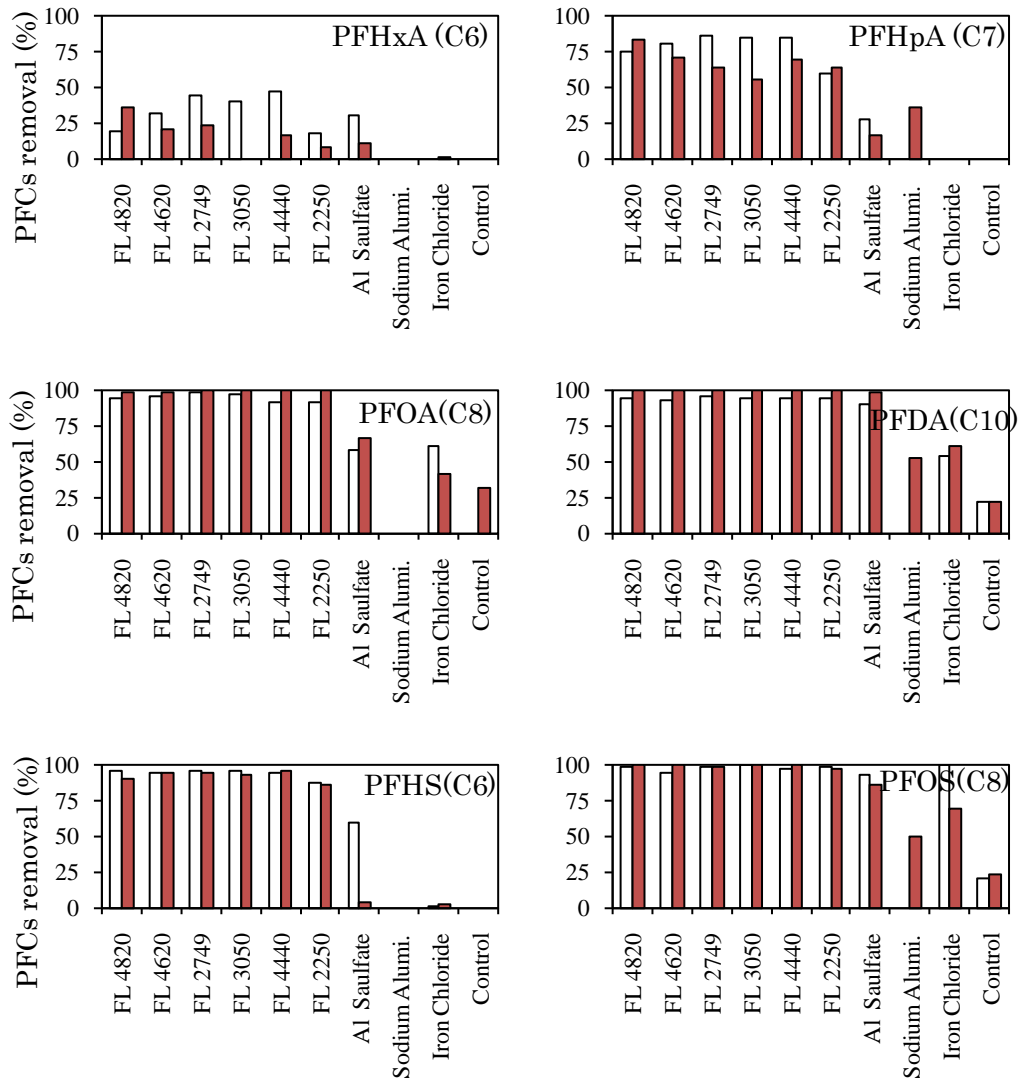


Fig. 5.8 Percentage reduction of each PFCs by various organic and inorganic coagulants for □ MilliQ water spiked with a mixture of PFCs ■ industrial wastewater spiked with a mixture of PFCs

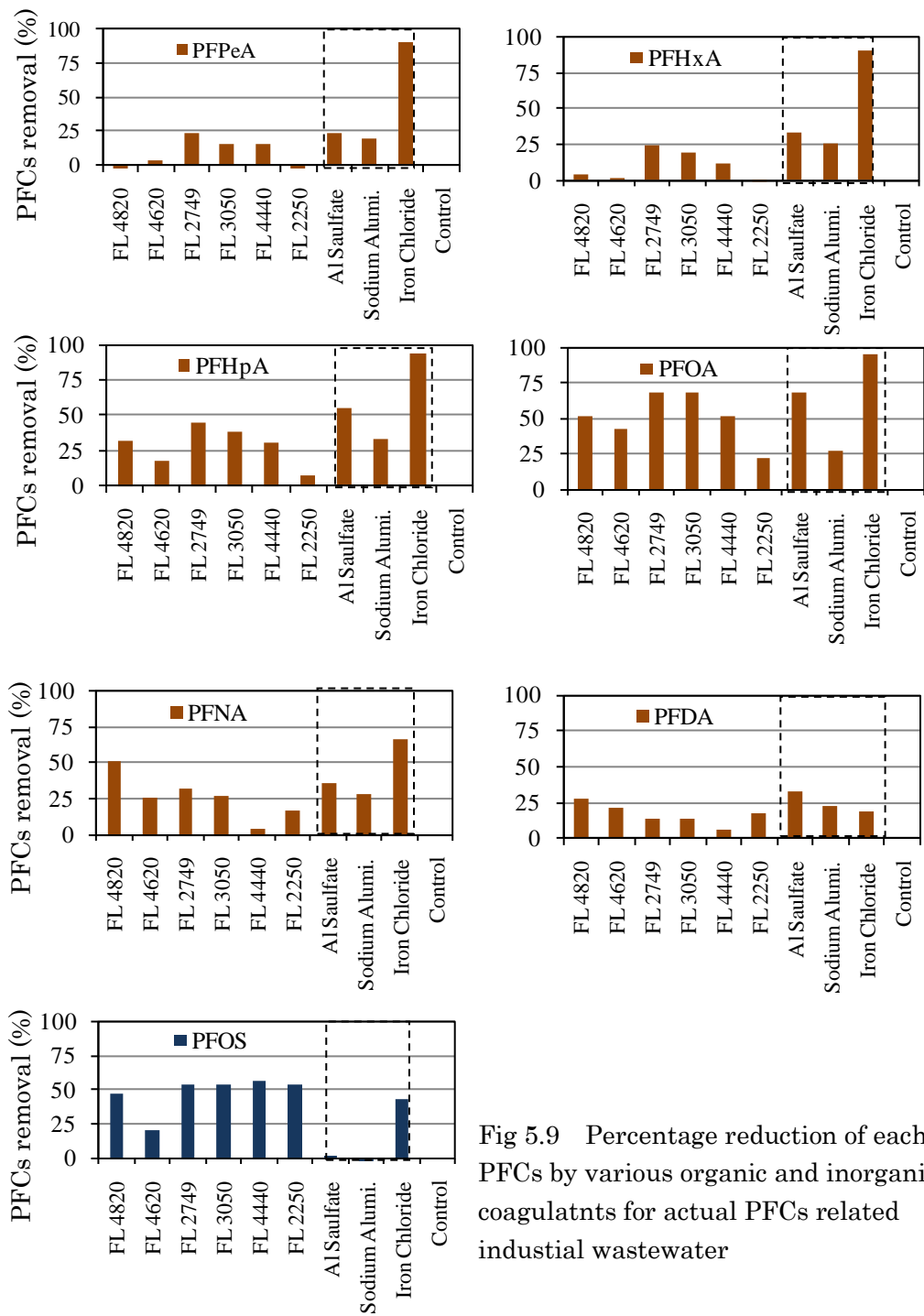


Fig 5.9 Percentage reduction of each PFCs by various organic and inorganic coagulants for actual PFCs related industrial wastewater

5.4.6 The role of filtration in the treatment process.

The filtration process was introduced after the Jar test experiment to simulate the actual treatment process for eliminating flocs and remaining coagulants to make sure the samples was free from suspended particles to analyze with LC/MS/MS. Each sample was filtered at least two times before analysis. First filtration was done at the end of the jar test (after 30 min of settling time) with 0.45 μ m syringe filters and the filtrate was again filtered by 0.2 μ m syringe filters. The control experiment carried out without coagulants showed that this pore size cannot filter PFCs.

The results of experiment 3 and 4 of this chapter suggest that the positively charged organic coagulates drastically improve the efficiency of PFCs filtration by micro filtration (0.2 μ m). Further studies to be done to determine the optimum pore size to prevent PFCs by combine coagulation-micro filtration process.

5.4.7 Possible removal mechanism of organic coagulants for PFCs spiked waters

Once a polymeric coagulant was added to a solution the first expected process is mixing. In the mixing process the polymer becomes distributed evenly throughout the solution. The mixing was achieved in this experiment by rapid mixing at 80 rpm for 3 min. Comparatively low mixing speed was selected as there is a possibility to break some long chain polymers with a high degree of turbulence (Sikora et al., 1981). Since concentrated polymer solutions are quite viscous, mixing usually becomes easier, and flocculation more effective, with more dilute dosing solutions (Gregogy et al., 1991). Mixing effects are generally more important for more concentrated suspensions. **Figure 5.10.a** schematically shows mixing process.

The second possible process is the attachment of polymers with the charged particles in the solution. The rate of attachment mainly depends on their concentrations and it follows the Smoluchowski kinetics (Gregory et al., 1988). This process is schematically shown in **Figure 5.10.b**. According to the literature data, the dose of optimum polymeric coagulant and adsorption rate are proportional to particle concentration (Bolto et al., 2001). The PFCs concentration in the experiment was 10 μ g/L and it was noticed that the longer slow mixing process showed better PFCs removal. Also we noticed that the optimum dose of polymeric coagulant for the elimination of PFCs at tracer level concentration is comparatively high (200 μ L/L).

The third identified process is rearrangement of adsorbed chains (**Figure 5.10.c**). The polymer chain reaches its equilibrium adsorbed configuration with a characteristic distribution of loops, trains and tails. According to the literature data, high mw polymers take several seconds to reach equilibrium concentration (Pelssers et al., 1990), during which, the adsorbed polymers

have more extended configuration and form bridging contacts. Since the coagulant dose applied in this experiment is 250 $\mu\text{L/L}$, TOC level in wastewater was less than 10 mg/L and PFCs concentration was 10 $\mu\text{g/L}$, there was an unbalanced concentrations of opposite charges in the solution and total charge neutralization in polymer coagulants could not be achieved. Also there is a possibility for charge pockets or patch mechanism; it occurs when high charge density cationic polymers adsorb negative surfaces with a fairly low density of charged sites (Kasper, 1971). There is a possibility for some polymers to remain without attaching to a surface or a PFCs.

The final expected process is flocculation, mainly by bridging mechanism (**Figure 5.10.d**). Flocculation is a second order rate process, so that the rate depends on the square of the particle concentration. The mechanism of charge-neutralisation/ precipitation has been proposed for the removal of humic substances by cationic polymers. In many cases (Galser et al., 1979) it has been shown that mw has little or no effect, indicating that polymer bridging is not a significant mechanism. But in this experiment we identified the polymer bridging is important than charge neutralization and we identified the optimum mw is around 100,000 for best PFCs elimination.

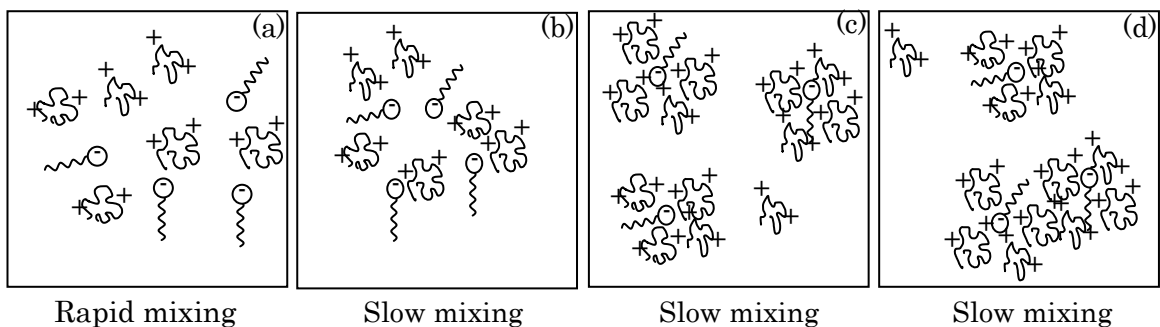


Fig. 5.10 Schematic diagram to explain possible PFCs coagulation mechanism. (a) Mixing (b) attachment (c) rearrangement (d) flocculation

5.5 Conclusion

Following conclusions were derived from the results of this experiment.

1. The experiment with deionized water spiked with PFCs suggested that comparatively higher coagulant dose is required to get a good PFCs removal efficiency by organic coagulants.
2. The results of the experiments with deionized water spiked with PFCs and wastewater spike with PFCs showed that the efficiency of PFCs coagulation by organic coagulant is almost double than that of inorganic coagulants.
3. Among the organic coagulants tested, FL 2749 was identified as the best candidate to eliminate any PFCs.
4. The results of PFCs coagulation by different organic coagulants suggest that a mixture of multipolymers is better than single polymer coagulants to coagulate PFCs.
5. The results of the experiment with actual wastewater spiked with PFCs indicated that occurrence of other organic matters discourages coagulation of short chain PFCs, but it encourages the coagulation of long chain PFCs.
6. The results of the experiment with actual PFCs related industrial wastewater indicated that organic coagulants are not effective as it showed in wastewater spiked with PFCs to coagulate PFCs. The PFCs appear in real wastewater seems to be incorporated with other polar molecules in the wastewater.
7. Organic coagulation followed by microfiltration seems to be an effective combination to eliminate PFCs for some wastewaters, but more studies to be done on this topic.

Chapter 6 - PFOS adsorption (column experiment)

6.1 Introduction

Four kinds of non ion-exchange polymers, which were identified by the batch experiment in Chapter 4, were tested with a column experiment. This experiment setup is approximately simulated the real application of selected polymeric filter materials.

In the column experiment, the process of adsorption was accomplished by passing water through the porous filter medium for the removal of targeted PFCs (PFOS). We initiated this experiment with the latest POPs of PFOS and our research group will continue this experiment with other PFCs. Actually, the columns are designed for adsorbing soluble organic matters onto the media. Most filter columns are designed to operate in a down flow manner but up flow filters are occasionally used ahead of another filter in series.

The process of adsorption could be successfully simulated using the filter columns. However, special attention should be taken to minimize the flow ratio of the sidewall to cross section, which results in significant short circuiting and excessive bed expansion/compression (E.E Baruth, 1969). In addition it is essential to maintain a fixed flow rate.

6.1.1 Key variables for the design of synthetic resin sorbent systems

6.1.1.1 Types of synthetic resins

The results of isotherm experiments can be used to get an idea on candidate materials to eliminate target compound (in this study PFOS). Isotherm experiments and determined coefficients for seven granular materials are shown in Chapter 4. Although isotherm studies are useful for screening resins, it is important to note that these isotherm data are based on batch equilibrium sorption studies. That may not be directly representative of dynamic performance configurations. The actual mass loading on a resin may be significantly lower than that predicted from an isotherm study depending on numerous variables such as competitive sorption effects, background water quality and contact time. Tests performed by Calgon Carbon (Pittsburgh, PA) have shown that operating carbon usage rates, based on capacity at the time of breakthrough, can be estimated at 45 to 55 percent of the equilibrium capacity for VOCs (Stenzel and Merz, 1988). In order to determine a similar relationship for resins, it would be necessary to conduct dynamic column tests. For the usage in drinking-water applications, the synthetic resins have to be certified by the relevant authority to apply in portable water.

6.1.1.2 Background water quality

There is limited data currently available on the effects of background water quality on the PFOS removal efficiency by synthetic resins. One of our previous researchers has found that NOM can discourage the PFCs adsorption onto GAC by carbon foiling and competitive adsorption. Also he suggested that the effect of NOM on adsorption kinetics is minimum (Yong, 2007).

According to the available data on other target organics, the performance of Amberlite resins is unaffected by pH (6.5-8.5), temperature (10°C-25°C), oxidants (HOCl, H₂O₂, and O₃) and the presence of NOM. Amberlite resins have also been found to be unsusceptible to biofouling.

The issue of PFOS desorption would need to be addressed to determine the potential need for selection a mode of regeneration, multiple resin vessels in series, a greater number of sampling locations and a higher frequency of sampling, and a more frequent regeneration of resins.

To reduce the organic loading on the resin and to eliminate disinfection byproduct in tap water it may be prudent to use GAC columns at the front end of the process flow. GAC is cheaper on a per unit basis and is generally more effective for the removal of highly hydrophobic compounds.

6.1.1.3 Process flow configuration

In the real applications, the process flow configuration of synthetic resin systems is very similar to that of GAC systems. The main difference between a resin system and a GAC system is that the provision for a regeneration process. Sorption columns can be used in either down-flow or up-flow service mode. In general, the system configuration will be dependent on a number of factors, including the effluent standard, regeneration technique, and vessel design constraints. In situations where low effluent standards must be met and, thus, low leakage levels are allowed, a resin system works best under countercurrent operation and regeneration, with operation in the up-flow mode and regeneration in the down-flow mode (Rohm and Haas, 1992). Using the down-flow mode for regeneration has been found to have better removal efficiencies and lower leakage levels once the column is returned to service after regeneration (Rohm and Haas, 1992). Sorbent columns can be operated in series, in parallel (also referred to as carousel), or as a combination of the two configurations depending on a number of factors, including the need for continuous operation, space constraints, effluent criteria, service cycle time constraints, operation logistics, and requirements for multi-barrier treatment.

Many field systems do not exhibit ideal, narrow breakthrough curves, but show elongated curves with tailing on the front and back end (Suffet, 1999 and Sun, 1999). This would suggest that the in-series operation offers an

economic advantage over the carousel operation. **Table 6.1** shows the design flow rates of some GAC filters available in the market.

Table 6.1 Design flow rates for some GAC filters available in the market

Brand	Model	Maximum Dimensions	Initial ΔP (psi) @ Flow Rate (gpm)	Chlorine Taste & Odor Reduction @ Flow Rate (gpm)
Pentec filtration	GAC-5	2-7/8" x 4-7/8" (73 x 124 mm)	3.0 psi @ 0.5 gpm (0.2 bar @ 1.9 L/min)	250 gallons @ 0.5 gpm (900 liters @ 1.9 L/min)
	GAC-10	2-7/8" x 9-3/4" (73 x 248 mm)	7.0 psi @ 1.0 gpm (0.5 bar @ 3.8 L/min)	5,000 gallons @ 1.0 gpm (18,900 liters @ 3.8 L/min)
	GAC-20	2-7/8" x 20" (73 x 508 mm)	16 psi @ 2.0 gpm (1.1 bar @ 7.6 L/min)	10,000 gallons @ 2.0 gpm (37,800 liters @ 7.6 L/min)
	GAC-BB	4-1/2" x 9-3/4" (114 x 248 mm)	6.0 psi @ 2.0 gpm (0.4 bar @ 7.6 L/min)	12,500 gallons @ 2.0 gpm (47,000 liters @ 7.6 L/min)
	GAC-20BB	4-1/2" x 20" (114 x 508 mm)	5.0 psi @ 4.0 gpm (0.3 bar @ 15 L/min)	25,000 gallons @ 4.0 gpm (95,000 liters @ 15 L/min)
Siemens Water Tec.		2.875" (7.3 cm) 9.75" (24.8 cm) 2.875" (7.3 cm) 20" (50.8 cm)	1.0 gpm (3.8 L/min) 2.0 gpm (7.6 L/min)	

6.1.2 Regeneration of granular materials

All the granular materials used as adsorbents in filters must be regenerated. In the case of GAC, normally regeneration is done at a separate plant. **Table 6.2** shows the main steps involved with this process (for GAC). Regeneration allows recovery of approximately 70% of the original carbon with this process. The re-activated carbon can be mixed with a portion of new carbon for higher effectiveness and is then returned to its place in the plant process (Clark, 1989). Off site regeneration of adsorbant materials is not cost effective. Also it requires time to install and uninstall filter materials.

Table 6.2 The basic steps involve with GAC regeneration

	Stage	Temperature (degrees C)	Action
1	Drying	< 100	GAC dewatered to 50% of original weight
2	Desorption	100 - 649	volatile materials driven off
3	Pyrolysis	100 - 649	heavy organics burnt leaving residue
4	Gasification	>>649 and >>1038	vapors and residues from previous stages driven out of pores

In the case of synthetic resins, there is a possibility to regenerate the materials on site, which is one of the main advantages over conventional GAC filters. Several alternatives are available for regeneration including steam regeneration, solvent regeneration, and microwave regeneration.

6.1.2 .1 Steam Regeneration

In steam regeneration, saturated steam is passed through a loaded/saturated resin bed, condensed, and collected. The steam is used to desorb organic compounds from the resin and to transport them away from the column. The condensed steam is typically discarded or treated through “superloading.” In superloading, the condensate is passed through a sorbent column just prior to the column’s regeneration cycle, taking advantage of the additional capacity of the sorbent at higher concentrations. The use of steam has been demonstrated to be an effective means of regenerating Ambersorb 563 resins loaded with a variety of organic compounds such as trihalomethanes (THMs) (Vandiver and Isacoff, 1994) and TCE (Parker and Bortko, 1991). In these cases, steam regeneration was able to fully restore the resin’s sorption capacity for these compounds. Suri et al. (1999) confirmed these findings, which showed that six regeneration cycles each with 28 to 40 bed volumes (BVs) of steam (160°C) effectively regenerated resins saturated with p-PCB, perchloroethylene (PCE), and CCl₄. In the case of o-PCB, there was a 20 percent loss in capacity observed after the first regeneration cycle. However, subsequent cycles did not result in further loss of sorption capacity (Suri et al., 1999).

6.1.2 .2 Solvent Regeneration

In solvent regeneration, a solvent in which the adsorbate is highly soluble is passed through the saturated bed. In this experiment, organic regeneration was carried out for regeneration of several non ion-exchange polymers which have adsorbed PFOS.

6.1.2 .3 Microwave Regeneration

Most studies on the use of microwave regeneration of sorbents examined vapor-phase applications in which the sorbents are used to remove volatile organic compounds (VOCs) from gaseous emission streams. However, the use of microwave regeneration for a liquid phase sorbent system is likely to be a similar process. Unlike steam regeneration, which uses steam to heat up the sorbent system, microwave irradiation generates heat directly in the sorbent bed by exciting sorbent and sorbate molecules. Contaminants adsorbed onto a resin column are volatilized and subsequently extracted through an induced vacuum (AmeriPure, Inc., 1999). Microwave heating has been shown to effectively eliminate the heat and mass transfer

resistances that limits the rate of regeneration in conventional steam systems (Price and Schmidt, 1997).

6.2 Aim and objectives

Major aim of this chapter is to study selected non ion-exchange polymer materials with a column experiment. Only non ion-exchange polymers were specifically selected for the column test mainly for two reasons. First reason is that it was found in the isotherm experiment that non ion-exchange polymers are possible candidates to adsorb PFOS; prior studies on this are rarely available. The second reason is easy regeneration of materials than other materials tested. The tested polymer materials were selected by the batch experiment conducted in Chapter 4. The results of the column experiment must be explained by the results of the batch test, which was conducted to determine adsorption isotherms. Also the results of this experiment are useful to determine some design and operational parameters in the real application in the field. The objectives in details are listed as below.

6.2.1 Objectives

1. To obtain column breakthrough curves up to 90% of PFOS removal for selected non ion-exchange filter materials.
2. To develop a mathematical model to explain the behaviors of the selected filter materials in the column.
3. To check the regenerability of non ion-exchange filter materials by washing of organic solvent.

6.3 Methodology

6.3.1 Adsorbent Pretreatment

Prior to the usage in the sorption experiment, Dowex polymers were first washed in ultrapure water to remove dirt and then dried at 50°C until reached a constant weight. Amberlite was also washed with deionized water first and then dried at 30°C. Once the polymers reached a constant weight, each column was filled with a required volume of each polymer. Similarly, the coal-based activated carbon of Filtrasorb 400 was first rinsed with deionized water for several times and then washed in 80°C deionized water for 2 hrs to remove the impurities. After being dried in an oven at 105°C for 48 hrs, they were crushed by a mortar and passed through 0.25 -0.5 mm sieve. After selecting the GAC with required size, again it was washed by deionized water to remove PAC particles attached with GAC. Washed GAC was dried and measured the required volume and installed into the column.

6.3.2 Analytical Equipments and Methods for PFOS Determination

At each sampling event, about 500mL of sample was collected from 1 column for the analysis of TOC and remaining PFOS. For the analysis of PFOS, 100mL was measured from the collected sample and sent through a Precip-C agri cartridge by using a concentrator (flow rate 5mL/min). Then, the cartridge was air dried for 1 hr using a vacuum manifold and then eluted it with methanol 3 mL. Eluted methanol was completely dried by flow of nitrogen gas at 60° C. Then, dried tube was reconstituted with 40% ACN solution and at the same time the concentration was adjusted such it did not exceed 10 µg/L. Final solution was analyzed and measured using HPLC/MS/MS (Agilent, Japan) and final concentration was calculated. In Agilent 1200SL HPLC, 5mM ammonium acetate and acetonitrile were used as mobile phases. Agilent 6400 triple quadrupole MS/MS was used in multiple reaction monitoring (MRM) at negative ionization mode for the detection of m/z of parent ion (499) and daughter ion (80) of PFOS.

6.3.3 Column Experiment

The column experiment setup is schematically shown in **Figure 6.1**. PP columns with dimensions of 30 cm length and 2 cm internal diameter were used to contain four types of filter materials as fixed-bed adsorbers. One column was run without a filter material as a control. The columns were first filled with measured pre treated material volume of 20 cm³. Then the columns were filled with MilliQ water and applied a vacuum for 24 hrs, which ensured all entrapped air bubbles in material surfaces were released. Tap water filtered with an activated carbon filter (to eliminate residual chlorine) was mixed with PFOS stock solution to adjust the feed PFOS concentration to 10 µg/L. The mixed PFOS solution was fed through five columns in down-flow mode and channeling of bed materials were avoided by mesh fixed at the bottom of each filter beds (Figure 6.1). Peristaltic pumps were used to control the flow rates at the inlets of each column and the mixing tank. The effluent of each column were collected periodically and analyzed for the remaining PFOS concentration (C) using LC/MS/MS. The desired break through concentration (C_b) was determined at 10% of the inlet feed concentration (C₀), which is 0.1 C₀ or 1 µg/L. The flows through the tested columns were continued until the PFOS concentration of all columns effluent approached 0.2 C₀ which took about 60 days.

6.3.4 PFOS regeneration

All filter materials of each column were completely removed after operation and dried in 60°C for 48 hrs. The dried materials were thoroughly mixed to make it homogenous. For the regeneration experiment, 0.02 g of each dry material were added to 1L of LC/MS grade methanol and shaken at control

temperature of 25°C. Sampling was done at different time intervals of 0, 20, 80 and 270 min. 2 mL of each collected samples were dried with nitrogen gas at 55°C and then reconstituted with 40% acetonitril (4mL). After filtration (0.2µm), the final samples were analyzed with LC/MS/MS for recovered PFOS.

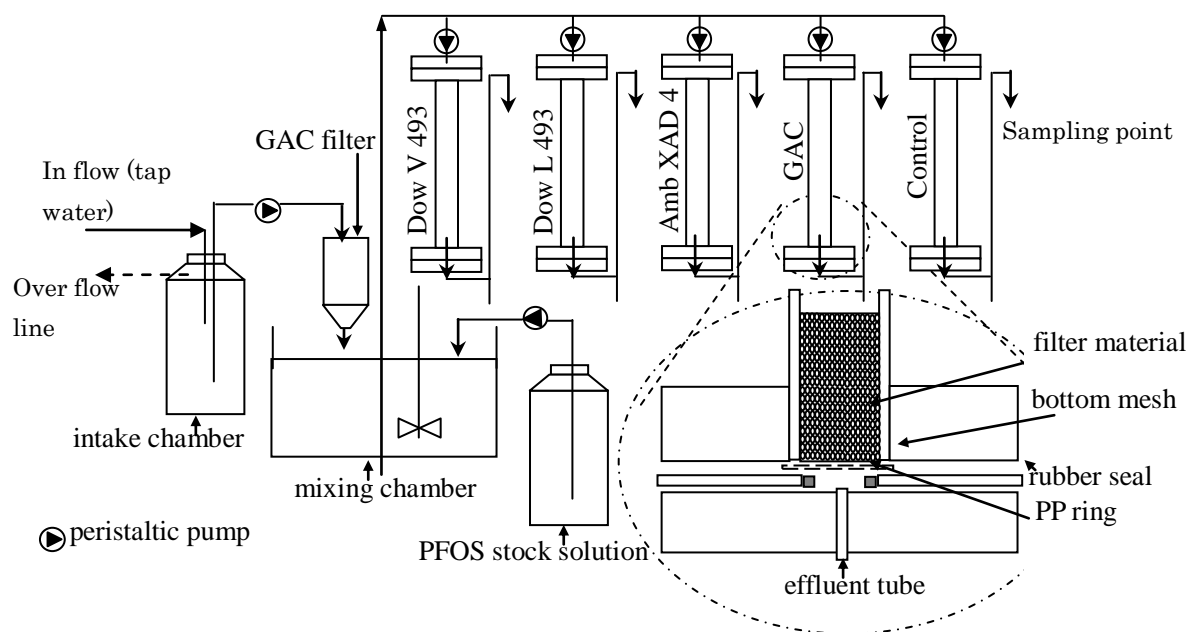


Fig 6.1 Column experiment setup for PFOS adsorption onto different filter materials

6. 4 Results and discussion

6.4.1 Forces effect on adsorption

Previous studies have demonstrated that anionic surfactants uptake by a adsorbent surface is strongly dependent on electrostatic interactions between a surfactant molecule and the surface (Dobson et al., 2000; Johnson et al., 2007). In addition, the Columbic repulsion between adjacent PFOS molecules is likely to play an important role. Other non electrostatic interactions, such as hydrophobic interaction (Dobson et al., 2000; Torn et al., 2003), may also contribute to surfactant adsorption onto mineral surfaces. Thus, the change in total free energy ((ΔG) adsorption) associated with PFOS adsorption can breakdown into three components:

$$(\Delta G) \text{ adsorption} = (\text{PFOS} - \text{surface electrostatic interaction}) + (\text{PFOS} - \text{PFOS electrostatic interaction}) + (\text{non} - \text{electrostatic interactions})$$

6.4.1.1 PFOS-surface electrostatic interaction

PFOS, being a strong acid with an estimated pKa of around -3 (OECD, 2002), carries a negatively charged site at its sulfonate head group under all environmentally relevant pH. In general, a mineral surface becomes more positively charged (or less negatively charged) at lower pH. This results in an enhanced electrostatic attraction force (or reduced electrostatic repulsion force) between the negatively charged PFOS molecules and the surface, which is expected to promote PFOS adsorption at lower pH. Another important parameter that affects the electrostatic interaction between PFOS molecules and the adsorbent surface is ionic strength. The electrostatic interaction can be significantly weakened at higher ionic strength due to the double layer compression effect. For a positively charged mineral surface, the amount of adsorbed PFOS tends to be reduced due to the weaker electrostatic attraction (Chuyang et al., 2010).

6.4.1.2 PFOS-PFOS electrostatic repulsion.

In addition to the PFOS surface electrostatic interaction, two adjacent PFOS molecules on a surface will also repel each other due to their negatively charged sulfonate head groups. A strong PFOS-PFOS repulsion tends to prevent these molecules getting close to each other. Thus, a solution with high ionic strength has a tendency to promote PFOS adsorption as a result of the suppressed electrostatic repulsive force. In contrast, the PFOS-PFOS electrostatic repulsion is not directly affected by pH since these molecules carry a constant charge over all environmentally relevant pH values (Chuyang et al., 2010).

6.4.1.3 Other non-electrostatic interactions.

Non-electrostatic interactions such as hydrophobic interaction (Higgins and Luthy, 2006; Ochoa-Herrera and Sierra-Alvarez, 2008; Torn et al., 2003) may also contribute to PFOS adsorption, given the strong hydrophobic nature of its perfluoroalkyl chain. For example, hydrophobic interaction may arise between the hydrophobic chain of a PFOS molecule and the hydrophobic moiety on a mineral surface or between the hydrophobic chains of different PFOS molecules. Such non-electrostatic interaction has much weak or little dependence on the solution chemistry compared to the PFOS-surface and PFOS-PFOS electrostatic interactions.

6.4.1. 4 Effect of pH

In general, lowering pH makes a surface more positively charged, which promotes PFOS adsorption (enhanced PFOS-surface interaction). However, the effect of pH diminishes at high ionic strength, as the PFOS-surface electrostatic interaction becomes screened by counter ions as a result of

electrical double layer compression (Chuyang et al., 2010).

6.4.1.5 Effect of ionic strength

Increasing ionic strength tends to suppress the PFOS-surface as well as PFOS-PFOS electrostatic interactions. The net result on PFOS adsorption depends on the competition between the two types of interactions. For a weakly charged mineral surface ($\text{pH} \sim \text{H}_{\text{pzc}}$), the PFOS-surface electrostatic interaction is negligible compared with the PFOS-PFOS interaction. Consequently, increasing ionic strength promotes PFOS adsorption as a result of reduced repulsive force between adjacent PFOS molecules. In contrast, the PFOS-surface interaction dominates for a highly charged surface.

6.4.2 Overall Performance of the columns with time

We applied comparatively higher flow rate of 15 mL/min which ensures at least 1.3 min retention time and inflow PFOS concentration was kept constant at 10 $\mu\text{g/L}$. **Figure 6.2 a and b** show the percentage removal of PFOS in each column over the time (60 days) and the variation of effluent PFOS concentration with operation time and filtered bed volume. It was noticed for all polymers that the percentage removal efficiency for first 5000 bed volume is more than 99%. Amb XAD showed excellent performance by removing more than 99.99% PFOS from first 23,000 bed volumes passing through it. The column break through point was assumed at 90% removal because the PFOS concentration in environmental water is in ng/L level.

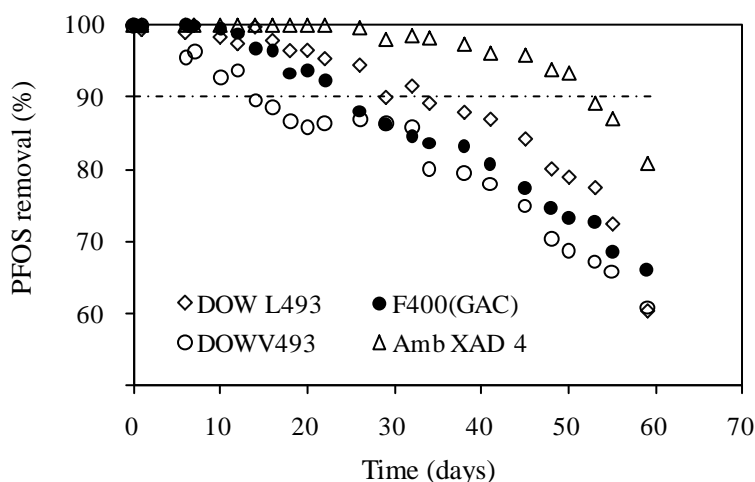


Fig. 6.2(a) Variation of percentage PFOS removal with time (60 days) for different filter materials in the column experiment

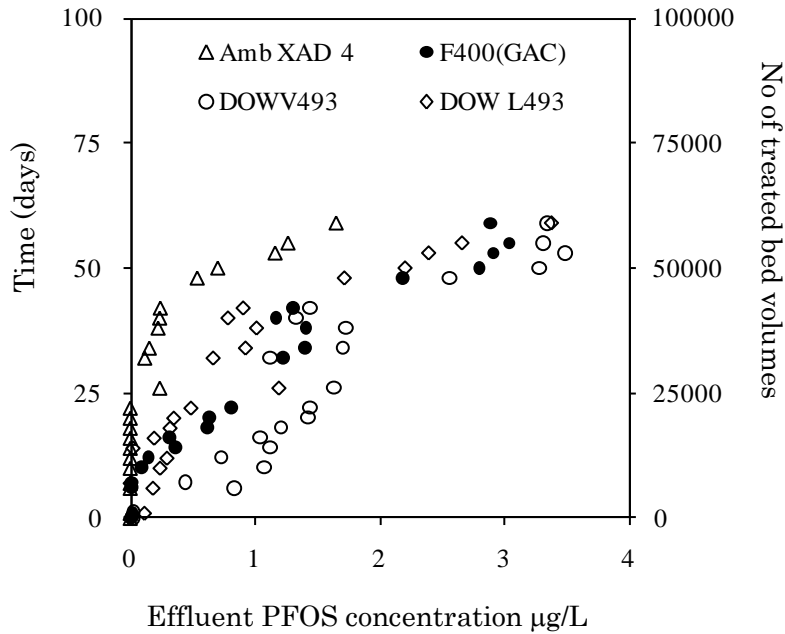


Fig 6.2(b) Variation of effluent PFOS concentration with operation time and filtered bed volume

6.4.2 .1 Dowex L493

The PFOS removal efficiency of the column with Dow L493 was more than 99% for first 7 days. It took 30 days to reduce the removal efficiency from 100% to 90%, another 18 days to reduce it from 90% to 80% and 9 days to reduce from 80% to 70%. **Figure 6.3** shows the percentage relative abundance with time.

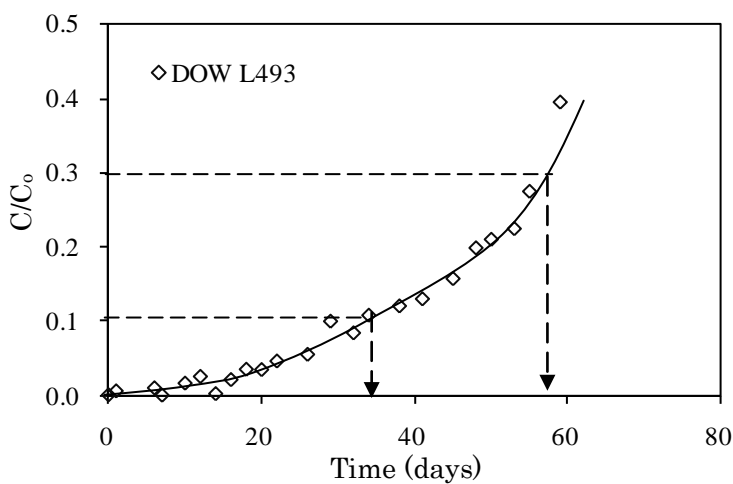


Fig 6.3 Fractional effluent PFOS concentration in the column with DOW L493

6.4.2.2 Amberlite XAD 4

Amb XAD 4 was the best candidate among the tested filter materials. The effluent PFOS concentration of AmbXAD4 was less than detectable level for first 20 days (**Figure 6.4(a)**).

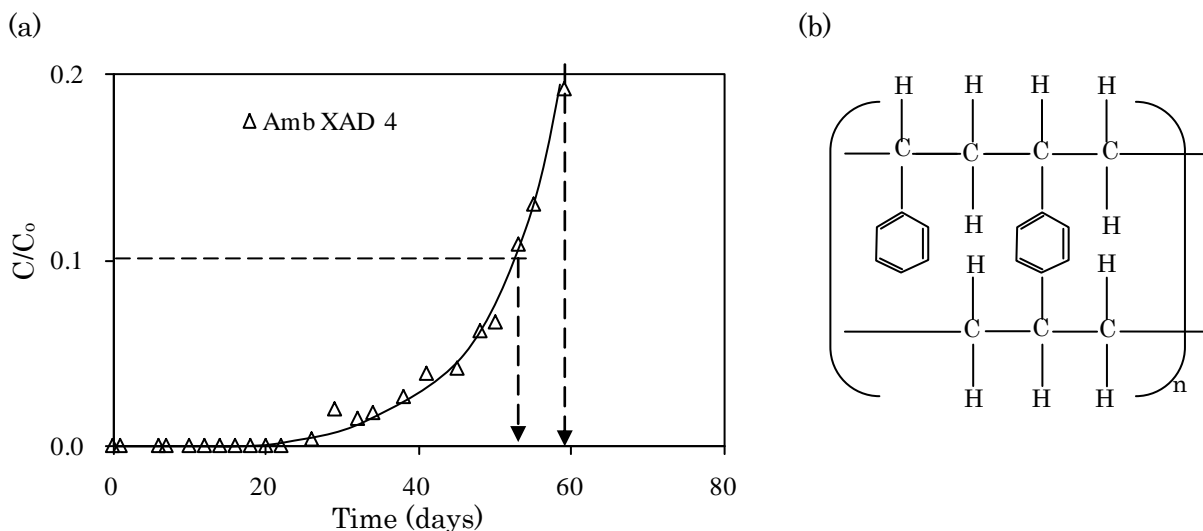


Fig 6.4 (a) Fractional effluent PFOS concentration in the column with Amb XAD 4; (b) Basic structure of Amb XAD 4;

The removal efficiency was decreased to 96% during next 20 days and showing a sudden efficiency drop from 40 days removal efficiency was 80% after 60 days. This behavior emphasizes the superior performance of AmbXAD at low PFOS concentrations.

Amberlite XAD 4 is a non-ionic cross linked polymer which derives its adsorptive properties from its macroreticular structure (containing both continuous polymer phase and continuous pore phase), high surface area and the aromatic nature of its surface (**Figure 6.4 (b)**). This structure gives Amb XAD polymer adsorbent an excellent physical, chemical and thermal stability. Average surface area of other granular materials tested was around 1,000 m²/g. The surface area of AmbXAD4 is unknown, but it is said by the manufactures that the minimum surface area is 750 m²/g. it can be reasonably assumed that the actual surface are of Amb XAD4 is more than other materials tested.

6.4.2.3 Granular Activated carbon

GAC showed more than 99.95% of PFOS removal for first 7 days and then started to reduce the performance. Unlike other granular materials tested, it was noticed that the relative abundance of PFOS is linearly increased

with time (filtered volume) (**Figure 6.5**) for this material. GAC column took about 22 days to reduce the removal efficiency by 10% (from 100% to 90%) and 40 days to reduce it by 20%.

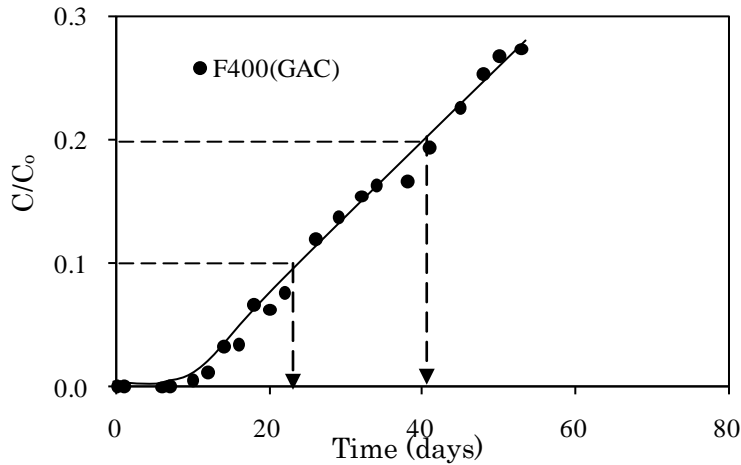


Fig 6.5 Fractional effluent PFOS concentration in the column with F400

6.4.2.4 Dowex V493

Among all the granular materials tested, DowV493 showed the minimum performance to remove PFOS. The performance of the column was reduced by 10% within 12 days and by 20% within 35 days (**Figure 6.6**).

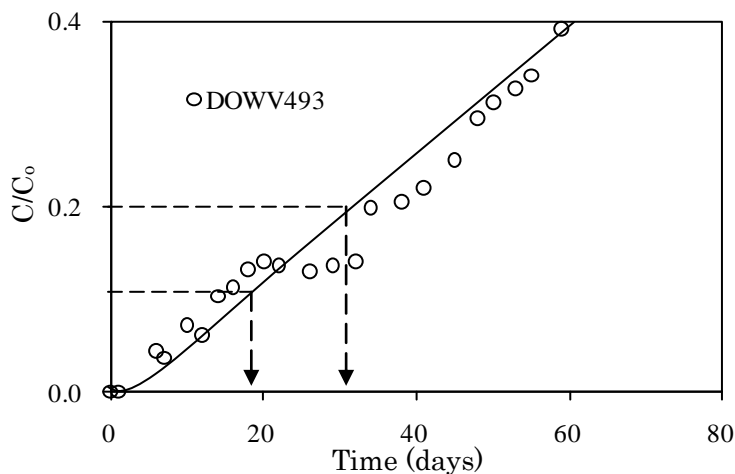


Fig 6.6 Fractional effluent PFOS concentration in the column with DOW V493

6.4.3 Column test results and Batch test results

The results of column test experiment can be explained by the results of batch test and kinetic test experiments. The PFOS concentration of the column outflow is decided by two main factors. First factor is the amount of

vacant sites of the filter media which can attach PFOS molecules and the second factor is the time requirement to make the bond between sorbent and sorbate. Isotherm experiment gives an idea on available vacant sites and kinetic experiment implies the speed of attachment. Amb XAD4 showed higher sorption rate constant ($k = 0.48$) and Freundlich isotherm constant ($K_f = 79.1$) and it was the best material even in the column test. GAC also showed higher sorption rate constant ($k = 80.28$) but lower Freundlich isotherm constant ($K_f = 28.4$) whereas for Dow L493 and Dow V493 showed higher Freundlich isotherm constants ($K_f = 54.6$ and 81.3) but lower sorption rate constants ($k = 0.07$ and 0.08).

6.4.4 Mathematical modeling

Lin and Huang (2007) proposed a mathematical model for the change of sorbate concentration in a column (with short column operation time of 1-5 min). using the same assumption they made, we come up with a modeling equation as derived below.

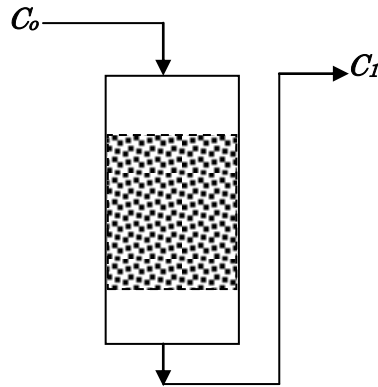


Fig 6.7 Schematic representative of a column for modeling

$$\text{Fraction of adsorption} \quad A = \frac{C_0 - C_1}{C_0} \quad 6.1$$

$$\text{Fraction of discharge} \quad P = \frac{C_1}{C_0} \quad 6.2$$

$$A + P = 1 \quad 6.3$$

$$\text{The rate of change of fraction of adsorption} = \frac{dA}{dt} = \frac{d[(C_0 - C_1)/C_0]}{dt} \quad 6.4$$

According to Lin and Huang (1999) it can be assumed that the rate of change of adsorption fraction is linearly promotional to the fraction of adsorption (A) itself

and the fraction of discharge (P).

With this assumption it can be written as

$$-\frac{dA}{dt} \propto AP \quad 6.5$$

Same expression can be rewritten with a constant as

$$-\frac{dA}{dt} = kAP \quad 6.6$$

From equations 6.3 and 6.6

$$-\frac{dA}{dt} = kA(1-A) \quad 6.7$$

With the initial conditions of $A = A_a$ and $t = t_a$, the equation can be integrated as

$$\int_{A_a}^A \frac{dA}{A(1-A)} = - \int_{t_a}^t k dt \quad 6.8$$

$$\ln \frac{A(1-A_a)}{A_a(1-A)} = k(t_a-t) \quad 6.9$$

Which is the same as:

$$\ln \left[\frac{P_a(1-P)}{P(1-P_a)} \right] = k(t_a-t) \quad 6.10$$

if the half removal time is denoted by τ , P (remaining fraction of PFOS) is 0.5 at $t = \tau$

$$P = \frac{1}{1 + \exp [k(\tau - t)]} \quad 6.11$$

Or

$$t = \tau + \frac{1}{k} \ln \left[\frac{P}{(1-P)} \right] \quad 6.12$$

Since the inflow and the outflow of the column is same, the remaining fraction of PFOS at the outflow can be represented by the concentration ratio, C/C_0 . Where C is the PFOS concentration at the outflow of the column and C_0 is the inflow PFOS concentration.

Then, the equation 6.12 can be rewritten as

$$t = \tau + \frac{1}{k} \ln \left[\frac{C}{(C_0 - C)} \right] \quad 6.13$$

According to equation 6.13, a linear plot of adsorption time (t) vs $\ln[C/(C_0 - C)]$ can be used to determine the half saturation time (τ) and column constant k .

Figure 6.8.a shows such a plot for PFOS adsorption on to different filter materials and **Table 6.3** shows the calculated τ and k . **Figure 6.8b** shows the theoretical curves which have been drawn with calculated τ and k and actual data point for first 60 days.

Table 6.3. parameters of the theoretical model proposed by Lin and Huang (1999) for a column experiment for PFOS adsorption onto different filter materials.

Adsorbent	τ (days)	k (1/days)	R^2
Dow V493	64.5	0.049	0.93
Amb XAD 4	70.7	0.117	0.97
Dow L493	67.4	0.069	0.98
Filtrisorb 400	65.5	0.060	0.94

Note: Half saturation time (τ) and column constant k with 10 $\mu\text{g/L}$ inflow concentration and 0.75 bed volume /min flow rate

6.4.5 Material regeneration by organic solvents

In the real application of solvent regeneration, a solvent in which the adsorbate is highly soluble is passed through the saturated bed. Studies by Rohm and Haas (1992) have demonstrated that the use of solvents such as methanol or acetone at a flow rate of two bed volumes per hour can successfully regenerate resin columns. In one study, methanol was found to extract more than 99% of 280 mg of trichloroethylene adsorbed per gram of Amb 563 (Parker and Bortko, 1991). A second study showed that 4 to 5 BVs of methanol at a flow rate of 1 bed volume per hour can remove more than 95% of 1,2-dichloroethane loaded on an Amb 563 column (Isacoff et al., 1992). Rinsing with water or steam is typically performed after regeneration to remove any residual regenerant prior to the next sorption cycle. In another experiment by Malley et al. (1993), methanol was demonstrated to be ineffective in regenerating some synthetic resins. The published data on the effectiveness of solvent regeneration specifically for PFCs-saturated columns is rarely available.

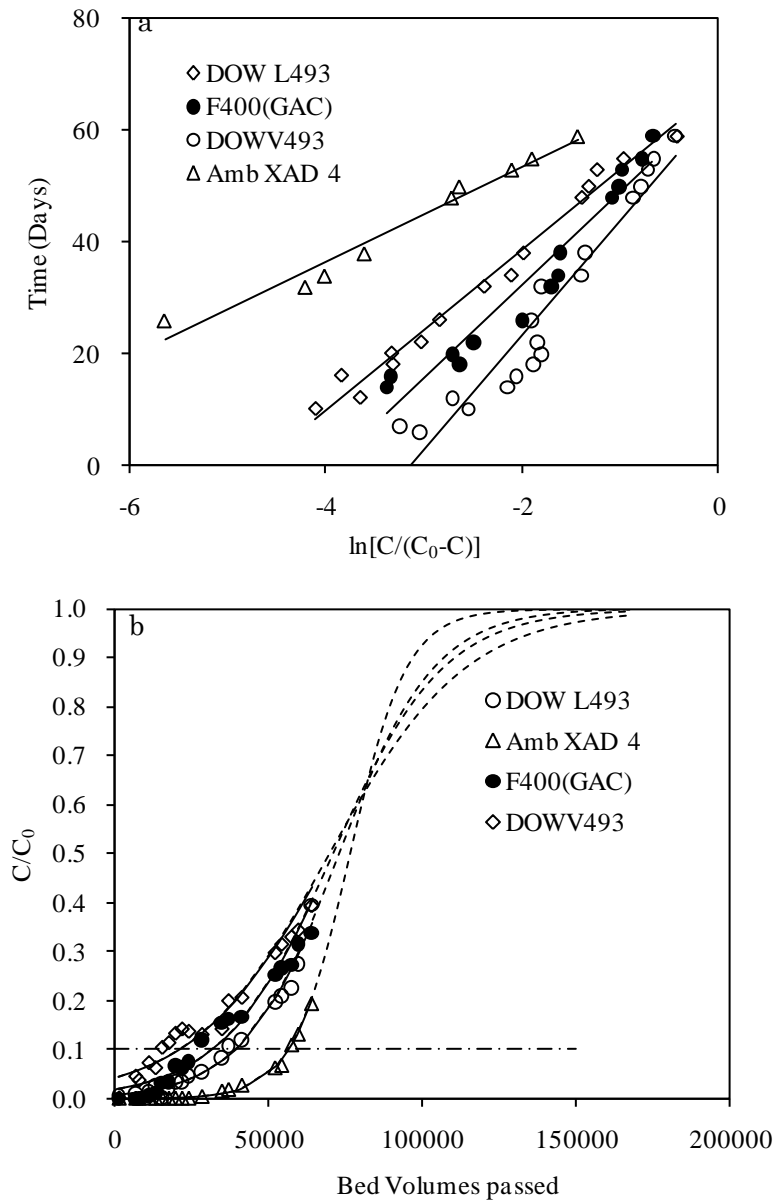


Fig. 6.8 Linear plot of t vs. $\ln[C/(C_0-C)]$ (a) and comparison of the observed and predicted breakthrough curves (b) of PFOS adsorption in columns with different filter materials.

The accumulation of PFOS over the operation of column test of 60 days is shown in **Figure 6.9**. The cumulative PFOS inflow into the column is also shown in the same figure. We only measured the PFOS concentration at in-flow and out-flow at different times (days) and the PFOS accumulation in the granular materials were calculated considering the difference of concentrations, sampling intervals and flow rates.

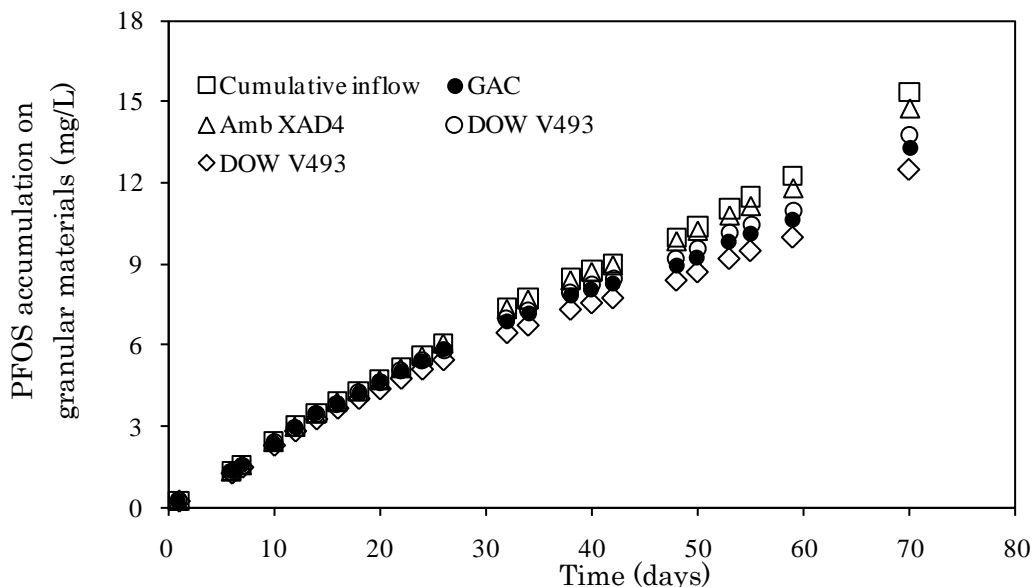


Fig 6.9 Variation of cumulative PFOS accumulation on various filter materials with time

Figure 6.10 shows the variation of percentage PFOS recoveries of each granular material with time. As reported by many researchers in previous studies (Rohm and Haas, 1992, Parker and Bortko, 1991, Isacoff et al., 1992) for other organic compounds, methanol has been identified as an ideal organic solvent to regenerate PFOS adsorbed synthetic resins.

For the synthetic polymers, a sudden recovery was observed for first 30 min and they reached the maximum recovery of 100% within 80 min. For GAC it was observed that the percentage recovery just reached 40% after 270 min of shaking time. One possible reason for faster desorption kinetics of synthetic resins than GAC is the strength of sorbent - sorbate. There is a physico-chemical bond between the internal surface of adsorbent and adsorbate at any adsorption process (Montgomery, 2008). The bond between GAC surface and PFOS seems to be stronger than that of synthetic resins and PFOS. The second possible explanation is pore diffusion. PFOS seems to be diffused into deep pores in the active GAC surface and it takes time to dissolve PFOS back in organic solvent. In the case of synthetic resins, PFOS attachment to the outer surface is dominant suggesting minimum pore diffusion. This may be the reason for higher PFOS recovery from synthetic resins than from GAC mainly during the first few minutes. The results suggest onsite regeneration of synthetic resins by organic solvents is much more feasible than regeneration of GAC. PFOS might be easily recovered from methanol by evaporation and it can be reused.

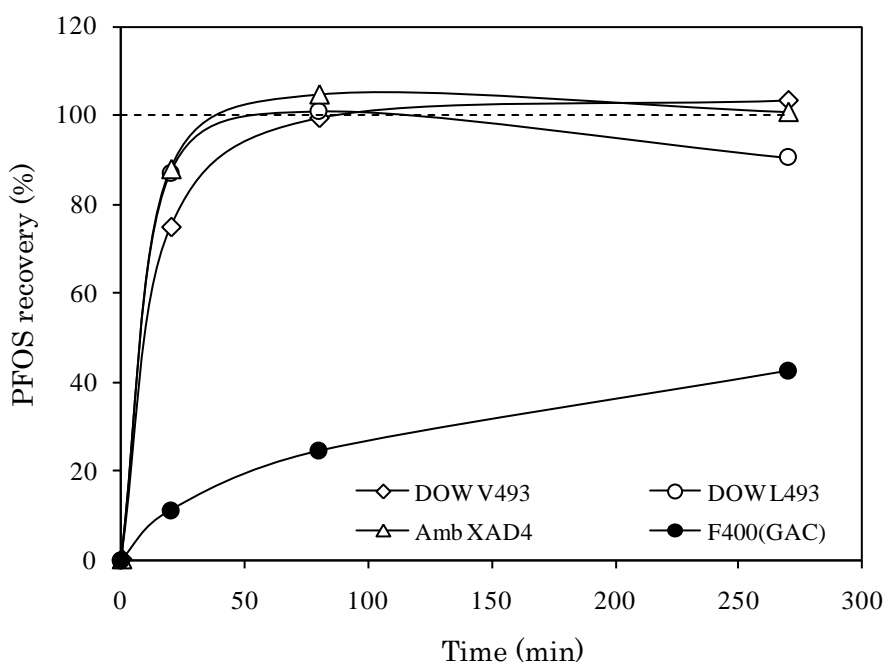


Fig 6.10 Variation of percentage PFOS recovery with time by organic solvent

6.5 Summary

In this chapter, non ion exchange polymer materials, which were selected by the batch experiment in Chapter 4 was tested with a continues column experiment. Three synthetic granular materials and one GAC material were tested by the column experiment, which was continuously run for 60 days. The conclusions of the experiment are summarized below.

1. Amb XAD 4 was recognized as the best candidate among the tested four filter materials to eliminate PFOS.
2. It was observed that the results of column experiment cannot be explained by individual results of isotherm experiment or kinetic experiment suggesting the importance of both isotherm (available vacant sites in the materials to adsorb) and kinetics (the speed of attachment) in the real application.
3. It was interesting to notice in the column experiment that Amb XAD 4 removed 99.99% PFOS up to 23,000 bed volumes pass through with the condition of 10 $\mu\text{g/L}$ inflow concentration and flow rate of 15 ml/min (0.75 bed volumes/min).
4. Within 80 min, all most 100% PFOS was recovered from synthetic resins in the regeneration experiment suggesting that synthetic polymers can be effectively regenerated by an organic solvent.

Chapter 7 - Combined treatment of PFOS

7.1 Introduction

The combined process of coagulation and filtration is not a new concept. Coagulation, flocculation and clarification, followed by rapid gravity sand filtration, are the key steps in conventional water treatment systems. This is a well-proven technology for the significant removal of color and particulate matter including protozoa (e.g. *Cryptosporidium* oocysts and *Giardia* cysts), viruses, bacteria, and other micro-organisms. Iron, manganese, tastes and odors may also be removed from the water by these processes (Mercalf & Eddy, 2003; Fiksdal et al., 2006, Dugan et al, 2001). This chapter combines the two unit operations of coagulation, adsorption and filtration, studied under Chapter 5 and 6 to remove PFOS from water. Conventional treatment (coagulation, sedimentation and sand filtration), has several distinct stages. A coagulant is added to neutralize the natural electrical charges on the colloidal particles that prevent them from agglomerating, and is rapidly mixed into the water to be treated. The processed water will then enter a flocculation chamber, where further chemicals may be added. Gentle mixing during this stage allows particles to agglomerate and form settleable flocs. We tried to simulate the process in the lab scale with polymer type organic coagulants and non ion exchange granular materials. It was assumed that the attachment of PFCs into long chain organic coagulant can be further enhanced the adsorption process and can be achieved superior performance than the individual coagulation and adsorption process.

7.2 Aim and objectives

The overall objective of this experiment was to examine the improvement of adsorption process by prior coagulation by organic coagulants. Non ion-exchange polymer adsorbents tested in Chapter 4 and the organic coagulants tested in Chapter 5 were used in this experiment. Coagulation and flocculation processes were simulated by lab scale unit and same column setup used in Chapter 6 was used to treat coagulated water.

The specific objectives of the experiment are as follows.

1. To observe the PFOS adsorption characteristics of non ion-exchange polymers for coagulated water by obtaining the column break through curves.
2. To determine the effect of TOC on PFOS adsorption.
3. To check the effectiveness of micro-filtration to eliminate PFOS from coagulated water.

7.3 Methodology

7.3.1 Adsorbent Pretreatment

Pretreatment of granular materials were similar to that of column experiment at Chapter 6. Prior to the use in the sorption experiment, Dowex polymers were first washed in ultrapure water to remove dirt and then dried at 50° C until reached a constant weight. Amberlite also washed with ultrapure water first then dried at 30° C. Once the polymers reach the constant weight, each column was filled with the required volume of each polymer. Similarly, the coal-based activated carbon of Filtrasorb 400 was first rinsed with deionized water for several times and then washed in 80° C deionized water for 2 hrs to remove the impurities. After being dried in an oven at 105°C for 48 hrs, they were crushed by a mortar and passed through 0.25 -0.5 mm sieve. After selecting the GAC with required size, again it was washed by deionized water to remove PAC particles attached with GAC. Washed GAC was dried and measured the required volume and installed into the column.

7.3.2 Analytical Equipments and Methods for PFOS Determination

At one sampling, about 1 L of sample was collected from one column. 100 mL was measured from the collected sample and first it was filtered with 0.2mm syringe filters. The main purpose of this step is to eliminate all the remaining coagulants in the sample as they can interfere with LC/MS/MS analysis. The filtrate was sent through a Presep-C agri cartridge by using the concentrator (flow rate 5mL/min). Then, the cartridge was air dried for 1 hr using a vacuum manifold and then eluted it with methanol 2 mL and Acetonitrile 2mL. Eluted methanol was completely dried by a flow of nitrogen gas at 55° C. Then, dried tube was reconstituted with 40% ACN solution and at the same time the concentration was adjusted such that it did not exceed 10 µg/L. Final solution was analyzed and measured by using LC/MS/MS and final concentration in the initial solution was calculated. In Agilent 1200SL HPLC, 5mM ammonium acetate and acetonitrile were used as mobile phases. Agilent 6400 triple quadrapole MS/MS was used in multiple reaction monitoring (MRM) at negative ionization mode for the detection of m/z of parent ion (499) and daughter ion (80) of PFOS.

7.3.3 Column Experiment

The column experiment setup is schematically shown in **Figure 7.1**. Similar kind of PP columns used in the column test in Chapter 6 with dimensions of 30 cm length and 2 cm internal diameter were used. Four non ion-exchange filter materials already tested in Chapter 4 and Chapter 6 were placed in the columns. Fifth column was run without a filter material and only coagulated water was collected at the effluent of column 5. The

columns were first filled with measured pre treated material volume of 20 cm³. Then, the columns were filled with deionized water and applied a vacuum for 24 hrs which ensured all entrapped air bubbles in material surfaces were released.

As an addition to the previous column test, rapid mixing tank was introduced for this experiment. Tap water filtered with an activated carbon filter (to eliminate residual chlorine) was mixed with PFOS stock solution (to adjust the feed concentration to 10 µg/L) and coagulation stock solution at the rapid mixing tank. The coagulated PFOS solution was sent to a slow mixing tank at which flocculation process is enhanced. Then, the solution was fed through five columns in down-flow mode and channeling of bed materials were avoided by mesh fixed at the bottom of each filter beds (Figure 7.1).

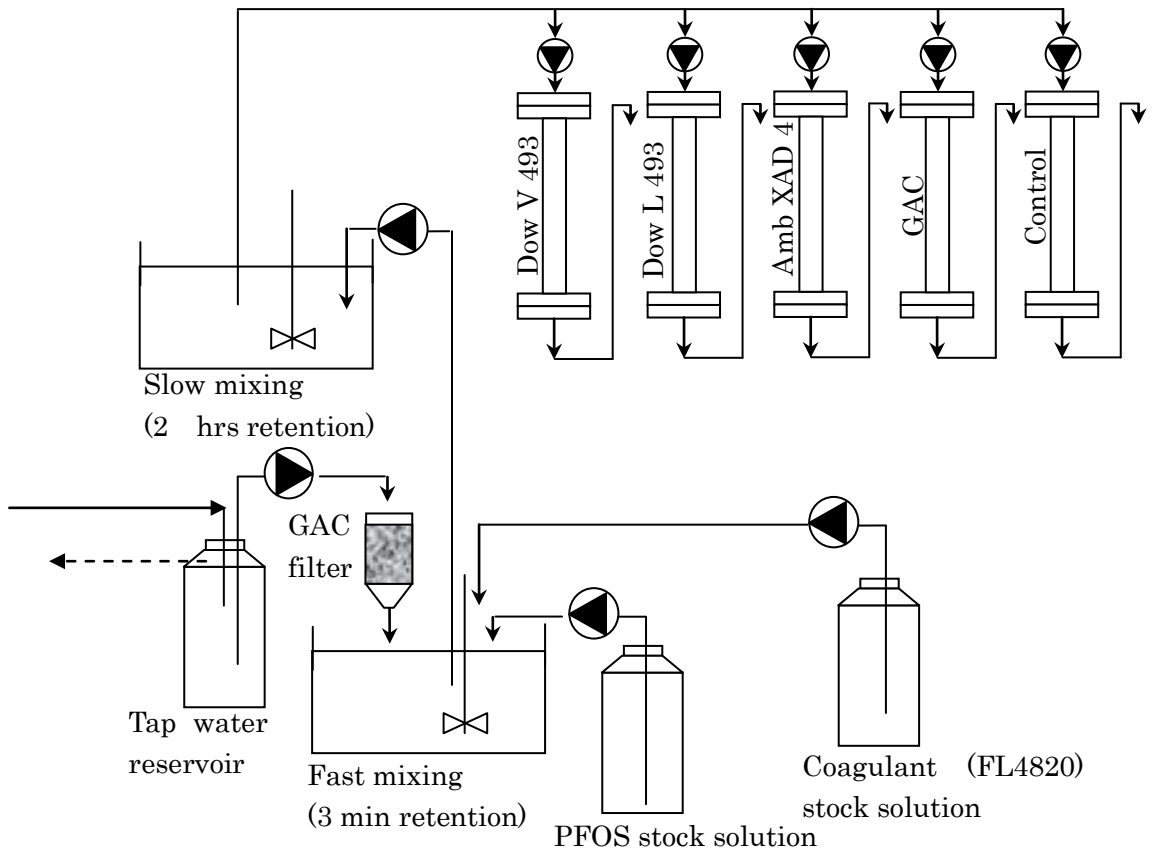


Fig 7.1 Schematic diagram of the experimental setup for combined treatment processes

Peristaltic pumps were used to control the flow rates at the inlets of each column and the mixing tanks. The effluent of each column were collected periodically and analyzed for the remaining PFOS concentration using LCMS/MS as described above. The conditions of the experiment are shown in Table 7.1.

Table 7.1 Experimental conditions for combined treatment process

Parameter	Set value
Feed concentration -PFOS	10µg/L
Feed concentration -Coagulant	6.5µL/L
Retention time – rapid mixing tank	4 min
Retention time – slow mixing tank	5 hrs
Flow rate in columns	15 mL/min
Retention time - column	1.3 min

7.4 Results and Discussion

Figure 7.2 compares the percentage removal of PFOS at each column (with different granular materials) for previous column experiment (Chapter 6) and this column experiment.

First observation in Figure 7.2 is the overall improvement of columns by organic coagulation to remove PFOS. The main reason for the improvement is the combined effect of coagulation and adsorption process. As schematically shown in **Figure 7.3**, coagulated water was sent through the adsorption column in this experiment whereas in the previous experiment only adsorption columns were used.

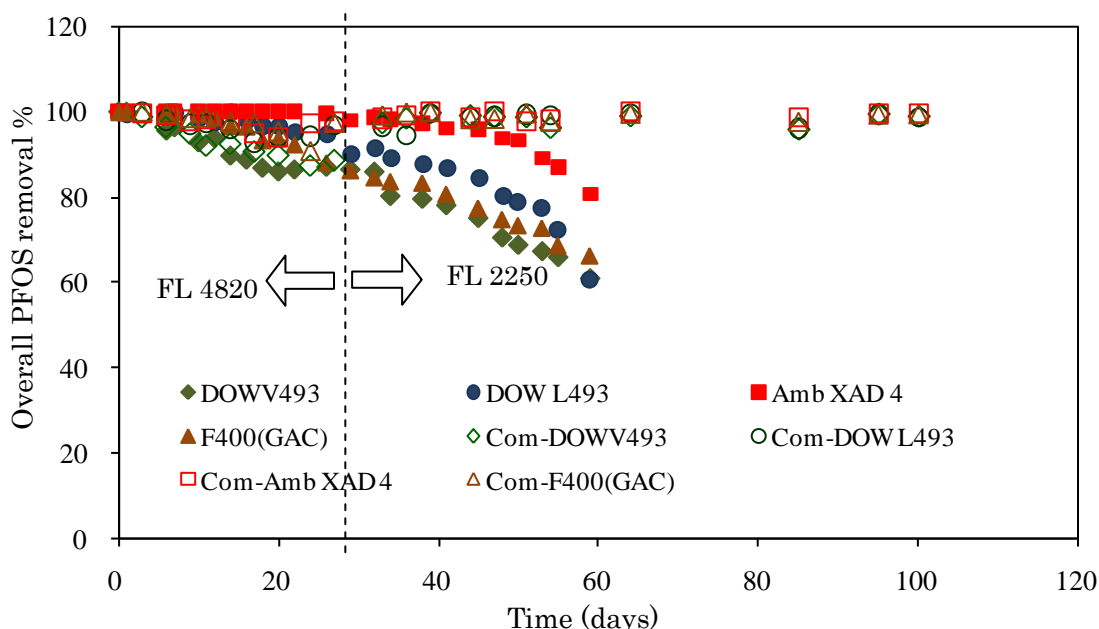


Fig. 7.2 Percentage PFOS removal with time by adsorption process and combined coagulation and adsorption process for non ion exchange filter materials.

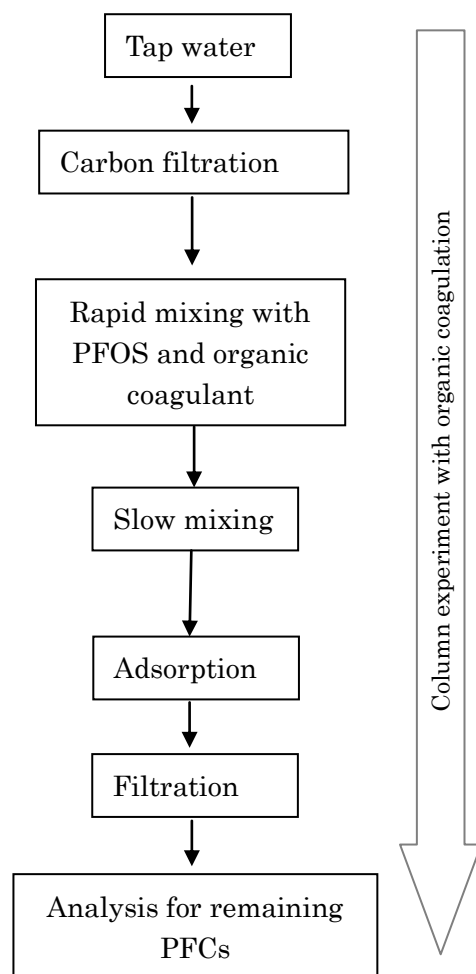


Fig 7.3 schematic diagram to explain the combined treatment process

Since an organic coagulant was added in the experiment three possible mechanisms can be expected. First obvious phenomenon is pure coagulation, which did not appear in the first column test discussed in Chapter 6. The coagulated PFOS can be settled in slow mixing tank and filter columns. The second PFOS removal mechanism in this column test is adsorption. Similar to the first column experiment, non coagulated PFOS molecules can be adsorbed onto the granular materials packed in the column. But in the second column experiment some organic coagulants also occupied the filter bed. Most of the time these coagulants negatively affect material adsorption capacity as they can block the macropores of granular materials preventing the access into inner micro pores. The effect is more serious as the retention time of the column is just 1.5 min. The retaining coagulants in the granular materials also have a positive effect on PFOS removal as it can add some active sites to the filter materials. Unfilled active sites of long chained polymeric coagulates attached to the filter media can attach some free PFOS molecules as it passes through the columns. It can be reasonably assumed that the real performance of the column is the net effect of above two phenomena (one negative and one positive).

The third PFOS removal mechanism is filtration. Filtration (0.2 μ m syringe filters) was done as an essential step in LC/MS analysis for both column tests before analysis. It was tested and observed that the PFOS removal by filtration (0.2 μ m syringe filters) is almost zero for non coagulated samples. As discussed in the Chapter 5 we observed that micro filtration is very effective to eliminate PFOS in coagulated water.

7.4.1 Reduction of PFOS by coagulation and filtration process in the combine treatment process

PFOS reduction by the coagulation and filtration process is determined by measuring the remaining PFOS after filtration in the effluent of control column. The control column was kept empty and the PFOS reduction was only by coagulation and filtration processes. **Figure 7.4** shows the percentage PFOS removal by coagulation with time. For the first month a long range polymer coagulant of FL4820 was used as the coagulant. It was observed in the experiment that the coagulation was increased for the first week from 65% to 85%. After that the performances of coagulation was deteriorated with time from 85% to 70% within the next 3 weeks. From the second month onward, another long range coagulant of FL 2250 was applied and found that the percentage PFOS removal was around 95% and it was stable with time.

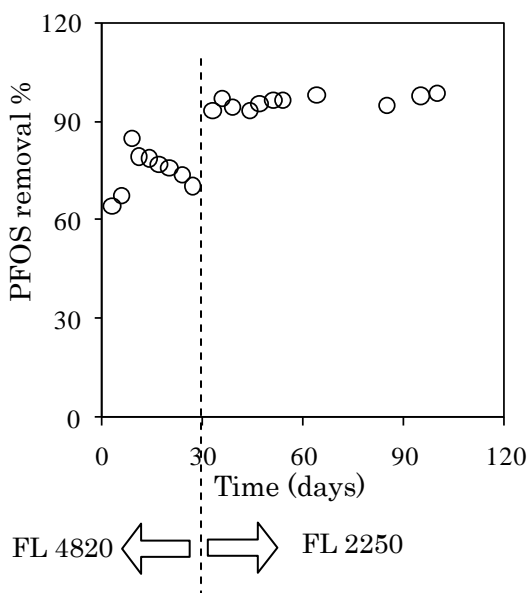


Fig. 7.4 Percentage PFOS removal with time by coagulation and filtration processes

7.4.2 Reduction of PFOS by adsorption process in the combined treatment process

PFOS reduction by adsorption process was calculated with overall PFOS reduction and the PFOS reduction by coagulation and filtration. It was assumed in the calculation that the adsorption process in the column was independent and it did not affect with coagulation and filtration process and vice versa. **Figure 7.5** shows the percentage PFOS removal by adsorption. Compared with the previous column experiment (Chapter 6) it was noticed that the column capacities did not reduce smoothly with time. It was also noticed in the first month that the removal efficiencies of the columns for all filter materials were less than that of first column experiment (Chapter 6). With the introduction of new organic coagulant (FL 2250) some performance improvement was observed for some polymers, particularly for AMB XAD 4. Disturbances by coagulants on adsorption process at the filter bed may be the main reason for the fluctuation and reduction (than previous column test) of column efficiencies. Also it was interesting to notice that the properties of coagulants affect the adsorption capacity in the column.

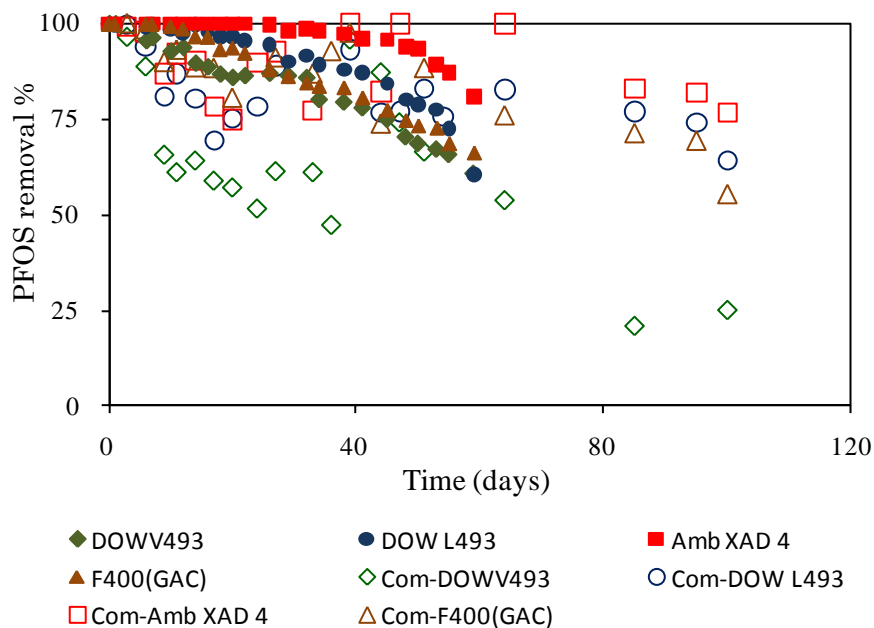


Fig. 7.5 Percentage PFOS removal by adsorption (with and without coagulation process)

7.4.3 TOC and PFOS removal

Figure 7.6 shows the variation of TOC with time. Tap water was used in this experiment as the inflow source where average TOC was measured as 2.5 mg/L. PFOS stock solution and organic coagulant solution were mixed with

tap water before feeding in to the column to adjust PFOS concentration to 10µg/L and coagulant concentration 6 mg/L. After all the additions, TOC should be around 8 mg/L but it was noticed that measured TOC was around 1 mg/L. The TOC could have been reduced in the process at several places. One place for the reduction of the TOC concentration is by the carbon filter installed to eliminate residual chlorine. The TOC added with the coagulant could have been reduced at the slow mixing tank by settling it, at filtration column and final filtration process before analysis. One of the main disadvantages with this experimental set up was that there was no proper provision to flush out settled coagulants in slow mixing tank and filter beds. Due to this fault, sudden TOC peaks were observed and it was overcome by cleaning the tanks manually and flushing the columns with tap water (free of residual chlorine). First such peak was observed after 60 days of operation as shown in **Figure 7.6**.

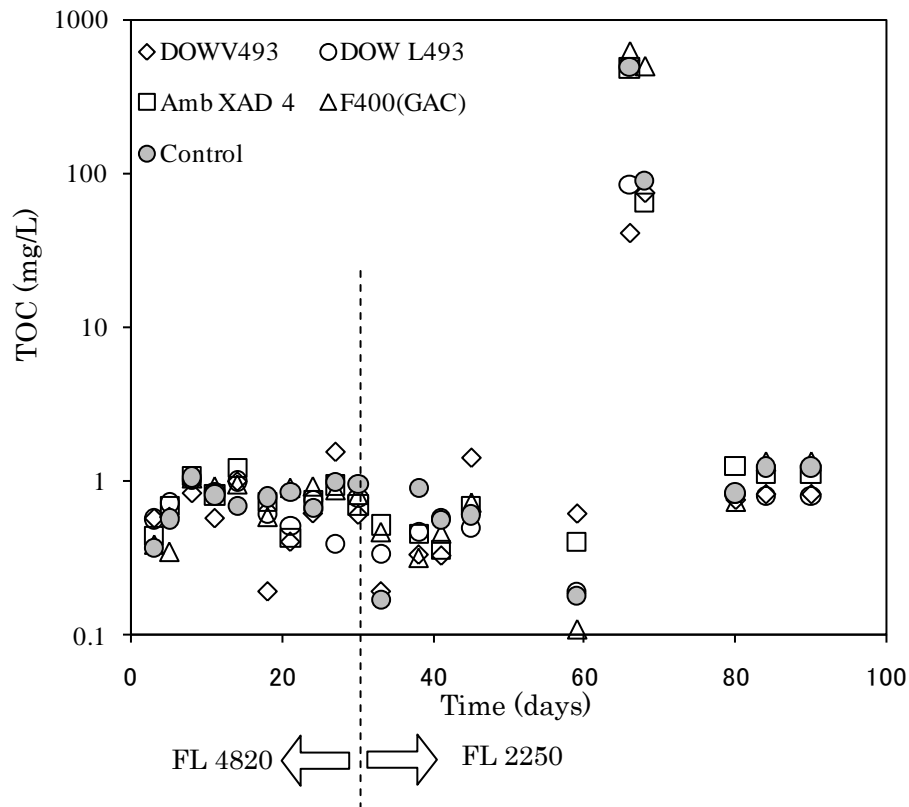


Fig. 7.6 Variation of TOC in the effluent of each column at the combine treatment process

It was noticed that there was a reduction of TOC with the introduction of different organic coagulants, which may be the reason for the improvement of adsorption capacity in some granular materials. It can be deduced with this observation that the filtration capacity of granular materials tested

were reduced by coagulants (may be due to material fouling) but the degree of effect was minimum for some granular materials such as AMB XAD 4.

7.5 Economic Analysis

7.5.1 Objective and Background

The primary purpose this basic economical analysis was to determine the potential cost saving granular material for treating water contaminated with PFOS. Since the column experiment and the material regeneration experiment were limited to non ion-exchange polymers, cost analysis also limited to the same granular materials.

7.5.2 Assumptions

This analysis was a basic cost comparison considering only two parameters of adsorption capacity and material regeneration. Following assumptions were made to figure out some parameters to be used in the calculation as described below.

1. Unit price of each polymer material and GAC were assumed to be same as the supply price to the laboratory. Table 7.3 shows the unit price of each granular material.
2. The performance of the column experiment can be applied to the real scale applications.
3. Three times bed volumes of organic solvent is sufficient to regenerate the synthetic polymer materials
4. Cost of organic solvent (Methanol) is same to the supply price to the laboratory.
5. 60% of material cost of GAC is required for regenerating them (for one time).
6. Handling of recovered PFOS is a separate business and will not involve with regeneration process.
7. The time required to reduce the column efficiency by given valve will not change with initial PFOS concentration for a given flow rate.
8. The column efficiency curve will not change for further low inflow concentration

Table 7.2 Cost of Granular Materials

Polymer brand	Producer	Supplier	Amount purchased (g)	Bill value (Yen)	Unit cost (Yen/kg)
Dow V493	Dow Chemical		100	9000	90000
Dow L493	Dow Chemical		500	18000	36000
Amb XAD 4	Rohm and Haas	Sigma-	500	21000	42000
F400 (GAC)	Calgon Company	Aldrich	500	8500	17000
Amb IRA-400	Rohm and Haas	Japan	500	16700	33400
Dow Marathon	Dow Chemical		250	11000	44000

7.5.3 Cost Scenarios

For this economic analysis, some common factors were not considered because the purpose of this analysis was to compare the materials, but not compare the PFOS treatment techniques. For example minimum by-product formation in the treatment process was not considered for the analysis because it is common for all granular materials. Two main factors considered for economical analysis were adsorption capacities of each material and their cost of regeneration. Some data related to the calculation was not available in the experiment and also in the literature data. For example still it is unknown how many times non ion-exchange polymers can be regenerated while keeping the acceptable removal efficiency. Also it is unknown the amount of organic solvent required for material regenerations. The economic analysis was done for three scenarios, for different inflow PFOS concentrations, different outflow PFOS concentrations and different times of regeneration. For the inflow PFOS concentrations, 10,000 ng/L, 4,000 ng/L and 1000 ng/L were considered and for outflow PFOS concentrations 100 ng/L and 10 ng/L were considered. The cost implications were also calculated for 10, 5 and 2 times of materials regenerations before replacing them with new materials.

7.5.4 Methodology

This economic analysis was done by comparing the material installation cost and the operational cost for four filters containing the target non ion-exchange filter materials. It was assumed that the filter bed volume is 1 L for each filter. For easy comparison, material installation cost and operational cost were calculated for the daily basis. Each component of the cost was calculated as described below.

7.5.4.1 Material installation cost

For this comparative study, it was assumed that the material supply price

remained as same as the laboratory supply price (Table 7.3). However, in the real application there is a significant price reduction for bulk purchasing.

7.5.4.2 Material regeneration interval

Material regeneration interval of each material was determined by considering the results of column experiment in Chapter 6 based on the required removal efficiencies of each scenario. Table 7.4 shows the drop of removal efficiencies of each material with time (based on the results of Chapter 6).

7.5.4.3 Material regeneration cost

It was assumed that three times bed volumes of methanol (3 L) is sufficient to regenerate synthetic polymers and since the methanol cost is dominant other costs can be negligible. Based on the literature data 60% of material cost was allocated for the offsite regeneration of GAC.

Table 7.3. Drop of PFOS removal efficiencies with time

Days	No of bed volumes	% Removal			
		DOWV493	DOW L493	Amb XAD 4	F400(GAC)
0	0	99.95	99.95	100.00	99.98
1	1080	99.90	99.41	100.00	99.95
6	6480	95.47	99.00	100.00	100.00
7	7560	96.27	100.00	100.00	99.96
10	10800	92.72	98.37	100.00	99.44
12	12960	93.74	97.46	100.00	98.79
14	15120	89.61	99.79	100.00	96.70
16	17280	88.65	97.89	100.00	96.56
18	19440	86.75	96.49	100.00	93.31
20	21600	85.87	96.54	100.00	93.75
22	23760	86.35	95.38	100.00	92.36
26	28080	86.98	94.48	99.64	88.06
29	31320	86.36	90.01	98.02	86.23
32	34560	85.84	91.58	98.53	84.56
34	36720	80.12	89.20	98.22	83.64
38	41040	79.46	87.94	97.35	83.30
41	44280	77.96	86.98	96.10	80.65
45	48600	74.96	84.25	95.82	77.36
48	51840	70.37	80.10	93.80	74.67
50	54000	68.65	78.95	93.32	73.25
53	57240	67.16	77.50	89.12	72.64
55	59400	65.774	72.47	86.96	68.54
59	63720	60.80	60.42	80.73	66.11

Table 7.4 Results of economic analysis for three times material regenerations

Material	Operation parameters				cost factors		Total
	IF	OF	MRI	RV	C _{mi}	C _{mr}	
Dow V493			3	99.00	90000	1200	91200
Dow L493	10000	100	7	99.00	15429	514	15943
Amb XAD 4			26	99.00	4846	138	4985
F400(GAC)			10	99.00	5100	1020	6120
Dow V493			14	90.00	19286	257	19543
Dow L493	1000	100	32	90.00	3375	113	3488
Amb XAD 4			50	90.00	2520	72	2592
F400(GAC)			23	90.00	2217	443	2661
Dow V493			3	99.75	90000	1200	91200
Dow L493	4000	10	7	99.75	15429	514	15943
Amb XAD 4			26	99.75	4846	138	4985
F400(GAC)			7	99.75	7286	1457	8743

Note

IF- Inflow PFOS concentration (ng/L), OF- Targeted outflow PFOS concentration (ng/L), MRI-Material regeneration interval (days), RV-PFOS removal efficiency, C_{mi}-Material installation cost, C_{mr}- Material regeneration cost

Assumptions: 1. three times bed volume of organic solvent is needed for material regeneration 2. 60% of materials cost (GAC) is needed for one time GAC regeneration 3. Cost of organic solvent is 1200 JPY/L

Table 7.5 Results of economic analysis for five times material regenerations

Material	Operation parameters				cost factors		Total
	IF	OF	MRI	RV	C _{mi}	C _{mr}	
Dow V493			3	99.00	150000	1200	151200
Dow L493	10000	100	7	99.00	25714	514	26229
Amb XAD 4			26	99.00	8077	138	8215
F400(GAC)			10	99.00	8500	1020	9520
Dow V493			14	90.00	32143	257	32400
Dow L493	1000	100	32	90.00	5625	113	5738
Amb XAD 4			50	90.00	4200	72	4272
F400(GAC)			23	90.00	3696	443	4139
Dow V493			3	99.75	150000	1200	151200
Dow L493	4000	10	7	99.75	25714	514	26229
Amb XAD 4			26	99.75	8077	138	8215
F400(GAC)			7	99.75	12143	1457	13600

Note

IF- Inflow PFOS concentration (ng/L), OF- Targeted outflow PFOS concentration (ng/L), MRI-Material regeneration interval (days), RV-PFOS removal efficiency, C_{mi}-Material installation cost, C_{mr}- Material regeneration cost

Assumptions: 1. three times bed volume of organic solvent is needed for material regeneration 2. 60% of materials cost (GAC) is needed for one time GAC regeneration 3. Cost of organic solvent is 1200 JP¥/L

Table 7.6 Results of economic analysis for eight times material regenerations

Material	Operation parameters				cost factors		Total
	IF	OF	MRI	RV	C _{mi}	C _{mr}	
Dow V493	10,000	100	3	99.00	240000	1200	241200
Dow L493			7	99.00	41143	514	41657
Amb XAD 4			26	99.00	12923	138	13062
F400(GAC)			10	99.00	13600	1020	14620
Dow V493	1,000	100	14	90.00	51429	257	51686
Dow L493			32	90.00	9000	113	9113
Amb XAD 4			50	90.00	6720	72	6792
F400(GAC)			23	90.00	5913	443	6357
Dow V493	4000	10	3	99.75	240000	1200	241200
Dow L493			7	99.75	41143	514	41657
Amb XAD 4			26	99.75	12923	138	13062
F400(GAC)			7	99.75	19429	1457	20886

Note

IF- Inflow PFOS concentration (ng/L), OF- Targeted outflow PFOS concentration (ng/L), MRI-Material regeneration interval (days), RV-PFOS removal efficiency, C_{mi}-Material installation cost, C_{mr}- Material regeneration cost

Assumptions: 1. three times bed volume of organic solvent is needed for material regeneration 2. 60% of materials cost (GAC) is needed for one time GAC regeneration 3. Cost of organic solvent is 1200 JP¥/L

7.5.5 Results

Nine different combinations of removal efficiencies and material regenerations were compared in terms of financial aspects. It was found in each calculation that Dow V493 was the least cost effective followed by Dow L493. Amb XAD 4 and GAC showed similar range of cost effectiveness for 90% and 99% PFOS removals. For the higher removal of 99.75%, Amb XAD4 showed the best cost effectiveness.

7.5.5.1 Factors affecting cost effectiveness

Higher sorption capacities

Since the environmental PFOS concentration is in ng/L level, it is essential to meet high removal efficiencies at the unit operation to treat PFOS, especially at industrial wastewater treatment. It was observed in this experiment that non ion-exchange polymers, especially Amb XAD4 showed an excellent performance for PFOS removal. Higher sorption capacity at lower equilibrium concentrations (outflow concentration) increases the duration of column operation between material regeneration which ultimately reduces the operation cost.

Material regeneration by organic solvent

Despite the high initial capital investment in resins compared to GAC, resins can be regenerated and reused on-site whereas carbon must be taken off-site, reactivated, and replaced. Consequently, if resin regeneration costs are sufficiently low and resin usage rates are less than carbon usage rates, the lifecycle costs for a resin system can be less than those for a carbon system.

Hydraulic retention time.

The hydraulic retention time applied in the experiment was 1.35 min, which is less than conventional GAC treatment units. It was observed that a comparatively better performance was given by non ion-exchange polymers than GAC with this retention time. Similar performance can be expected from the GAC column with lower flow rate. Consequently, resin vessels can sustain a much higher flow-through than equivalently sized carbon vessels, resulting in either a reduction in the total number of required resin vessels or a reduction in the size of the resin vessels. The smaller volume of resins required may lead to lower costs.

Minimal interference with other organics.

The results of combine treatment of coagulation and adsorption suggest the interferences for adsorption by other organics are comparatively less for some non ion-exchange polymers than GAC. This observation indicates the direct applicability of non ion-exchange polymers especially in the industrial wastewater.

7.6 Summary

1. Combined treatment process of coagulation (by organic coagulants) followed by adsorption and filtration was identified as an excellent method to treat PFCs in water. The combination with some adsorbents, more than 99% removal was obtained even after 100 days of continuous run.
2. Removal of PFCs by coagulation was higher than that determined by the jar test in Chapter 5. This may be due to the higher retention time at slow mixing tank.
3. Addition of coagulants negatively affected the adsorption of most of the adsorbents, but for AmbXAD4, the effect was positive.
4. Economical analysis with different scenarios for the level of treatment and regenerations identified AmbXAD as the cheapest material for PFOS adsorption.

Chapter 8 - Conclusions and Recommendations

8.1 Conclusions

Perfluorinated compounds are anthropogenic organic pollutants with the properties of persistence, bio-accumulation and toxicity. Many researchers have reported that conventional water and wastewater treatment methods can not eliminate PFCs. Fully saturated C-F bonds give the stability and polarity to the PFCs molecules. This study tried to eliminate PFCs by using the property of polarity. Main removal mechanisms tested were adsorption and coagulation. The conclusions are drawn by chapters as follows;

In Chapter 2, available literature was summarized, basically on PFCs treatment. It was noticed that PFCs oxidation is extremely difficult at environmental temperature and pressure. Adsorptions by GAC and membrane filtration were identified as attractive methods to eliminate PFCs.

Chapter 3 tested the ferrate technique to oxidize PFCs at trace concentrations (from 0.1 to 25 $\mu\text{g/L}$). Ferrate(VI) technique has been identified as an emerging water purification technique and proved its effectiveness to treat many organic and inorganic pollutants. Conclusions of this chapter are shown below

1. The best ferrate to PFCs molar ratio to reach maximum PFCs reduction was identified as 100.
2. It was noticed that the average elimination of PFCs with sulfonane functional group was 18% and acid functional group was 24%.
3. PFCs reduction by ferrate(VI) might occur due to the adsorption than oxidation. It was also found that high ferrate(VI) to PFC molar ratio discouraged PFC removal. Coagulation property of ferrate(VI), which flocculate ferrite(III) particles might be reducing the adsorption effect.
4. It was concluded that ferrate technique alone is not sufficient to oxidize PFCs at environmental pressure and temperature. The oxidation numbers of carbon atoms in the PFCs chain are +2 and +3.
5. Since the ferrate(VI) can oxidize many pollutants in water except PFCs, it might be useful in methodology development in PFCs determination, especially to degrade organic matrices in wastewater samples.

Chapter 4 studied the PFCs adsorption by batch experiments. Ion-exchange polymers, non ion-exchange polymers and GAC were studied in detail for kinetic and isotherm characteristics. Conclusions of this chapter were shown as follows.

1. Constant sorbent method was identified as the best method to determine sorption isotherm, where sorbent concentration was kept constant and sorbate concentration was changed.
2. Ion-exchange resins and GAC showed faster adsorption characteristics than non ion-exchange polymers. To reach the equilibrium concentration for all kind of granular materials, at least 100 hrs shaking was needed.
3. Synthetic polymer materials were identified as better filter materials (in terms of adsorption capacity) to eliminate PFCs in water at low concentration (1 $\mu\text{g/L}$). The magnitude of Freundlich isotherm constants (K_f) decreases in the following order for most of the long chain and medium chain PFCs tested: Ion-exchange polymers > Non ion-exchange polymers > GAC, but in some cases at further low equilibrium concentrations (100 ng/L) non ion-exchange polymers showed higher adsorption capacity than other adsorbents.
4. Amb IRA- 400 was identified as the best filter material to eliminate PFOS at equilibrium concentrations > 1 $\mu\text{g/L}$. Considering both adsorption isotherm and adsorption kinetics, Amb XAD 4 and Dow MarathonA can be recommended for eliminating PFOS at ng/L equilibrium concentrations.
5. Further studies are to be done to understand the sorption mechanisms of PFOS, but it can be suspected that the chemisorption must be the dominant process.

Chapter 5 studied PFCs coagulation by a series of jar tests. Long chain polymer type cationic coagulants and conventional inorganic coagulants were comparatively studied for PFCs coagulation. Conclusions are listed in detail as follows.

1. The experiment with deionized water spiked with PFCs suggested that comparatively higher coagulant dose is required to get a good PFCs removal efficiency by organic coagulants.

2. The results of the experiments with deionized water spiked with PFCs and wastewater spiked with PFCs showed that the efficiency of PFCs coagulation by organic coagulants is almost double than that of inorganic coagulants.
3. Among the organic coagulants tested, FL 2749 was identified as the best candidate to eliminate any PFCs.
4. The results of PFCs coagulation by different organic coagulants suggest that a mixture of multipolymers is better than single polymer coagulant to coagulate PFCs.
5. The results of the experiment from actual wastewater spiked with PFCs indicated that existence of other organic matter discourages coagulation of short chain PFCs, but it encourages the coagulation of long chain PFCs.
6. The results of the experiment from actual industrial wastewater related to PFCs industry indicated that organic coagulants are not effective as it showed in wastewater spiked with PFCs to coagulate PFCs. The PFCs that appear in real wastewater seems to be incorporated with other polar molecules in the wastewater.
7. Organic coagulation followed by microfiltration seems to be an effective combination to eliminate PFCs for some wastewaters, but more studies to be done on this topic.

Chapter 6 studied the PFOS adsorption by column experiment. Non ion-exchange synthetic polymers identified in chapter 4 were tested with long run column experiment (60 days) for PFOS adsorption. At the end of the experiment, the granular materials were tested for PFOS recovery. The conclusions of the chapter are summarized as following.

1. Amb XAD 4 was recognized as the best candidate among the tested four filter materials to eliminate PFOS.
2. It was observed that the results of column experiment cannot be explained by individual results of the isotherm experiment or the kinetic experiment suggesting the importance of both isotherm (available vacant sites in the materials to adsorb) and kinetics (the speed of attachment) in the real application.
3. It was interesting to notice that in the column experiment with Amb XAD 4 removed 99.99% PFOS up to 23,000 bed volumes pass through with the condition of 10 $\mu\text{g/L}$ inflow concentration and flow rate of 15 ml/min (0.75 bed volumes/min).

4. Within 80 min, all most 100% PFOS was recovered from synthetic resins in the regeneration experiment suggesting that synthetic polymers can be effectively regenerated by an organic solvent.

Chapter 7 studied the combined treatment process of adsorption (studied in Chapter 4 and Chapter 6) and coagulation (studied in Chapter 5) for PFOS elimination. This study was done in a continuous run column experiment (>100 day). Later part of Chapter 7 calculated the cost effectiveness of each polymer material. The conclusions of this chapter are summarized as following.

1. Combined treatment process of coagulation (by organic coagulants) followed by adsorption and filtration was identified as an excellent method to treat PFCs in water. Some polymers showed more than 99% removal even after 100 days of continuous run.
2. The higher removal of PFCs by coagulation than that was determined by the jar test at Chapter 5 may be due to the higher retention time at slow mixing tank.
3. Addition of coagulants negatively affected the adsorption of most of the adsorbents, but for AmbXAD4, the effect was positive.
4. Economical analysis with different scenarios for the level of treatment and regeneration identified AmbXAD 4 as the cheapest material for PFOS adsorption.

8.2 Recommendations

The results of this study suggest the following recommendations. A limited number of synthetic materials were tested in this experiment. Four synthetic resins out of six (two ion-exchange resins and four non ion-exchange resins) studied in this experiment showed better performance than conventional GAC for PFCs adsorption. It is highly recommended to test more synthetic materials for material optimization. Also the dominancy of chemisorption was observed and further studies are recommended for complete understanding of PFCs adsorption process. Medium molecular weight (around 100,000Da) cationic organic coagulants showed the best PFCs coagulation and further studied to be done to confirm it. Organic coagulation followed by micro filtration seems to be an effective combination for tap water treatment and further research on this is recommended. Among the inorganic coagulants, ferric chloride showed better performance for PFOA coagulation and it can be recommended for WWTPs. In

the column experiment, best performance was given by Amb XAD4. It was found that this material can be regenerated on site (solvent regeneration) and economically viable than other granular materials tested. It is highly recommended to install a filter column with Amb XAD4 in a PFCs related industry to study the performance in the real field conditions.

References

- 1 Adams B. A. and Holmes E. L., 1935 *J. Soc. Chem. Ind.* 54,1-6T.
- 2 Akid R, Darwent J R. Heteropolytungstates as catalysts for the photochemical reduction of oxygen and water. *Journal of the Chemical Society. Dalton Transactions*, 1985, 2: 395–399
- 3 Anipsitakis G P, Dionysiou D D. Radical generation by the interaction of transition metals with common oxidants. *Environmental Science & Technology*, 2004, 38(13): 3705–3712
- 4 Atkins. P.W *Physical Chemistry*", Oxford University Press, 6th ed., 1998, ISBN 0-19-850101-3
- 5 Audette, R.J., Quail, J.W., 1972. Potassium, rubidium, cesium, and barium ferrates 6. Preparations, infrared spectra and magnetic susceptibilities. *Inorg. Chem.* 11, 1904.
- 6 AWWA (2000). *Operational Control of Coagulation and Filtration Processes. Manual M37, 2nd Edition.*
- 7 Ball D L, Edwards J O. The Kinetics and mechanism of the decomposition of Caro's acid. 1. *Journal of the American Chemical Society*, 1956, 78(6): 1125–1129
- 8 Beck, F., Kaus, R., Orberts, M., 2001. Transpassive dissolution of iron to ferrate (VI) in concentrated alkali hydroxide solutions. *Electrochimica Acta* 30 (2), 173–183.
- 9 Blanksby SJ, Ellison GB 2003. "Bond dissociation energies of organic molecules". *Acc. Chem. Res.* 36 (4): 255–63.
- 10 Bolto B., Dixon D., Eldridge R., King S, 2001, Cationic polymer and clay or metal oxide combinations for natural organic matter removal, *Water Res* 35, 2669–2676.
- 11 Boulanger, B., Peck, A.M., Schnoor, J.L., Hornbuckle, K.C., 2005-2. Mass budget of perfluorooctane surfactants in Lake Ontario. *Environ. Sci. Technol.* 39, 74–79.
- 12 Boulanger, B., Vargo, J., Schnoor, J.L., Hornbuckle, K.C., 2004. Detection of perfluorooctane surfactants in Great Lakes water. *Environ. Sci. Technol.* 38, 4064–4070.
- 13 Boulanger, B., Vargo, J.D., Schnoor, J.L., Hornbuckle, K.C., 2005-1. Evaluation of perfluorooctane surfactants in a wastewater treatment system and in a commercial surface protection product. *Environ. Sci. Technol.* 39, 5524–5530.
- 14 Bouzek, K., Rousar, I., 1993. The study of electrochemical preparation of ferrate(VI) using alternating current superimposed on the direct current. Frequency dependence of current yields. *Electrochem. Acta* 38 (13), 1717–1720.
- 15 Bouzek, K., Rousar, I., 1996. Influence of anode material on current yields during ferrate (VI) production by anodic iron dissolution. Part 1: current efficiency during anodic dissolution of grey cast iron to ferrate (VI) in concentrated alkali hydroxide solutions. *J. Appl. Electrochem.*

26 (9), 919–924.

- 16 Bouzek, K., Rousar, I., Bergmann, H., Herwing, K., 1998. The cyclic voltametric study of ferrate production. *Electroanal. Chem.* 425 (1–2), 125–137.
- 17 Bouzek, K., Schmidt, M.J., Wragg, A.A., 1999-1. Influence of electrolyte composition on current yield during ferrate (VI) production by anodic iron dissolution. *Electrochem. Commun.* 1, 370–374.
- 18 Bouzek, K., Schmidt, M.J., Wragg, A.A., 1999-2. Influence of anode material composition on the stability of electrochemically prepared ferrate(VI) solutions. *J. Chem. Technol. Biotechnol.* 74, 1188–1194.
- 19 Busca, G., Berardinelli, S., Resini, C. and Arrighi, L, 2008. Technologies for the removal of phenol from fluid streams: A short review of recent developments. *Journal of Hazardous Materials*, 160, 265–288.
- 20 Carr, J.D. Kelter, P.B. Tabatabai, A. Splichal, D. Erickson J. and McLaughlin, C.W. 1985. Properties of ferrate(VI) in aqueous solution: an alternate oxidant in wastewater treatment. In: R.L. Jolley, Editor, *Proceedings of Conference on Water Chlorination Chemistry. Environment Impact Health Lewis Chelsew* , pp. 1285–1298.
- 21 Carr, J.D., Kelter, P.B., Tabatabai, A., Splichal, D., Erickson, J. and McLaughlin, C.W. 1985. Properties of ferrate (VI) in aqueous solution: an alternate oxidant in wastewater treatment. *Proceedings of Conference on Water Chlorination Chemistry. Environment Impact Health Lewis Chelsew.* 1285–1298.
- 22 Chen J, Zhang P Y, Zhang L. 2006-1. Photocatalytic decomposition of environmentally persistent perfluorooctanoic acid. *Chemistry Letters*, 35(2): 230–231
- 23 Chen, J, Zhang P. 2006-2 Photodegradation of perfluorooctanoic acid in water under irradiation of 254 nm and 185 nm light by use of persulfate. *Water Science & Technology*, 54(11-12): 317–325
- 24 Chen, J, Zhang P. Photodegradation of perfluorooctanoic acid in water under irradiation of 254 nm and 185 nm light by use of persulfate. *Water Science & Technology*, 2006, 54(11-12): 317–325
- 25 Cheung C.W., Porter J.F., McKay G. 2001. Sorption kinetic analysis for the removal of cadmium ions from effluents using bone char. *water research*, vol 35, pp.605–612.
- 26 Christian, G.D., Sensmeier, R.K., Wagner, W.F., 1975. Electrochemical studies of potassium ferrate(VI). *Monatshefte fuer Chemie* 106 (3), 813–822.

- 27 Chuyang Y. Tanga, , Q. Shiang Fub, c, d, Dawen Gaod, e, Craig S. Criddled and James O. Leckied, 2010, Effect of solution chemistry on the adsorption of perfluorooctane sulfonate onto mineral surfaces, *Water Research* 44(8), 2654-2662
- 28 Darling, E. S . and Reinhard M. 2008 Nanofiltration for Trace Organic Contaminant Removal: Structure, Solution, and Membrane Fouling Effects on the Rejection of Perfluorochemicals. *Environ. Sci. Technol*, 42, 5292–5297
- 29 Davis, K.L., Aucoin, M.D., Larsen, B.S., Kaiser, M.A., Hartten, A.S., 2007. Transport of ammonium perfluorooctanoate in environmental media near a fluoropolymer manufacturing facility. *Chemosphere* 67, 2011–2019.
- 30 Denver, A., Pletcher, D., 1996-1. Electrochemical generation of ferrate 1. Dissolution of an ironwool bed anode. *J. Appl. Electrochem.* 26, 815–821.
- 31 Denver, A., Pletcher, D., 1996-2. Electrochemical generation of ferrate. 2. Influence of anode composition. *J. Appl. Electrochem.* 26, 823–827.
- 32 Ding, Z., Yang, C., Wu, Q., 2004. The electrochemical generation of ferrate at porous magnetite electrode. *Electrochimica Acta* 49 (19), 3155–3159.
- 33 Dobson K.D, Roddick-Lanzilotta A.D and McQuillan A.J, 2000, An in situ infrared spectroscopic investigation of adsorption of sodium dodecylsulfate and of cetyltrimethylammonium bromide surfactants to TiO₂, ZrO₂, Al₂O₃, and Ta₂O₅ particle films from aqueous solutions, *Vibrational Spectroscopy* 24 (2), 287–295
- 34 Dugan, N., K. Fox, J. Owens, and R. Miltner 2001. Controlling *Cryptosporidium* oocysts using conventional treatment. *J. AWWA.* 93 (12), pp 64–76.
- 35 Earth Negotiations Bulletin. 2009 International Institute for Sustainable Development. 15(172), 1-4.
- 36 Ellis, D.A., Martin, J.W., De Silva, A.O., Mabury, S.A., Hurley, M.D., Sulbaek Andersen, M.P., Wallington, T.J., 2004. Degradation of fluorotelomer alcohols: A likely atmospheric source of perfluorinated carboxylic acids. *Environ. Sci. Technol.* 38, 3316–3321.
- 37 Eng, Y.Y., Sharma, V.K., Ray, A.K., 2006. Ferrate (VI): Green chemistry oxidant for degradation of cationic surfactant. *Chemosphere* 63, 1785–1790.
- 38 Environmental health perspectives National Institutes of Health U.S. Department of Health and Human Services
- 39 *Environmental Science and Technology* 31 (9): 2445-2454.

- 40 European Commission, Directive 2006/122/EC of the European Parliament and of the Council of 12 December 2006 amending for the 30th time Council Directive 76/769/EEC on the approximation of the laws, regulations and administrative provisions of the Member States relating to restrictions on the marketing and use of certain dangerous substances and preparations (perfluorooctane sulfonates), Off. J. Europ. Commun., L 372/32, 27.12.2006.
- 41 Fan, M.H., Brown, R.C., Huang, C.P., 2002. Preliminary studies of the oxidation of arsenic(III) by potassium ferrate. *Int. J. Environ. Pollut.* 18 (1), 91–96.
- 42 Fricke, M., Lahl, U., 2005. Risk evaluation of perfluorinated surfactants as contribution to the current debate on the EU Commission's REACH document. *Z. Umweltchem. Ökotox.* 17 (1), 36–49.
- 43 Fujii S., Polprasert C., Tanaka S., Lien P.H. and Qiu, Y. 2007. New POPs in the water environment: distribution, bioaccumulation and treatment of perfluorinated compounds- a review paper. *Water Supply Research and Technology - AQUA.* 56.5, 313-326.
- 44 Furdui, V. I., N. L. Stock, D. A. Ellis, C. M. Butt, D. M. Whittle, P. W. Crozier, E. J. Reiner, D. C. G. Muir and S. A. Mabury (2007). Spatial distribution of perfluoroalkyl contaminants in lake trout from the Great Lakes, *Environ. Sci. Technol.*, 41 (5), 1554.
- 45 Gauthier S A, Mabury S A. Aqueous photolysis of 8: 2 fluorotelomer alcohol. *Environmental Toxicology and Chemistry*, 2005, 24(8): 1837–1846
- 46 Giesy, J.P., Kannan, K., 2001. Global distribution of perfluorooctane sulfonate in wildlife. *Environ. Sci. Technol.* 35, 1339–1342.
- 47 Glaser H.T., Edzwald J.K., 1979, Coagulation and direct filtration of humic substances with polyethylenimine, *Environ. Sci. Technol.* 13, 299–305.
- 48 Gomez, V., Larrechi, M.S. and Callao, M.P. 2007. Kinetic and adsorption study of acid dye removal using activated carbon. *Chemosphere.* 69 ,1151–1158.
- 49 Graham, N., Jiang, C.H., Li, X.Z., Jiang, J.Q., Ma, J., 2004. The influence of pH on the degradation of phenol and chlorophenols by potassium ferrate. *Chemosphere* 56, 949–956.
- 50 Gregory J, 1973, Rates of flocculation of latex particles by cationic polymers, *J. Colloid Interface Sci*, 42, 448–456.
- 51 Gregory J, 1988, Polymer adsorption and flocculation in sheared suspensions, *Colloids Surf* 31, 231–253.
- 52 Gregory J. and Li G.B, 1991, Effects of dosing and mixing conditions on polymer flocculation of concentrated suspensions, *Chem. Eng. Commun* 108, 3–21

- 53 Hansen, K.J., Johnson, H.O., Eldridge, J.S., Butenhoff, J.L., Dick, L.A., 2002. Quantitative characterization of trace levels of PFOS and PFOA in the Tennessee River. *Environ. Sci. Technol.* 36, 1681–1685.
- 54 Hatfield, T. L. (2001a), Hydrolysis reactions of perfluorooctanoic acid (PFOA), 3M Environmental Laboratory, USEPA docket: EPA-HQ-OPPT-2002-0051-0013.
- 55 Hatfield, T. L. (2001b), Screening studies on the aqueous photolytic degradation of perfluorooctanoic acid (PFOA), 3M Environmental Laboratory, USEPA docket: EPA-HQ-OPPT-2002-0051-0023.
- 56 Haukas, M., Berger, U., Hop, H., Gulliksen, B., Gabrielsen, G.W., 2007. Bioaccumulation of per- and polyfluorinated alkyl substances (PFAS) in selected species from the Barents Sea food web. *Environ. Poll.* 148, 360–371.
- 57 He, W., Wang, J., Shao, H., Zhang, J., Cao, C.-N., 2005. Novel KOH electrolyte for onestep electrochemical synthesis of high purity solid K_2FeO_4 : comparison with NaOH. *Electrochem. Commun.* 7, 607–611.
- 58 He, W., Wang, J., Yang, C., Zhang, J., 2006. The rapid electrochemical preparation of dissolved ferrate (VI): effects of various operating parameters. *Electrochem. Acta* 51 (10), 1967–1973.
- 59 Hekster F.M., Laane R.W.P.M. and de Voogt P. 2003. Environmental and toxicity effects of perfluoroalkylated substances. *Reviews of Environmental Contamination and Toxicology* 179:
- 60 Higgins C.P and Luthy R.G, 2006, Sorption of perfluorinated surfactants on sediments, *Environmental Science and Technology* 40 (23), 7251–7256
- 61 Hill T. and A. Langdon 1991. Porous ceramic dual media filtration. *Water & Wastes in New Zealand*, 66, 19-20, 22.
- 62 Hori, H., Hayakawa, E., Einaga, H., Kutsuna, S., Koike, K., Ibusuki, T., iatagawa, H., Arakawa, R.. Decomposition of environmentally ersistent perfluorooctanoic acid in water by photochemical pproaches. *Environmental Science & Technology*, 2004-a, 38(22): 118–6124
- 63 Hori, H., Hayakawa, E., Einaga, H., Kutsuna, S., Koike, K., Ibusuki, T., Kiatagawa, H., Arakawa, R. , 2004. Decomposition of environmentally persistent perfluorooctanoic acid in water by photochemical approaches. *Environmental Science & Technology*, 38(22): 6118–6124
- 64 Hori, H., Hayakawa, E., Koike, K., Einaga, H., Ibusuki, T.. Decomposition of nonafluoropentanoic acid by heteropolyacidphotocatalyst $H_3PW_{12}O_{40}$ in aqueous solution. *Journal of olecular Catalysis A—Chemical*, 2004-b, 211(1-2): 35–41

- 65 Hori, H., Nagaoka, Y., Murayama, M., Kutsuna, S. Efficient decomposition of perfluorocarboxylic acids and alternative fluorochemical surfactants in hot water. *Environmental Science & Technology*, 2008, 42, 7438–7443
- 66 Hori, H., Nagaoka, Y., Yamamoto, A., Sano, T., Yamashita, N., Taniyasu, S., Kutsuna, S., Osaka, I., Arakawa, R. 2006. Efficient decomposition of environmentally persistent perfluorooctanesulfonate and related fluorochemicals using zerovalent iron in subcritical water. *Environmental Science & Technology*, 40(3): 1049–1054
- 67 Hori, H., Yamamoto, A., Hayakawa, E., Taniyasu, S., Yamashita, N., Kutsuna, S., Kiatagawa, H., Arakawa, R. 2005. Efficient decomposition of environmentally persistent perfluorocarboxylic acids by use of persulfate as a photochemical oxidant. *Environmental Science & Technology*, 39(7): 2383–2388
- 68 Hori, H., Yamamoto, A., Koike, K., Kutsuna, S., Osaka, I., Arakawa, R. 2007. Photochemical decomposition of environmentally persistent shortchain perfluorocarboxylic acids in water mediated by iron(II)/(III) redox reactions. *Chemosphere*, 68(3): 572–5781
- 69 Houde, M., Martin, J.M., Letcher, R.J., Solomon, K.R., Muir, D.C.G., 2006. Biological monitoring of polyfluoroalkyl substances: a review. *Environ. Sci. Technol.* 40, 3463–3473.
- 70 Huheey, pps. A-21 to A-34; T.L. Cottrell, "The Strengths of Chemical Bonds," 2nd ed., Butterworths, London, 1958; B. deB. Darwent, "National Standard Reference Data Series," National Bureau of Standards, No. 31, Washington, DC
- 71 Inoue, K., F. Okada, R. Ito, S. Kato, S. Sasaki, S. Nakajima, A. Uno, Y. Saijo, F. Sata, Y. Yoshimura, R. Kishi and H. Nakazawa (2004a). Perfluorooctane sulfonate (PFOS) and related perfluorinated compounds in human maternal and cord blood samples: Assessment of PFOS exposure in a susceptible population during pregnancy, *Environ. Health Perspect.*, 112 (11), 1204-1207.
- 72 International Institute for Sustainable Development. 2009. *Earth Negotiations Bulletin*, vol 15, pp.1-4.
- 73 Jakob L, Hashem T M, Burki S, Guindy N M, Braun A M. Vacuum-ultraviolet (VUV) photolysis of water: Oxidative degradation of 4-chlorophenol. *Journal of Photochemistry and Photobiology A: Chemistry*, 1993, 75(2) 97–103
- 74 Jan, H., Michaela, B., Karel, B., Sharma, V.K., 2006. Electrochemical formation of ferrate (VI) in a molten NaOH–KOH system. *Electrochem. Commun.* 8, 1737–1740.
- 75 Jiang, J.Q., 1988. Study on the anodic passivation in an electrocoagulator in water treatment. *Wat. Treatment* 3 (3), 344–352.

- 76 Jiang, J.Q., 2003. Ferrate: a dual functional water treatment chemical. In: Proceedings of the First IWA Leading Edge Conference on Drinking Water and Wastewater Treatment Technologies, Noordwijk/Amsterdam, 26–28 May 2003.
- 77 Jiang, J.Q., 2007. Research progress in the use of ferrate(VI) for the environmental remediation. *J. Hazard. Mater.* 146, 617–623.
- 78 Jiang, J.Q., Graham, N., Andre, C., Kelsall, G.H., Brandon, N., 2002. Laboratory study of electro-coagulation-flotation for water treatment. *Water Res.* 36, 4064–4078.
- 79 Jiang, J.Q., Lloyd, B., 2002. Progress in the development and use of ferrate(VI) salt as an oxidant and coagulant for water and wastewater treatment. *Water Res.* 36, 1397–1408.
- 80 Jiang, J.Q., Lloyd, B., Grigore, L., 2001. Disinfection and coagulation performance of potassium ferrate for potable water treatment. *Environ. Eng. Sci.* 18 (5), 323–328.
- 81 Jiang, J.Q., Panagouloupoulos, A., Bauer, M., Pearce, P., 2006-2. The application of potassium ferrate for sewage treatment. *J. Environ. Manag.* 79 (2), 215–220.
- 82 Jiang, J.Q., Wang, S., 2003. Enhanced coagulation with potassium ferrate(VI) for removing humic substances. *Environ. Eng. Sci.* 20 (6), 627–633.
- 83 Jiang, J.Q., Wang, S., Panagouloupoulos, A., 2006-1. The exploration of potassium ferrate(VI) as a disinfectant/coagulant in water and wastewater treatment. *Chemosphere* 63 (2), 212–219.
- 84 Jiang, J.Q., Wang, S., Panagouloupoulos, A., 2007. The role of potassium ferrate (VI) in inactivation of *Escherichia coli* and in the reduction of COD for water remediation. *Desalination* 210, 266–273.
- 85 Jiang, J.Q., Yin, Q., Zhou, L.J., Pearce, P., 2005. Occurrence and treatment trails of endocrine disrupting chemicals (EDCs) in wastewaters. *Chemosphere* 61, 244–550.
- 86 Jia-Qian Jiang and Barry Lloyd. 2002 Progress in the development and use of ferrate (VI) salt as an oxidant and coagulant for water and wastewater treatment. *Water Research* 36, 1397–1408.
- 87 Jin, Y.E., Liu, W., Sato, I., Nakayama, S.F., Sasaki, K., Saito, N., and Tsuda, S. 2009. PFOS and PFOA in environmental and tap water in China. *Chemosphere.* 77, 605–611
- 88 Jing C., Peng Z. and Jian L. 2007. Photodegradation of perfluorooctanoic acid by 185 nm vacuum ultraviolet light. *Journal of Environmental Sciences*, vol 19(4), pp.387-390.
- 89 Johnson R.L, Anschutz A.J, Smolen J.M, Simcik M.F and Lee Penn R, 2007, The adsorption of perfluorooctane sulfonate onto sand, clay, and iron oxide surfaces, *Journal of Chemical and Engineering Data* 52 (4), 1165–1170
- 90 Ka`rrman, A., Ericson, I., Van Bavel, B., Danerud, P.O., Aune, M., Glynn, A., Lignell, S., Lindstrvm, G., 2007. Exposure of perfluorinated chemicals through lactation: levels of

- matched human milk and serum and a temporal trend, 1996–2004, in Sweden. *Environ. Health Perspect.* 115, 226–230.
- 91 Kannan, K., Corsolini, S., Falandysz, J., Fillmann, G., Kumar, K.S., Loganathan, B.G., Mohd, M.A., Olivero, J., Wouwe, N.V., Yang, J.H., Aldous, K.M., 2004. (1), 128–134. Perfluorooctanesulfonate and related fluorochemicals in human blood from several countries. *Environ. Sci. Technol.* 38, 4489–4495.
- 92 Kannan, K., Corsolini, S., Falandysz, J., Oehme, G., Focardi, S., Giesy, J.P., 2002. Perfluorooctanesulfonate and related fluorinated hydrocarbons in marine mammals, fishes, and birds from coasts of the Baltic and the Mediterranean Seas. *Environ. Sci. Technol.* 36, 3210–3216.
- 93 Kannan, K., L. Tao, E. Sinclair, S. D. Pastva, D. J. Jude and J. P. Giesy (2005). Perfluorinated compounds in aquatic organisms at various trophic levels in a Great Lakes food chain, *Arch. Environ. Contam. Toxicol.*, 48 (4), 559-566.
- 94 Kasper D.R., 1971, Theoretical and Experimental Investigation of the Flocculation of Charged Particles in Aqueous Solution by Polyelectrolytes of Opposite Charge, California Institute of Technology, Pasadena, .
- 95 Kato, K., Kazama, F., 1991. Biocidal characteristics of potassium ferrate. In: Proceeding of the Third IAWPRC Regional Conference on Asian Water Quality, November 20–24, Shanghai, China II-50-II-55.
- 96 Kawamura S. 2000. Integrated Design and Operation of Water Treatment Facilities. 2nd Edition, New York: John Wiley and Sons.
- 97 Kazama, F., 1994. Inactivation of coliphage QB by potassium ferrate. *FEMS Microbiol. Lett.* 118, 345–350.
- 98 Kazama, F., 1995. Viral inactivation by potassium ferrate. *Wat. Sci. Technol.* 31, 165–168.
- 99 Kennedy, G.L., Butenhoff, J.L., Olsen, G.W., O'Connor, J.C., Seacat, A.M., Perkins, R.G., Biegel, L.B., Murphy, S.R., Farrar, D.G., 2004. The toxicology of perfluorooctanoate. *Crit. Rev. Toxicol.* 34, 351–384.
- 100 Key B.D., Howell R.D. and Criddle C.S. 1997. Fluorinated organics in the biosphere.
- 101 Knappe, D.R.U., Rossner, A., Snyder, S.A., Strickland, C. 2007. Alternative Adsorbents for the Removal of Polar Organic Contaminants. American Water Works Association Research Foundation, Denver, CO.
- 102 Koninck, M.D., Belanger, D., 2003. The electrochemical generation of ferrate at pressed iron powder electrodes: comparison with foil electrode. *Electrochem. Acta* 48, 1435–1442.

- 103 Koninck, M.D., Brousse, T., Belanger, D., 2003. The electrochemical generation of ferrate at pressed iron powder electrodes: effect of various operating parameters. *Electrochem. Acta* 48, 1425–1433.
- 104 Kudo, N. and Y. Kawashima (2003). Toxicity and toxicokinetics of perfluorooctanoic acid in humans and animals, *Journal of Toxicological Sciences*, 2, 49-57.
- 105 Kutsuna S, Hori H. 2007 Rate constants for aqueous-phase reactions of SO_4^{2-} with $\text{C}_2\text{F}_5\text{C}(\text{O})\text{O}^-$ and $\text{C}_3\text{F}_7\text{C}(\text{O})\text{O}^-$ at 298 K. *International Journal of Chemical Kinetics*, 39(5) 276–288
- 106 Kutsuna S, Nagaoka Y, Takeuchi K, Hori H. 2006. TiO_2 -induced heterogeneous photodegradation of a fluorotelomer alcohol in air. *Environmental Science & Technology*, 40, 6824–6829
- 107 Labique, F., Valentin, G., 2002. Direct electrochemical preparation of solid potassium. *Electrochem. Commun.* 4 (10), 764–766.
- 108 Lampert D.J., Frisch M.A., Speitel Jr. and G.E. 2007. Removal of perfluorooctanoic acid and perfluorooctane sulfonate from wastewater by ion exchange. *Pract. Periodical Haz., Toxic, and Radioactive Waste Mgmt*, 11, 60–68.
- 109 Lange, F. T., C. Schmidt and H. J. Brauch (2006), Perfluoroalkylcarboxylates and -sulfonates: emerging contaminants for drinking water supplies?, 31 pp, Association of River Waterworks (RIWA), Netherlands.
- 110 Lau, C., J. L. Butenhoff and J. M. Rogers (2004). The developmental toxicity of perfluoroalkyl acids and their derivatives, *Toxicol. Appl. Pharmacol.*, 198 (2), 231-241.
- 111 Lau, C., J. R. Thibodeaux, R. G. Hanson, J. M. Rogers, B. E. Grey, M. E. Stanton, J. L. Butenhoff and L. A. Stevenson (2003). Exposure to perfluorooctane sulfonate during pregnancy in rat and mouse. II: Postnatal evaluation, *Toxicol. Sci.*, 74 (2), 382-392.
- 112 Lee C, Choi W, Kim Y G, Yoon J. UV photolytic mechanism of Nnitrosodimethylamine in water: Dual pathways to methylamine versus dimethylamine. *Environmental Science & Technology*, 2005, 39(7): 2101–2106
- 113 Lee J, Kim J, Choi W. Oxidation on zerovalent iron promoted by polyoxometalate as an electron shuttle. *Environmental Science & Technology*, 2007, 41(9): 3335–3340
- 114 Lee, Y., Cho, M., Kim, J.Y., Yoon, J., 2004-1. Chemistry of ferrate(Fe(VI)) in aqueous solution and its applications as a green chemical. *J. Ind. Eng. Chem.* 10 (1), 161–171.
- 115 Lee, Y., Um, I.H., Yoon, J., 2004-2. Arsenic(III) oxidation by iron(VI) (ferrate) and subsequent removal of arsenic(V) by iron(III) coagulation. *Environ. Sci. Technol* 37 (24), 5750–5756.
- 116 Lemal DM. . 2004 "Perspective on Fluorocarbon Chemistry" *J Org Chem*, volume 69, p 1–11.

- 117 Lescuras-Darrou, V., Lapicque, F., Valentin, G., 2002. Electrochemical ferrate generation for waste water treatment using cast irons with high silicon contents. *J. Appl. Electrochem.* 32, 57–63.
- 118 Li, C., Li, X.Z., Graham, N. and Gao, N.Y. 2008 The aqueous degradation of bisphenol A and steroid estrogens by ferrate. *Water Research* 42, 109 – 120
- 119 Licht, S., Naschitz, V., Liu, B., Ghosh, S., Halperin, N., Halperin, L., Rozen, D., 2001. Chemical synthesis of battery grade super-iron barium and potassium Fe(VI) ferrate compounds. *J. Power Sources* 99 (1–2), 7–14.
- 120 Licht, S., Tel-Vered, R., Halperin, L., 2002. Direct electrochemical of solid ferrate and super-iron battery. *Electrochem. Commun.* 4 (11), 933–937.
- 121 Licht, S., Yang, L., Wang, B., 2005. Synthesis and analysis of Ag₂FeO₄ Fe (VI) ferrate super-iron cathode. *Electrochem. Commun.* 7 (9), 931–936.
- 122 Lien, N.P.H., Fujii, S., Tanaka, S., Nozoe, M. and Tanaka, H. 2008. Contamination of perfluorooctane sulfonate (PFOS) and perfluorooctanoate (PFOA) in surface water of the Yodo River basin (Japan). *Desalination*. 226, 338–347.
- 123 Lin, S. and Juang, R., 2009. Adsorption of phenol and its derivatives from water using synthetic resins and low-cost natural adsorbents: A review. *Journal of Environmental Management*. 90, 1336-1349.
- 124 Loos, R., Wollgast, J., Huber, T., Hanke, G., 2007. Polar herbicides, pharmaceuticals, perfluorooctansulfonate (PFOS), perfluorooctanoate (PFOA), nonylphenol and its carboxylates and ethoxylates in surface and tap waters around Lake Maggiore in Northern Italy. *Anal. Bioanal. Chem.* 387, 1469–1478.
- 125 Lucas, J.S., Idle, C.N., Chao, A.C., 1996. Quality improvement of biosolids by ferrate (VI) oxidation of offensive odour compounds. *Wat. Sci. Technol.* 33 (3), 119–130.
- 126 Lui, W., Ma, J., 2002. Effects of ferrate (VI) preoxidation on the architecture of algal cells and the mechanism of enhanced coagulation. *Acta Scientiae Circumstantie* 22, 24–28.
- 127 Luthy R.G, Aiken G.R, Brusseau M.L, Cunningham S.D, Gschwend P.M, Pignatello J.J, Reinhard M, Traina S.J, Weber W.J and Westall J.C, 1997, Sequestration of hydrophobic organic contaminants by geosorbents, *Environmental Science and Technology* 31 (12), 3341–3347
- 128 Ma, J., Liu, W., 2002-1. Effectiveness of ferrate (VI) peroxidation in enhancing the coagulation of surface waters. *Water Res.* 36, 4959–4962.
- 129 Ma, J., Liu, W., 2002-2. Effectiveness and mechanism of potassium ferrate (VI) preoxidation for algae removal by coagulation. *Water Res.* 36, 871–878.

- 130 Malley J.P., Locandro R.R., Wagler J.L. 1993, Innovative Point-of-Entry (POE) Treatment for Petroleum Contaminated Water Supply Wells. Final Report. U.S.G.S. New Hampshire Water Resources Research Center. Durham, NH.
- 131 Martin, J. W., S. A. Mabury, K. R. Solomon and D. C. G. Muir (2003a). Bioconcentration and tissue distribution of perfluorinated acids in rainbow trout (*oncorhynchus mykiss*), *Environ. Toxicol. Chem.*, 22 (1), 196-204.
- 132 Martin, J.W., Smithwick, M.M., Braune, B.M., Hoekstra, P.F., Muir, D.C.G., Mabury, S.A., 2004-1. Identification of long-chain perfluorinated acids in biota from the Canadian Arctic. *Environ. Sci. Technol.* 38, 373–380.
- 133 Maruthamuthu P, Padmaja S, Huie R E. Rate constants for some reactions of free-radicals with haloacetates in aqueous solution. *International Journal of Chemical Kinetics*, 1995, 27(6): 605–612
- 134 McKay G. and Ho Y.S. 1999. Pseudo-second order model for sorption processes. *Process Biochem.* 34, 451-465.
- 135 McLachlan, M., Holmström, K.E., Reth, M., Berger, U., 2007. Riverine discharge of perfluorinated carboxylates from the European Continent, *Environ. Sci. Technol.*, in press.
- 136 Melin, G., 1999. Evaluation of the Applicability of Synthetic Resin Sorbents for MTBE Removal from Water, Center for Groundwater Restoration and Protection, National Water Research Institute, California.
- 137 Melzer, D., Rice, N., Depledge, H.M., Henley, e.W., Tamara, Galloway, S. 2010. Association Between Serum Perfluorooctanoic Acid (PFOA) and Thyroid Disease in the NHANES Study. *Env. Health perspective*
- 138 Metcalf & Dddy, 2003. *Wastewater Engineering – Treatment & Reuse* (fourth Edition), McGrawhill
- 139 Midasch, O., Schettgen, T., Angerer, J., 2006. Pilot study on the perfluorooctansulfonate and perfluorooctanoate exposure of the German general population. *Int. J. Hyg. Environ. Health* 209, 489–496.
- 140 Mohammad,A., Jia-Qian, J., Cecilia Stanford b. 2009. On-line production of ferrate with an electrochemical method and its potential application for wastewater treatment – A review *Journal of Environmental Management* 90 1350–1356
- 141 (Montgomery) James M. Montgomery Consulting Engineers, Inc. 2008, *Water Treatment Principles and Design*. John Wiley and Sons, Inc.
- 142 Moriwaki H., Takagi Y., Tanaka M., Tsuruho K., Okitsu K. and Maeda,Y. 2005 Sonochemical Decomposition of Perfluorooctane Sulfonate and Perfluorooctanoic Acid. *Environ. Sci.*

Technol. 39(9), 3388-3392.

- 143 Mursheda, M., Rockstrawb, D.A., Hansonc, A.T., Johnsond, M., 2003. Rapid oxidation of sulphide mine tailing by reacting with potassium ferrate. *Environ. Pollut.* 125, 245–253.
- 144 Neta P, Huie R E, Ross A B. Rate constants for reactions of inorganic radicals in aqueous solution. *Journal of Physical and Chemical Reference Data*, 1988, 17(3): 1027–1284
- 145 Nishiwaki T, Usui M, Anda K, Hida M. 1979. Dechlorination of polychlorinated biphenyls by UV-irradiation. 5. Reaction of 2,4,6- trichlorobiphenyl in neutral and alkaline alcoholic solution. *Bulletin of the Chemical Society of Japan*, 52(3): 821–825
- 146 Ochoa-Herrera V and Sierra-Alvarez R, 2008, Removal of perfluorinated surfactants by sorption onto granular activated carbon, zeolite and sludge, *Chemosphere* 72 (10), 1588–1593
- 147 Ockerman, L.T., Schereyer, J.M., 1951. Preparation of sodium ferrate(VI). *J. Am. Chem. Soc.* 73, 5479.
- 148 OECD report ENV/JM/RD(2002)17/FINAL, 21 Nov. 2002. Hazard assessment of perfluorooctanesulfonate (PFOS) and its salts.
- 149 O'Hagan D. 2008. "Understanding organofluorine chemistry. An introduction to the C–F bond". *Chem Soc Rev* 37 (2): 308–19
- 150 Oppenlander T, Gliese S. Mineralization of organic micropollutants (homologous alcohols and phenols) in water by vacuum-UV oxidation (H₂O-VUV) with an incoherent xenon-excimer lamp at 172 nm. *Chemosphere*, 2000, 40(1): 15–21
- 151 Osborne M C, Li Q, Smith I W M. Products of the ultraviolet photodissociation of trifluoroacetic acid and acrylic acid. *Physical Chemistry Chemical Physics*, 1999, 1(7): 1447–1454
- 152 Park H, Vecitis C D, Cheng J, Mader B T, Hoffmann M R. 2009. Reductive defluorination of aqueous perfluorinated alkyl surfactants: Effects of ionic headgroup and chain length. *Journal of Physical Chemistry A*, 113(4): 690–696
- 153 Parker G.R. and Bortko S, 1991. "Groundwater Remediation Using Amberlite Adsorbents." Presented at the Florida Environmental Chemistry Conference. October 30 - November 1,
- 154 Parker G.R. and Bortko S. 1991, Groundwater Remediation Using Amberlite Adsorbents. Presented at the Florida Environmental Chemistry Conference .
- 155 Pelssers E.G.M., Stuart M.A.C., Fleer G.J, 1990, Kinetics of bridging flocculation—role of relaxations in the polymer layer, *J. Chem. Soc.—Faraday Trans* 86, 1355–1361.
- 156 Prevedouros, K., Cousins, I.T., Buck, R.C., Korzeniowski, S.H., 2006. Sources, fate and

transport of perfluorocarboxylates. *Environ. Sci. Technol.* 40, 32–44.

- 157 Price D.W. and Schmidt P.S, 1997, Microwave Regeneration of Adsorbents at Low Pressure: Experimental Kinetics Studies, *Journal of Microwave Power and Electromagnetic Energy*. 32(3), 145-154.
- 158 Qiang Y., Ruiqi Z., Shubo D., Jun H. and Gang Y. 2009. Sorption of perfluorooctane sulfonate and perfluorooctanoate on activated carbons and resin: Kinetic and isotherm study. *Water Research*. 43, 1150-1158.
- 159 Qu, J.H., Liu, H.J., Liu, S.X., Lei, P.J., 2003. Reduction of fulvic acid in drinking water by ferrate. *J. Environ. Eng. ASCE* 129 (1), 17–24.
- 160 Quici N, Litter M I, Braun A A, Oliveros E. Vacuum-UV photolysis of aqueous solutions of citric and gallic acids. *Journal of Photochemistry and Photobiology A: Chemistry*, 2008, 197(2-3): 306–312
- 161 Quinete, N., Wub, Q., Zhang, T., Yun, H.S., Moreira, I. and Kannan, K. 2009. Specific profiles of perfluorinated compounds in surface and drinking waters and accumulation in mussels, fish, and dolphins from southeastern Brazil. *Chemosphere*. 77 , 863–869
- 162 Read, J.F., John, J., MacPherson, J., Schaubel, C., Theriault, A., 2001. The kinetics and mechanism of oxidation of inorganic oxysulfur compounds by potassium ferrate. Part I. Sulfite, thiosulfate and dithionite ions. *Inorganic Chimica* 315, 96–106.
- 163 Read, J.F., MacCormick, K.J., McBain, A.M., 2004. The kinetics and mechanism of the oxidation of DL ethionine and thiourea by potassium ferrate. *Trans. Metal Chem.* 29 (2), 149–158.
- 164 Read, J.F., Wyand, A.E.H., 1998. The kinetics and mechanism of the oxidation of seleno-DL-methionine by potassium ferrate. *Trans. Metal Chem.* 23 (6), 755–762.
- 165 Renner R. 2001. Growing Concern Over Perfluorinated Chemicals. *Environmental Science and Technology* 35 (7): 155A-160A.
- 166 Robert J., Sarah C.B., Miguel B., John K.B.J., Ripal N.S. and Ken D.S. 2000. Application of the Freundlich adsorption isotherm in the characterization of molecularly imprinted polymers. *Analytica Chimica Acta*. 435, 35-42.
- 167 Rohm and Haas, 1992-1999, Inc. Manufacturer Literature. 100 Independence Mall West, Philadelphia, PA 19106-2399.
- 168 Saito, N., Harada, K., Inoue, K., Sasaki, K., Yoshinaga, T., Koizumi, A., 2004-1. Perfluorooctanoate and perfluorooctane sulfonate concentrations in surface water in Japan. *J. Occup. Health* 46, 49–59.

- 169 Saito, N., Sasaki, K., Nakatome, K., Harada, K., Yoshinaga, T., Koizumi, A., 2004-2. Perfluorooctane sulfonate concentrations in surface water in Japan. *Arch. Environ. Contam. Toxicol.* 45, 149–158.
- 170 Schaefer, A., 2006. Perfluorinated surfactants contaminate German waters. *Environ. Sci. Technol.* 40, 7108–7109.
- 171 Schink, T., Waite, T.D., 1980. Inactivation of F2 virus with ferrate (VI). *Water Res.* 14, 1705–1717.
- 172 Schröder, H. F. and R. J. W. Meesters (2005). Stability of fluorinated surfactants in advanced oxidation processes - A follow up of degradation products using flow injection-mass spectrometry, liquid chromatography-mass spectrometry and liquid chromatography-multiple stage mass spectrometry, *J. Chromatogr. A*, 1082 (1), 110-119.
- 173 Schultz, M.M., Barofsky, D.F., Field, J.A., 2006. Quantitative determination of fluorinated alkyl substances by large-volume-injection liquid chromatography tandem mass spectrometry-characterization of municipal wastewaters. *Environ. Sci. Technol.* 40, 289–295.
- 174 Schwarzenbach R P, Gschwend P M, Imboden D M. *Environmental Organic Chemistry*. 2nd ed. New York: Wiley, 2003
- 175 Shao, H.B., Wang, J.M., He, W.C., Zhang, J.Q., Cao, C.N., 2005. EIS analysis on the anodic dissolution kinetics of pure iron in a highly alkaline solution. *Electrochem. Commun.* 7, 1429–1433.
- 176 Sharma, V.K., 2004. Use of iron (VI) and iron (V) in water and wastewater treatment. *Wat. Sci. Technol.* 49 (4), 69–74.
- 177 Sharma, V.K., 2007. A review of disinfection performance of Fe(VI) in water and wastewater. *Wat. Sci. Technol.* 55, 225–230.
- 178 Sharma, V.K., Mishra, S.K., 2006. Ferrate (VI) oxidation of ibuprofen: a kinetic study. *Environ. Chem. Lett.* 3 (4), 182–185.
- 179 Sharma, V.K., Mishra, S.K., Ray, A.K., 2006. Kinetic assessment of the potassium ferrate(VI) oxidation of antibacterial drug sulfamethoxazole. *Chemosphere* 62
- 180 Sharma, V.K. 2002 Potassium ferrate(VI): an environmentally friendly oxidant. *Adv. In env. Research.* 6, 143-156
- 181 Sharma, V.K. and Hollyfield, S. 1995 Ferrate(VI) oxidation of aniline and substituted anilines. *Am. Chem. Soc. Div. Environ. Chem.* 35, 63–66.
- 182 Sharma, V.K., Rendon, R.A., Millero, F.J. and Vazquez, F.G. 2000 Oxidation of thioacetamide by ferrate(VI), *Mar. Chem.* 270, 235–242.

- 183 Sharma, V.K., Rivera, W., Joshi, V.N., Millero, F.J. and Connor, D. 1999 Ferrate(VI) oxidation of thiourea. *Environ. Sci. Technol.* 33, 2645–2650.
- 184 Sikora M.D. and Stratton R.A, 1981, The shear stability of flocculated colloids, *Tappi* 64, 97–101
- 185 Simon, W.P., Michael, D.K., Jaap, V.R., Ropert, R., 2002. The use of hydrous iron (III) oxides for the removal of hydrogen sulphide in aqueous systems. *Water Res.* 36, 825–834.
- 186 Sinclair, E., Kannan, K., 2006. Mass loading and fate of perfluoroalkyl surfactants in wastewater treatment plants. *Environ. Sci. Technol.* 40, 1408–1414.
- 187 Sirinivasan R., Sorial G.A., Ononye G., Husting C. and Jackson E., 2008. Elimination of persistent odorous compounds from drinking water. *Water Science and Technology – Water Supply* 8.2, 121-127.
- 188 Skutlarek, D., Exner, M., Färber, H., 2006. Perfluorinated surfactants in surface and drinking waters. *Environ. Sci. Poll. Res.* 13 (5), 299–307.
- 189 So M.K., Taniyasu S., Yamashita N., Giesy J.P., Zheng J., Fang Z., Im S.H. and Lam P.K.S. 2004. Perfluorinated compounds in coastal waters of Hong Kong, South China, and Korea. *Environmental Science and Technology* 38 (15): 4056-4063.
- 190 Srinivasan P. T., T. Viraraghavan and K. S. Subramanian 1999. Aluminium in drinking water: An overview. *Water SA*, 25, No. 1, Jan, pp 47-55.
- 191 Stenzel M.H. and Merz W.J., 1988, Use of Carbon Adsorption Processes in Groundwater Treatment. *Proceedings of the American Institute of Chemical Engineers. 1988 Summer National Meeting, Denver, CO. Paper No. 6c.*
- 192 Suffet, I.M., 1999, Presentation to the MTBE Research Partnership Research Advisory Committee.
- 193 Takagi, S, F. Adachi, K. Miyano, Y. Koizumi, H. Tanaka, M. Mimura, Y. Watanabe, S. Tanabe and K. Kannan 2008. Perfluorooctanesulfonate and perfluorooctanoate in raw and treated tap water from Osaka, Japan, *Chemosphere.* 72(10), 1409-1412.
- 194 Tang, C.Y., Fu, Q.S., Robertson, A.P., Criddle, C.S., Leckie, J.O., 2006. Use of reverse osmosis membranes to remove perfluorooctane sulfonate (PFOS) from semiconductor wastewater. *Environ. Sci. Technol.* 40, 7342–7349.
- 195 Taniyasu, S., K. Kannan, Y. Horii and N. Yamashita (2002), The first environmental survey of perfluorooctane sulfonate (PFOS) and related compounds in Japan, paper presented at Dioxin 2002, Barcelona, Spain, August 11-16, 2002.
- 196 Thibodeaux, J. R., R. G. Hanson, J. M. Rogers, B. E. Grey, B. D. Barbee, J. H. Richards, J. L. Butenhoff, L. A. Stevenson and C. Lau (2003). Exposure to perfluorooctane sulfonate during

- pregnancy in rat and mouse. I: Maternal and prenatal evaluations, *Toxicol. Sci.*, 74 (2), 369-38
- 197 Thompson, G.W., Ockerman, L.T., Schreyer, J.M., 1951. Preparation and purification of potassium ferrate(VI). *Chem. Anal.* 8, 1379–1381.
- 198 Tiwari, D., Kim, H.U., Choi, B.J., Lee, S.M., Kwon, O.H., Choi, K.M., Yang, J.K., 2007. Ferrate (VI): a green chemical for the oxidation of cyanide in aqueous/waste water. *J. Environ. Sci. Health A Tox. Hazard Subs. Environ. Eng.* 42 (6), 803–810.
- 199 Tiwari, D., Yang, J.Q., Lee, S.M., 2005. Application of ferrate(VI) in the treatment of wastewaters. *Environ. Eng. Res.* 10 (6), 269–282.
- 200 Torn, L.H. , De Keizer A, Koopal L.K and Lyklema J, 2003, Mixed adsorption of poly(vinylpyrrolidone) and sodium dodecylbenzenesulfonate on kaolinite, *Journal of Colloid and Interface Science* 260 (1), . 1–8.
- 201 US EPA (2002), Hazard assessment of perfluorooctanoic acid and its salts, 107 pp, Office of Pollution Prevention and Toxics - Risk Assessment Division, US.
- 202 US EPA (2003), Preliminary risk assessment of the developmental toxicity associated with exposure to perfluorooctanoic acid and its salts, 64 pp, Office of Pollution Prevention and Toxics - Risk Assessment Division, US
- 203 Valeria, O. and Reyes, S. 2008. Removal of perfluorinated surfactants by sorption onto granular activated carbon, zeolite and sludge. *Chemosphere.* 72, 1588-1593.
- 204 Vandiver M. and Isacoff E.G., 1994 “THM Reductions with Amborsorb 563 Adsorbent.” Presented at the Society of Soft Drink Technologists 41st Annual Conference, Albuquerque, NM. April
- 205 Vecitis C D, Park H, Cheng J, Mader B T, Hoffmann M R. 2008 Enhancement of perfluorooctanoate and perfluorooctanesulfonate activity at acoustic cavitation bubble interfaces. *Journal of Physical Chemistry C*, 112(43): 16850–16857
- 206 Waite, T.D., 1979. Feasibility of wastewater treatment with ferrate. *ASCE J. Environ. Eng.* 105, 1023–1026.
- 207 Waite, T.D. and Gilbert, M. 1978 Oxidative destruction of phenol and other organic water residuals by iron(VI) ferrate. *Water pollution control.* 50, 543-558.
- 208 Waldemer R H, Tratnyek P G, Johnson R L, Nurmi J T. Oxidation of chlorinated ethenes by heat-activated persulfate: Kinetics and products. *Environmental Science & Technology*, 2007, 41(3): 1010–1015
- 209 Wardman P. Reduction potentials of one-electron couples involving free-radicals in aqueous-solution. *Journal of Physical and Chemical Reference Data*, 1989, 18(4): 1637–1755

- 210 Weinstock I A. Homogeneous-phase electron-transfer reactions of polyoxometalates. *Chemical Reviews*, 1998, 98(1): 113–170
- 211 Wood, R.H., 1958. The heat, free energy, and entropy of the ferrate(VI) ion. *J. Am. Chem. Soc.* 80, 2038–2041.
- 212 Xu, J., Wang, J., Yang, W., Chen, C., Zhang, J., 2004. Electrochemical synthesis of ferrate(VI) by anodic oxidation. *Dianhuaxue* 10 (1), 87–93.
- 213 Yamamoto T, Noma Y, Sakai S, Shibata Y. 2007 Photodegradation of perfluorooctane sulfonate by UV irradiation in water and alkaline 2-propanol. *Environmental Science & Technology*, 41(16): 5660–5665
- 214 Yamashita, N., Kannan, K., Taniyasu, S., Horii, Y., Okazawa, T., Petrick, G., Gamo, T., 2004. Analysis of perfluorinated acids at parts-per-quadrillion levels in seawater using liquid chromatography-tandem mass spectrometry. *Environ. Sci. Technol.* 38, 5522–5528.
- 215 Yamashita, N., Kannan, K., Taniyasu, S., Horii, Y., Petrick, G., Gamo, T., 2005. A global survey of perfluorinated acids in oceans. *Marine Poll. Bull.* 51, 658–668.
- 216 Yong Q., Fujii S. and Tanaka S. 2007. Removal of perfluorochemicals from wastewater by granular activated carbon adsorption. *Env Eng research.* 44, 185-193.
- 217 Yong Qiu , 2007, study on treatment technologies for perfluorochemicals IN wastewater, PhD thesis
- 218 Yong, Y. E., Sharma ,V.K and Ray,A. K. 2006 Green chemistry oxidant for degradation of cationic surfactant. *Chemosphere* 63,1785–1790
- 219 Yong,Q., Fujii,S., Tanaka,S. and Koizumi, A. 2006 Priliminary study on the treatment of Perfluorinated chemicals (PFCs) by Advanced Oxidation Process (AOPs). The12th Seminar of JSPS-MOE Core University Program on Urban Environment, Kyoto, Japan
- 220 Yuan, B., Li, Y., Huang, X., Lui, H., Qu, J., 2006. Fe(VI)-assissted photocatalyticx degradation of microcystin-LR using titanium dioxide. *J. Photochem. Photobiol.*
- 221 Yuan, B., Qu, J.-H., Fu, M.-L., 2002. Renoval of cyanobacterial microcystin – LR by ferrate oxidation–coagulation. *Toxicon* 40, 1129–1134.
- 222 Yuxi, R., Zhen, C., Yamin, G., Riyao, C., Xi, Z., 2008. Usage of anisomeric square pulse with fluctuating frequency for electrochemical generation of FeO₄²⁻ in CS–CMC bipolar membrane electrolysis cell. *Chem. Eng. Process* 47 (4), 708–715.
- 223 Zhu, J.H., Yan, X.L., Liu, Y., Zhang, B., 2006. Improvingalachlor biodegradability by ferrate oxidation. *J. Hazard. Mater.* B135, 94–99.

